13:25:13 OCA PAD AMENDMENT - PROJECT HEADER INFORMATION 05/14/92

Active

Project #: E-25-620 Cost share #: E-25-329 Rev #: 1
Center # : 10/24-6-R7315-0A0 Center shr #: 10/22-1-F7315-0A0 OCA file #:
Work type : RES
Contract#: 36053-S1 Mod #: LTR DTD 5/13/92 Document : PO
Prime #: Contract entity: GTRC

Subprojects ? : N CFDA: N/A
Main project #: PE #: N/A

Project unit: MECH ENGR Unit code: 02.010.126
Project director(s):
UMEAGUKWU I C MECH ENGR (404)894-7411

Sponsor/division names: MOTOROLA INC /
Sponsor/division codes: 212 / 049

Award period: 910601 to 930228 (performance) 930228 (reports)

Sponsor amount	New this change	Total to date
Contract value	0.00	121,000.00
Funded	0.00	121,000.00
Cost sharing amount		60,000.00

Does subcontracting plan apply ?: N

Title: EXPERIMENTAL & FINITE ELEMENT INVESTIGATION OF THERMALLY INDUCED PWB WARPAGE

PROJECT ADMINISTRATION DATA

OCA contact: Ina R. Lashley 894-4820

Sponsor technical contact

DR. KARL WYATT
(708)538-2388

MOTOROLA, INC.
MS/IL02 F31, ROOM 1014
1301 E. ALGONQUIN ROAD
SCHAUMBURG, IL 60196

Sponsor issuing office

GENE GOLEMO
(708)576-6139

MOTOROLA, INC.
SHARED SYSTEMS PURCHASING
1302 E. ALGONQUIN ROAD
SCHAUMBURG, IL 60196

Security class (U,C,S,TS) : U ONR resident rep. is ACO (Y/N): N
Defense priority rating : N/A N/A supplemental sheet
Equipment title vests with: Sponsor GIT X

Administrative comments -
MOTOROLA LTR DTD 5/13/92 AUTHORIZES A NINE-MONTHS NO-COST EXTENSION.

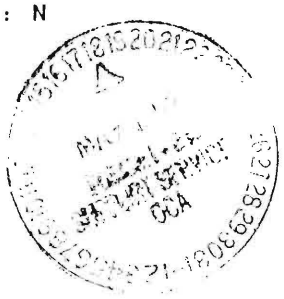

GEORGIA INSTITUTE OF TECHNOLOGY
OFFICE OF CONTRACT ADMINISTRATION

NOTICE OF PROJECT CLOSEOUT

Closeout Notice Date 09/20/93

Project No. E-25-620 Center No. 10/24-6-R7315-0A0

Project Director UMEAGUKWU I C School/Lab MECH ENGR

Sponsor MOTOROLA INC/

Contract/Grant No. 36053-S1 Contract Entity GTRC

Prime Contract No.

Title EXPERIMENTAL & FINITE ELEMENT INVESTIGATION OF THERMALLY INDUCED PWB WARP

Effective Completion Date 930228 (Performance) 930228 (Reports)

Closeout Actions Required:	Y/N	Date Submitted
Final Invoice or Copy of Final Invoice	Y	
Final Report of Inventions and/or Subcontracts	Y	
Government Property Inventory & Related Certificate	N	
Classified Material Certificate	N	
Release and Assignment	N	
Other	N	

CommentsEFFECTIVE DATE 6-1-91. CONTRACT VALUE $121,000.

Subproject Under Main Project No.

Continues Project No.

Distribution Required:

Project Director	Y
Administrative Network Representative	Y
GTRI Accounting/Grants and Contracts	Y
Procurement/Supply Services	Y
Research Property Managment	Y
Research Security Services	N
Reports Coordinator (OCA)	Y
GTRC	Y
Project File	Y
Other CARL BAXTER-FMD	Y
FRED CAIN-OOD	Y

NOTE: Final Patent Questionnaire sent to PDPI.

EXPERIMENTAL AND FINITE ELEMENT INVESTIGATION OF THERMALLY INDUCED PWB WARPAGE

Charles Ume
Jeff Garratt
School of Mechanical Engineering
Georgia Institute of Technology
Atlanta, GA 30332-0405

September 1993

A Final Report Submitted to:

Dr. Karl Wyatt
Motorola Inc.
CMRC Room 1014
1301 E. Algonquin Road
Schaumburg, IL 60196

Charles Ume

ACKNOWLEDGEMENT

The authors would like to acknowledge the support of the CMRC of Motorola, which provided the financial support to carryout this research under contract No. 36053-S1. Special thanks to Dr. Karl Wyatt who served as the project's technical mentor.

TABLE OF CONTENTS

LIST OF TABLES

LIST OF FIGURES

SUMMARY

The trend in printed wiring board (PWB) manufacturing is towards miniaturization of electronic circuitry, while simultaneously increasing product functionality. The result is more densely populated boards, with smaller components. The increasing use of surface mount devices (SMDs) in industry has sparked a great deal of research in the area of printed wiring board warpage. Thermal stresses resulting from manufacturing processes cause the PWB to deform, and thus can be a source of solder joint failure. The warpage is also a major cause of alignment errors during the component placement process.

Previous investigators have performed warpage analyses using published properties data, given in range format for room temperature. The current research outlines the development of procedures for the measurement of temperature dependent properties of thin lamina and laminates to be used for lay-up decisions in the early stages of the PWB design process. Experimental results of temperature dependent properties testing of the PWB's core materials are presented. These results were used in finite element analysis to predict warpage of a sample PWB undergoing a simulated wave soldering process. In addition to using measured properties for the finite element analysis, two other cases were considered. The first utilizes the minimum values of properties data for the PWB core materials(copper and prepreg, a glass/epoxy composite) , the second uses the maximum values. The three cases are compared to illustrate the importance of temperature dependent property testing in predicting thermally induced printed wiring board warpage.

CHAPTER I

INTRODUCTION

The technological revolution of the last decade can trace its roots to advances in the both the electronics and computer industries. With improvements in the computational power of modern digital computers and in processing speeds of telecommunications equipment, the efficiency of industrial operations has increased dramatically. The evolution of the electronics industry has given rise to increasingly complex circuitry to meet the ever growing demand for equipment which is faster, cheaper, smaller, and more functional than its predecessors. Today's electronic circuits have many more components in a much smaller area with a greater number of interconnections than did those of just a few years ago.

The building block for these modern electronic circuits is the printed wiring assembly (PWA). PWAs consist of electronic components mounted on printed wiring boards (PWBs) which have two primary functions: 1) provide the physical platform for electronic components, 2) provide the electrical interconnections necessary for circuit operation. Most PWBs consist of alternating layers of copper foil and dielectric materials which are often in the form of fiberglass reinforced epoxy composites.

As components decrease in size and population density increases, accuracy of component placement becomes more critical. In particular, placement is critical for surface mount devices (SMDs). Many manufacturers utilize robots to place these devices on the boards, requiring precise positioning to ensure that the component's leads are properly aligned with the solder pads. However, often times proper alignment is not possible due to PWB warpage or *bow* caused by thermal stress as a result of the

manufacturing processes(See figure 1.1 for illustration of Bow). One of these sources of thermal stress is the component soldering process, which was the focus of this research and is briefly described in the following paragraphs.

Soldering Processes

The wave solder process is just one of the methods PWB manufacturers use to secure electronic devices to the physical board, as well as complete the electrical interconnections of the circuits. The two predominant methods utilized in industry today are 1) the wave solder process, 2) and the reflow solder process, or a combination of both. In practice, when the board contains large numbers of thru-hole connections, wave soldering is the preferred choice. However, when the board is made up solely of surface mount devices, solder reflow methods are used [18].

Reflow soldering begins by applying *solder paste* through a process known as *screening*. If the manufacturer is using a one step process with components on both sides of the board, then adhesives may be applied in addition to the paste to prevent component detachment when the board is turned over to allow for opposite side device mounting. Once the components are in place, the board is then heated to a temperature 30-40°C above the solder liquidus temperature, allowing the solder to 'flow,' accounting for the process name, reflow. The two most common methods of reflow are vapor phase and convection/infrared. Vapor phase utilizes the latent heat of vaporization of an inert perflouracarbon [18] to increase the temperature of the board and achieve reflow. Convection/Infrared methods rely on radiation heat transfer as well as convection to reach desired reflow temperatures.

Wave soldering, as implied by the name, is achieved by passing the printed wiring board with components(both surface mount and through-hole devices) over a *wave* of

solder. The wave soldering method provides reliable performance at low cost, and remains the most commonly used method of applying solder. However, as compared to the reflow methods discussed earlier, wave soldering, in general, produces a larger thermal shock to the board [18]. It is the effects of this thermal shock on printed wiring boards that provided the impetus for the thesis. For the remainder of this paper, references to soldering will imply the wave soldering method.

Objective

This research is part of the on going research project in PWA technology conducted at the Georgia Institute of Technology's Advanced Electronic Packaging Laboratory (AEPL). The research represents the initial steps towards the development of a system for the *rapid* determination of printed wiring board thermo-mechanical behavior. The specific goals of this thesis were:

- Develop methods for measuring temperature dependent properties of thin lamina and laminates
- Automate temperature dependent property testing process
- Compare sample PWB warpage predictions using: 1) measured temperature dependent property data, and 2) maximum and minimum values of published property data, to illustrate the importance of temperature dependent property testing

System development began with strain gage selection and implementation. Various criteria for gage selection are discussed. Once the strain gage was chosen, the focus turned to the setup for the materials testing equipment, with an emphasis on system

automation. After verifying the testing system's accuracy, properties testing of the PWB's core materials began. These results were then used in a finite element analysis (FEA) to predict board warpage under conditions which simulated the wave soldering process. In addition to using the measured property data in the FEA, analyses were conducted using the maximum and minimum published property values. These three cases are compared, to illustrate the importance of properties measurement. Finally, suggestions are given for future enhancements to improve system automation and accuracy.

Review of Literature and Related Research

As previously stated, this research is part of a continuing research effort in the area of PWA technology [6]. PWB warpage due to the solder masking process has previously been investigated [14,26] with results leading to generalized guidelines for solder mask selection and application. The analytical models in the research utilized material properties data found in the literature. In addition, these properties were assumed to remain constant. The current thesis is an extension of this research, with the goal of determining the temperature dependent properties of the PWB materials, and utilizing them in the analytical models.

Existing documents discussing temperature dependent properties testing were also found in the literature [8,22]. The results of these papers are used for comparative purposes in this thesis. The work of Upthegrove [25] illustrated the temperature dependent properties of several different copper specimens (Annealed, cold worked, etc.). These vary from the current project in that copper foil specimens used in this research were fabricated through an electro-deposition process, and specimens are very thin, approximately 1.2 to 0.6 mils in thickness. Haque's paper [8] details the process used for experimentally determining the temperature dependent mechanical properties of kevlar-

graphite/epoxy hybrid composites. The composites tested for the paper had an average of 12.5 plies producing a total thickness of 72 mils. For this thesis, individual composite plies of prepreg were tested, with an approximate thickness of 3.5 mils.

Description of Thesis Chapters and Content

The remainder of this thesis is composed of five chapters as follows: Chapter II outlines the strain gage selection process, emphasizing the thinness of the test specimens. The chapter also discusses the techniques used in strain gage implementation. This chapter is very important to the entire research project, as all subsequent results are based upon the accuracy of the experimental strain measurements.

Chapter III details the methods used to automate the temperature dependent properties testing process. The chapter includes an illustration of the entire properties testing system as well as a discussion of the control hardware and software. Finally, operational procedures are discussed for the different tests and specimens.

Chapter IV contains the properties testing data for both the copper and prepreg (fiberglass/epoxy composite) specimens. Properties include Young's moduli, Poisson's ratio, shear modulus, and coefficient of thermal expansion for both copper and prepreg specimens.

Chapter V gives the details for the physical properties of the PWBs used for this paper. This includes an illustration of the sample PWB configuration investigated as well as the manufacturer's specifications of the core components (Copper foil and prepreg). The element chosen for the numerical analysis is also discussed, along with the assumptions made to facilitate the analysis. At this point, a short description is given for a computer program written by the author to aid in the automation of the finite element analysis. Results of the analytical PWB warpage predictions are compared, and the

importance of temperature dependent property testing is discussed. Experimental results from shadow moiré technique are also shown for illustrative purposes.

Chapter VI, the final chapter of the paper, summarizes the results of research, and discusses possible methods for improvement of the current system. Current project status as well as possible areas of future research are described.

The final portion of this thesis includes both a bibliographical listing as well as appendices. The appendices contain miscellaneous information used in the research, as well as additional materials testing data. The reader will be referred to the information in the appendices throughout the paper.

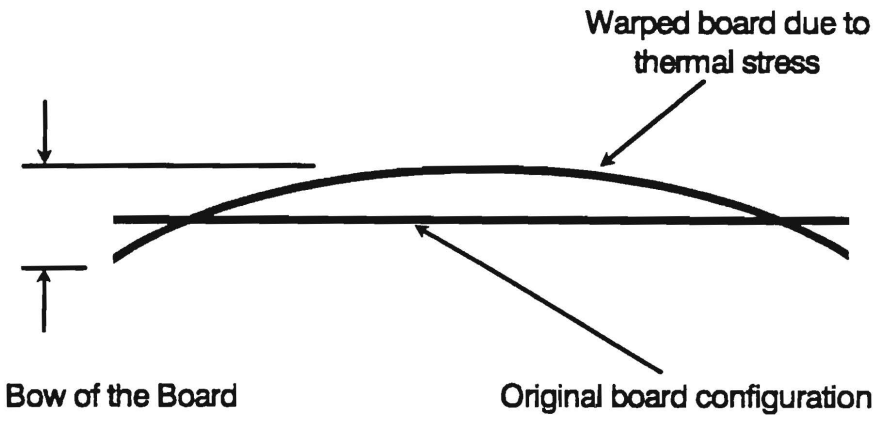

Figure 1.1 Illustration of PWB bow

CHAPTER II

STRAIN GAGE SELECTION AND IMPLEMENTATION

The following chapter details the criteria used in deciding what type of strain measuring system to use for experimental testing of the temperature dependent properties of the board materials. The decisions made based upon these criteria form the foundation for the entire research project. All subsequent work, to include board warpage prediction, is dependent upon the accuracy of the strain measurement system. To insure the greatest accuracy at reasonable cost , an electrical resistance strain gage (EA-13-250AE-350 from Measurements Group) was used for strain measurement. Though many strain-measuring systems exist today, electrical resistance strain gages remain the most widely used device [2].

The chapter begins with a comparison of the stacked rosette and the single open faced foil strain gage, and explains the reason for choosing the latter for the current project. The following section describes several characteristics of strain gages which must be considered during the selection process. Once the gage selection was completed, the focus then turned to the method of bonding the gage to the test specimen. Great care must be taken to insure proper bonding of the gage with the test specimen. The adhesive chosen as well as the curing process are briefly described. The final section of the chapter explains several methods for removing sources of error from strain measurements. It should be noted at this point that the author found the suggestions and information

supplied by the engineers at Measurements Group invaluable during the entire strain gage selection process.

Strain Gage Selection

Stacked Rosette vs. Single Open Faced Foil Gage

Due to the non-homogeneity of the test material, namely B-stage prepreg, it was desirable to measure the material properties in the same location, which would dictate the use of the 2 element 90° stacked rosette. However, the prepreg test specimens used for this paper were approximately 0.004 inches thick. The 2 element stacked rosette, once bonded to the specimen, would have an approximate thickness of 0.004 inches. This would equal the specimen's thickness, producing unacceptable reinforcement effects. A comparison of data from a stacked rosette and two separate gages is shown in figures 2.2 and 2.3. The slopes of each graph represent the coefficients of thermal expansion. The CTEs indicated by the stacked rosette configuration, 12.6 and 13.8E-6 in the x and y directions respectively, were much lower than those of the two gage configuration, 17.0 and 19.3E-6 for the same measurements. In addition to the reinforcement effects, the heat generation within the gage area would roughly double, increasing thermal output (Error in strain reading due to temperature effects). These two effects prompted the use of two open faced foil gages measuring transverse and longitudinal strains in relatively close but distinct locations. The actual gage layout is illustrated in figure 2.1.

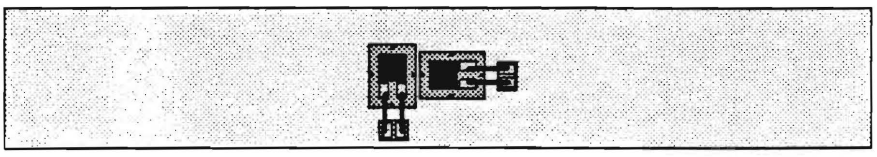

Figure 2.1 Lay-up of strain gages on test specimen

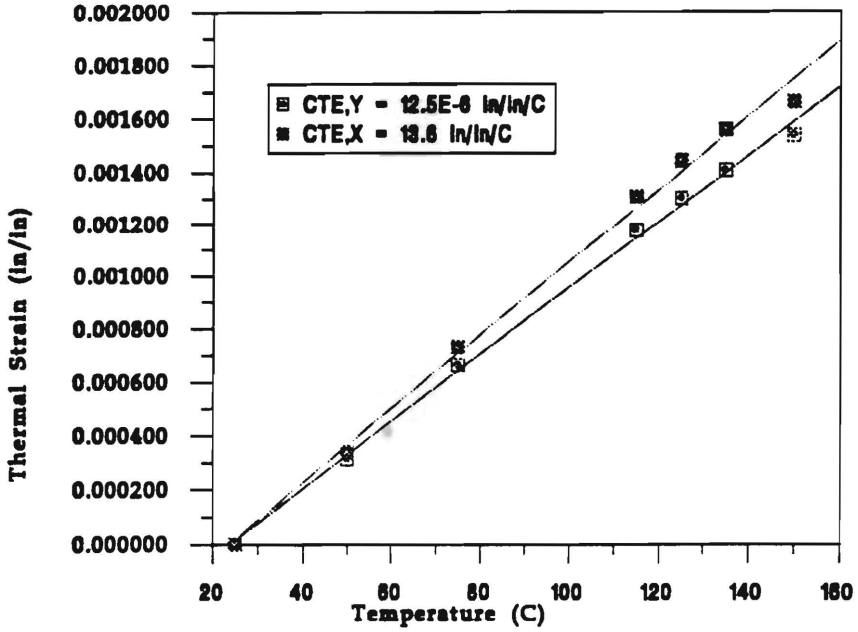

Figure 2.2 Thermal strain vs. temperature for Copper/FR-4 using stacked rosette

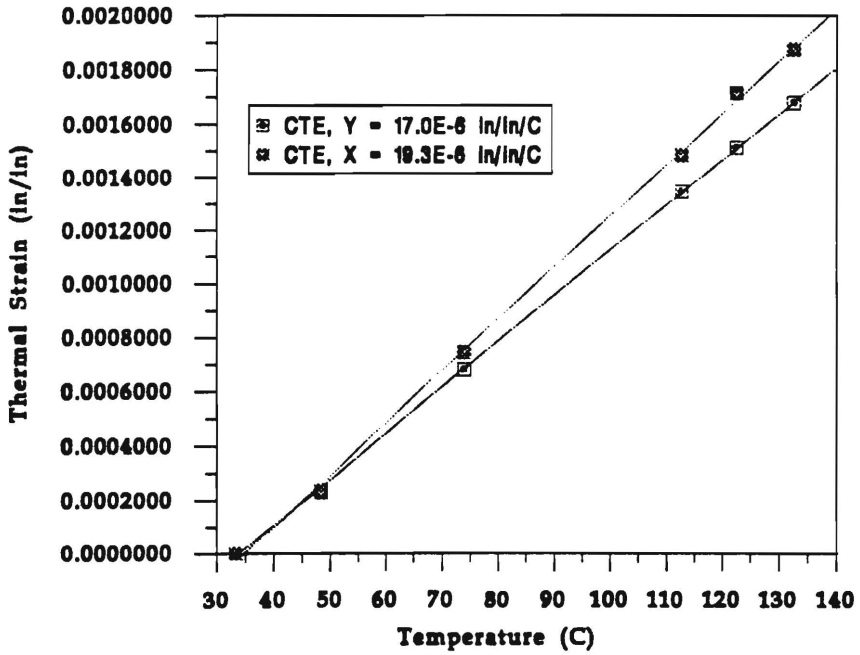

Figure 2.3 Thermal strain vs. temperature for Copper/FR-4 using 2 gage configuration

The error in Poisson's ratio measurements due to isolated transverse and longitudinal strain readings was considered more acceptable than the combined heat generation and reinforcement effects of the rosette gage.

Gage Characteristics

The first consideration is the size of the gage, which is usually specified by gage length (See figure 2.4 for illustration of gage length). Large gages are suggested for use with non-homogeneous materials, such as glass reinforced composites, to achieve better averaging over the strain area. Gage lengths of 0.125 to 0.25 inches are preferable, since larger ones do not noticeably improve fatigue life, stability, or elongation, while shorter ones usually are inferior [21]. For the given system, 0.25 inch gages were chosen to maximize surface coverage for more accurate averaging, as well as for availability from the manufacturer, Measurements group.

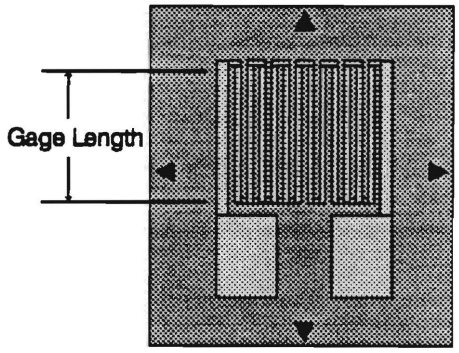

Figure 2.4 Foil Strain Gage with gage length indicated

In addition to the gage length, the width is also an important factor in strain gage selection. Particularly, if a large strain gradient exists perpendicular to the gage axis (As is the case with orthotropic materials), then a narrow grid width is better to minimize

averaging error. However, due to the poor heat transfer properties of the test material (prepreg), wide gages were used to enhance gage stability[21].

As the name implies, electrical resistance strain gages are available in varying resistances, with the 120 and 350 ohm gages being the most common. In general, when a choice exists, a 350 ohm gage is preferable because it reduces internal heat generation of the gage grid approximately by a factor of 3 as compared to the 120 ohm gage for the same excitation voltage (from $P = I^2R$). The 350 ohm has the advantage of decreasing leadwire effects such as circuit desensitization due to leadwire resistance, and unwanted signal variations caused by leadwire resistance changes with temperature fluctuations. Also, when the gage circuit includes switches, slip rings, or other sources of random resistance change (half bridge for example), the signal-to-noise ratio is improved with higher resistance gages operating at the same power level [21].

Adhesive selection and curing process

Due to temperature range of the properties testing, room temperature to 170°C, the choice of adhesive was critical. After consulting with applications engineers from Measurements Group, M-Bond 610 adhesive was chosen. M-bond 610 is a general-purpose epoxy-phenolic adhesive which proves useful for high temperature applications [16]. Another possible adhesive choice is M-Bond 600, an adhesive similar to 610 but with a shorter curing time. However, the 600 adhesive has more reactive curing agents than the 610. These agents could be reactive with the epoxy component of the prepreg specimens and is therefore was excluded from further consideration. An additional benefit of the 610 style epoxy-phenolic adhesive is that it can have a glueline less than 0.0002 inches thick, a very important feature considering the thickness of the test specimen themselves which were as thin as 0.0006 inches.

Figure 2.5 shows glueline temperature versus cure time in hours. The chart is used to determine the amount of time necessary to cure the adhesive for a given temperature. For the case of copper foil specimens, a cure temperature of 170°C for 1.5 hours was used, corresponding to recommended values.

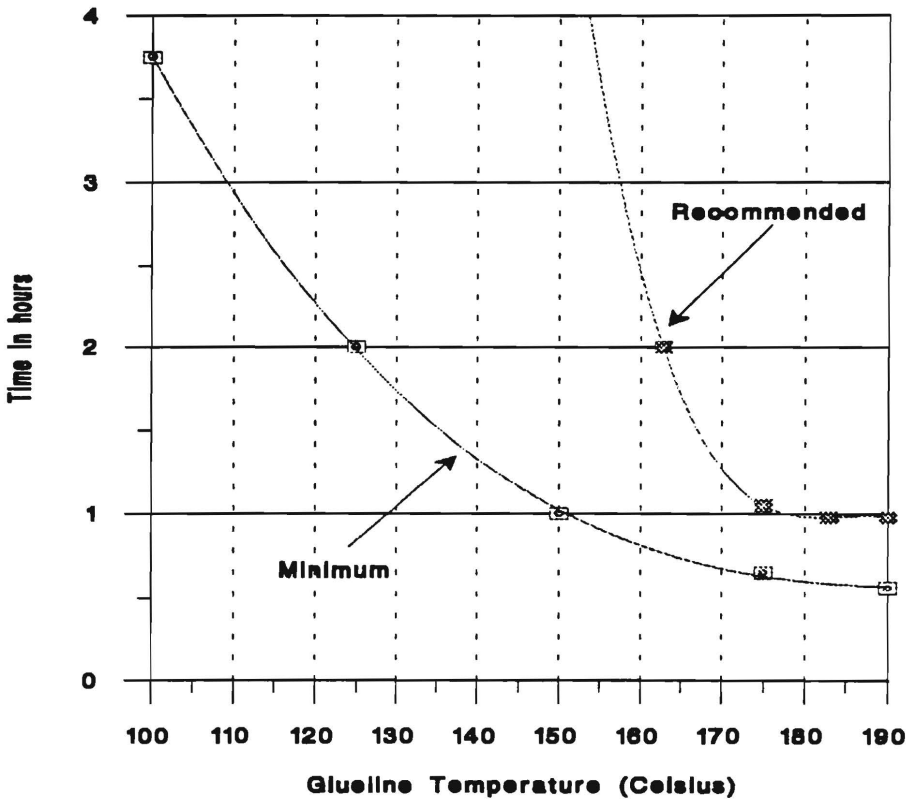

Figure 2.5 Glueline temperature vs. Time for M-Bond 610 Adhesive

Cure temperatures and duration were not critical for the copper foil specimens; however, more thought was necessary for determining the cure time and temperature for the B-stage prepreg samples. As a result, a cure temperature of 170°C for 1.5 hours was

again used. The decision was based upon lamination data provided by IBM [12]. Composite lamination parameters were given by IBM as follows:

- Lamination Time 160 min.
- Temperature 185°C
- Pressure 300 psi

Total cycle for the above parameters:

- Ramp 7 min.
- 185°C for 118 min.
- Cool down 40 min.

The time and temperature were reduced for the actual cure process due to lack of data for actual temperatures of the internal layers of the composite board and assuming insulating effects due to layering of prepreg material. The choice of an adhesive curing temperature and duration better simulating the lamination process of the B-stage prepreg material would improve experimental results but requires a more thorough investigation of the lamination process itself, which is beyond the scope of this paper.

Strain Gage Excitation Level

The optimum excitation level is based upon the following factors[17]:

- Strain gage grid area
- Gage resistance
- Thermal conductivity of the test material
- Testing temperature
- Accuracy

The most important of these factors for the purposes of this project was the heat sink capabilities of prepreg, a fiberglass/epoxy composite. When the temperature of the gage grid is much higher than that of the material, gage performance is affected in two ways. The temperature rating of the gage backing can be reduced by as much as 30°C (Of

	Thermal Conductivity of Test Material				
Accuracy Requirements for strain measurement	EXCELLENT Heavy Aluminum or Copper	GOOD Thick Steel	FAIR Thin Stainless Steel or Titanium	POOR Filled Plastic such as **Fiberglass/epoxy**	VERY POOR Unfilled Plastic such as Acrylic or Polystyrene
High	2-5	1-2	0.5-1	**0.1-0.2**	0.01-0.02
Moderate	5-10	2-5	1-2	0.2-0.5	0.02-0.05
Low	10-20	5-10	2-5	0.5-1	0.05-0.1

Table 2.1 Heat sink conditions data from Measurements Group, Inc. (watts/in^2)

primary concern considering temperature ranges for testing), and the stress-free stability of the gage is reduced, creating zero-shift, which is extremely important when using the half-bridge configuration [17]. Table 2.1 illustrates the heat sink capabilities of some common materials, including fiberglass/epoxy composites. Based upon data from table 2.1, prepreg (fiberglass/epoxy composite) has poor heat sink properties, warranting careful consideration of gage excitation levels. The power dissipated in the gage grid is given by the following equation [17]:

$$P_G = \frac{E_B^2}{4R_G} \qquad (2.1)$$

From which the power density in the gage grid is determined by:

$$P'_G = \frac{P_G}{A_G} \qquad (2.2)$$

where: R_G = gage resistance (ohms)

A_G = grid area (in^2)

E_B = bridge excitation voltage

The strain measurement system used for testing had an excitation voltage of 3.5 volts, and the gage resistance was 350 ohms with a grid area of 0.0625 in^2 (See Appendix A for gage specifications). From equations 2.1 and 2.2, the power dissipated in the gage grid is 0.00875 watts, producing a power density of 0.14 watts/in^2. Comparison of this value with the heat sink conditions from table 2.1 indicate that the system excitation level of 3.5 volts was within the optimum range for measurement accuracy.

Correcting for Thermal Output

Half Bridge Configuration

When a bonded gage undergoes a temperature change, the gage alloy usually undergoes a change in resistance. This resistance change is independent of the stress-induced strain of the test specimen. The temperature change of the gage assembly causes this apparent strain which is termed the *thermal output* of the gage [15].

The classical method for correcting for thermal output while measuring mechanical properties is the "dilatometer", which utilizes the half-bridge circuit with a dummy gage in one quarter of the bridge (See Figure 2.6). During the test, the dummy gage is mounted on a coupon identical to the test specimen (or approximately identical as is the case for this research due to the variation of composite materials). The thermal output for each gage will cancel due to the balancing effects of the bridge, provided both test and dummy gage assemblies are at the same temperature.

To achieve the highest accuracy possible in canceling thermal output, gages on both the test specimen and dummy should be as identical as possible [15]. Purchasing the dual element gage pattern available from Measurements Group would have guaranteed the closest match between thermal outputs of the gages, but were not available during the course of this research. In lieu of this choice, gages were ordered from the same lot.

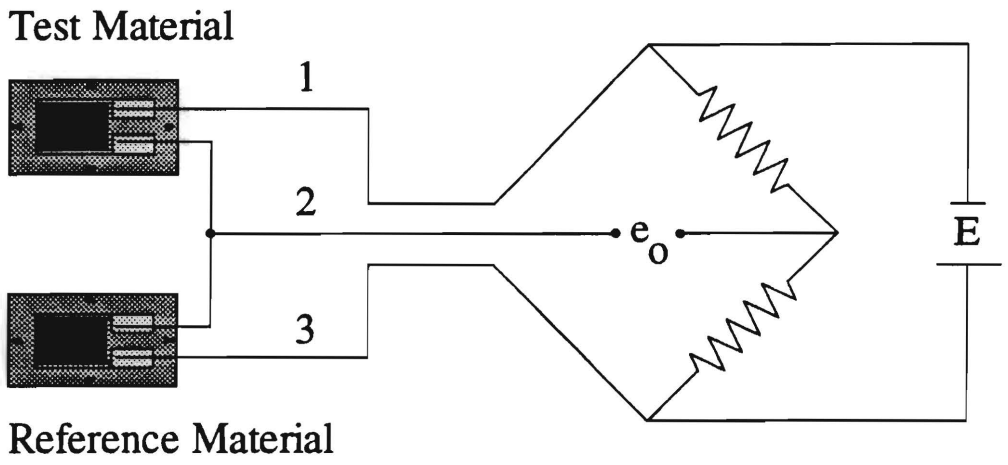

Figure 2.6 Strain gages in half-bridge configuration for measuring thermal expansion coefficients and correcting for thermal output

Second Order Error Correction

Transverse Sensitivity correction

To further enhance thermal expansion measurements, smaller effects need to be addressed. One of these factors is the transverse sensitivity of the strain gage [5]. This effect arises from the fact that the gage has been calibrated for a specific difference in thermal expansion between the gage grid and the specimen. When a test material is used that does not match the specified CTE value, errors will result. To correct these errors, it is necessary to multiply the difference in thermal outputs of the gage with respect to the specimen and gage with respect to the reference material by a correction factor [15] (These two sources of thermal output are discussed in detail in the following chapter, and are shown in equation 3.8). The difference in these thermal outputs is represented by the voltage reading from the bridge circuit, which is recorded as a strain value. The

correction procedure involves multiplying the recorded strain reading by a correction factor which is given by the following equation:

$$\frac{(1-0.285K_t)}{(1+K_t)} \qquad (2.3)$$

The factor K_t is a correction factor which is given in percentage form in the data sheet accompanying gages purchased from the Measurements Group. One important limitation of this correction procedure is that it is only applicable to isotropic materials [15]. For this reason, this correction procedure was only used for the copper foil specimens.

Gage Factor Correction

Much like transverse sensitivity error discussed above, gage factor correction accounts for relatively small inaccuracies. The procedure is also very much like that for transverse sensitivity correction. Again the difference in thermal outputs of the gage with respect to the specimen and the gage with respect to the reference material are multiplied by a correction factor. This correction factor is given as [15]:

$$\frac{1}{(1+\Delta F_G)} \qquad (2.4)$$

The factor ΔF_G is the change in gage factor with temperature. This factor is also given in percentage form in the data sheet accompanying the purchased gages. It must be put into decimalized form prior to use in the correction procedure.

Chapter Conclusion

Electrical resistance strain gages were chosen for the strain measurement system due to their high level of accuracy and cost effectiveness. Upon careful review of selection criteria, the EA-13-250AE-350 open faced foil strain gage, available from Measurements Group, was chosen for its low level of specimen reinforcement, relatively large grid length, and low level of heat generation. The thicknesses of test specimens for the research (as small as 0.0006 inches) produced unique problems in the selection process. The gage lay-up was non-traditional, but the reinforcing and heat generation affects of traditional stacked rosette gages were seen as unacceptable.

CHAPTER III

AUTOMATION OF PROPERTIES TESTING PROCESS

As stated in the introduction to the thesis, one of the objectives of the research is the development of an automated system for the rapid determination of the thermo-mechanical behavior of the board. Though the long term objective is the automation of each of the three phases outlined in the introduction, the current research focuses mainly on the temperature dependent properties testing portion. Specifically, the chapter discusses the experimental setup used for properties testing, briefly describing each facet of the testing process, to include CTE, Young's Moduli , Poisson's ratio, and shear modulus testing. Explanations of the corresponding software routines used to control testing are also given.

Hardware Setup

The hardware setup included an IBM 386 computer which served as the platform for the MTS Testar software package, an MTS load unit and hydraulic power system, a Honeywell UDC 3000 digital controller, an Infinity K-type thermocouple meter, and a Satec oven. The actual system is shown in figure 3.1. All commands are introduced to the system via computer which forms the user interface with the MTS Digital Controller, the heart of the properties testing system. All signals in the setup flow through and are processed by the MTS Digital Controller. However, the system can be separated into

three distinct subsystems, each performing a separate function. The subsystems include temperature control, signal processing, and load unit control.

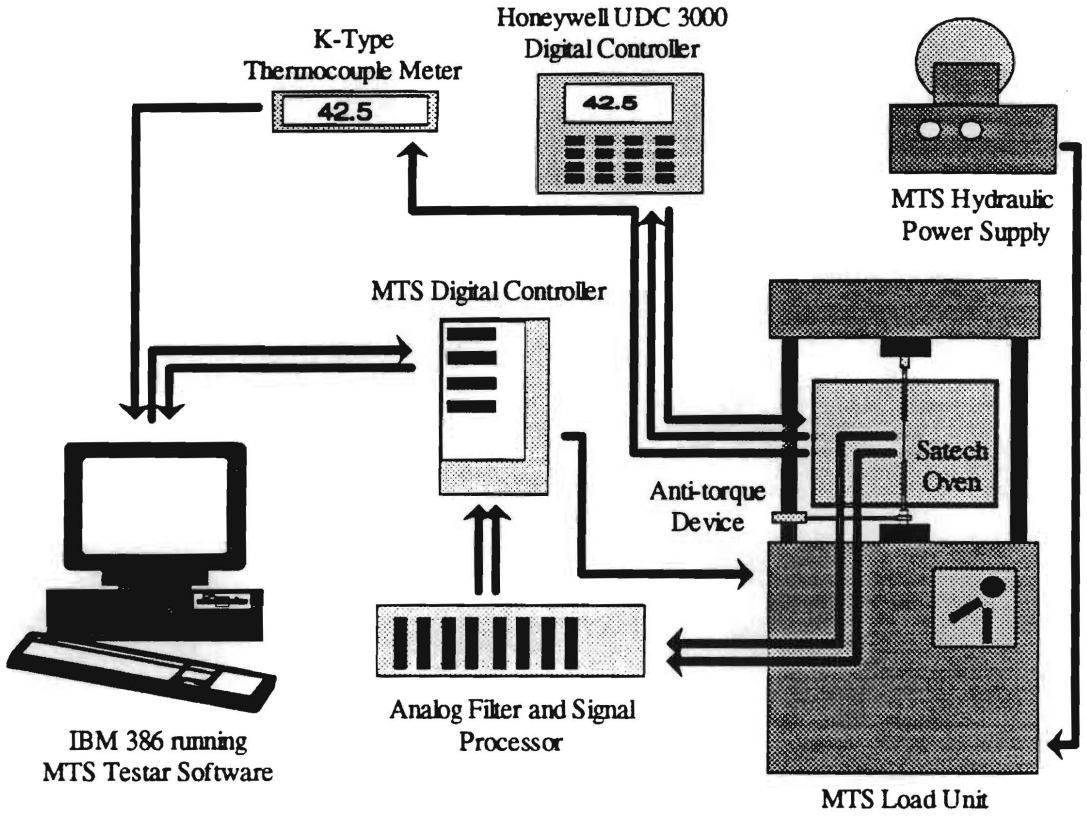

Figure 3.1 Hardware Setup for Automation of Properties Testing

Temperature control involved both the Honeywell Universal Digital Controller (UDC) and the K-type thermocouple meter, as well as the Testware-SX software which formed the interface with the MTS Digital Controller (The software program itself is discussed in the following section). Through commands using the Testware software, an analog signal ranging from 0 to 5 volts was sent from the MTS Digital Controller to the UDC. The UDC was fitted with an input card which allows for remote set point operation. With this card, the UDC interpreted the input signal as a set point for the

process variable, which for this project was the temperature of the oven. The input signal to set point conversion was based upon an internal scaling parameter. For the testing done for this project, a 0 to 5 volt input signal represented a 0 to 400°C set point for the oven temperature. The K-type thermocouple meter provided temperature feedback to the MTS Digital Controller which is monitored by the Testware software. The feedback was in the form of a 1 to 5 volt analog signal, which was then converted to Celsius degrees by a similar mechanism as described for the UDC.

The signal processing portion of the system included both the analog filter and the MTS Digital Controller. The analog filter and strain amplifier processed the signals from the strain gages prior to transfer to the MTS Digital Controller. The analog filter also provided the excitation voltage for the strain gage circuit.

The final subsystem handled load control and included the MTS Load Unit , MTS Digital controller and the Testware software. The user created software sent commands to the MTS Digital Controller which interpreted these commands and performed the necessary servo valve control commands to move the actuator as defined by the user's program. The load cell of the MTS Load Unit sent signals to the MTS Digital Controller which then calculated the current force on the specimen. To assure uniaxial stress on the test specimen, an anti-torque device was designed and mounted onto the main actuator of the MTS Load Unit. All desired data was recorded in a data file by the Testware software.

Test Software Description

Testware-SX is an application of the MTS Testar software package. Testware-SX allows the user to create property testing procedures through the use of an interactive window environment. These tests are broken up into *steps*, which in turn are made up of

processes. The types of processes available are[24]:

- Command:

  Cyclic Command

  Hold Command

  Monotonic Command
- Data Collection:
- Event Detectors:
- External Control:

The *Command* processes control the servo valve of the load unit using a closed loop control system, allowing for cyclic or monotonic load control as well as hold commands which maintain loads for a prescribed duration. *Data collection* commands store data from input channels to user defined files. *Event Detectors* provide the user greater control over tests by either responding to test conditions or by triggering other processes. *External Control* commands allow the user to output signals to devices which are external to the control loop, such as the Honeywell Digital Controller shown in figure 3.1. A sample test program is illustrated in figure 3.2. More detailed programs are discussed later in the chapter for specific types of tests (e.g. CTE, Modulus, etc.).

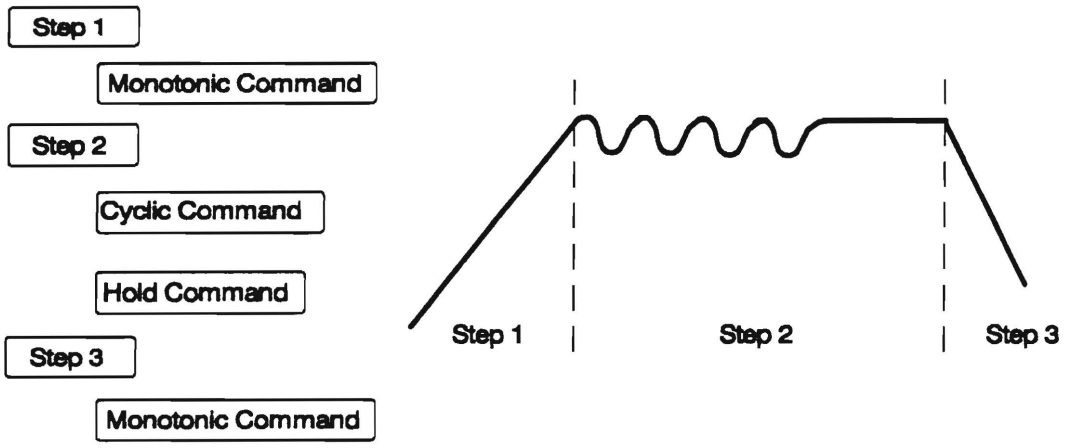

Figure 3.2 Sample program for Testware-SX application

Verification of System Accuracy

To evaluate the system performance, the coefficient of thermal expansion was measured for an aluminum specimen. The published value for the CTE for aluminum is 23.9E-6 in/in/C [19]. Curve fitting data points measured by the testing system produced the line shown in figure 3.3. The following equation gives change in strain based upon the CTE.

$$\Delta T\alpha = \Delta\varepsilon \qquad (3.1)$$

where: α = thermal expansion coefficient

$\Delta\varepsilon$ = change in strain

ΔT = change in temperature

Rearranging the equation gives:

$$\alpha = \frac{\Delta\varepsilon}{\Delta T} \qquad (3.2)$$

From equation 3.2 it can be seen that the coefficient of thermal expansion is the slope of the line shown in figure 3.3, which is 23.8E-6 in/in/C. This measurement compares favorably with the published value.

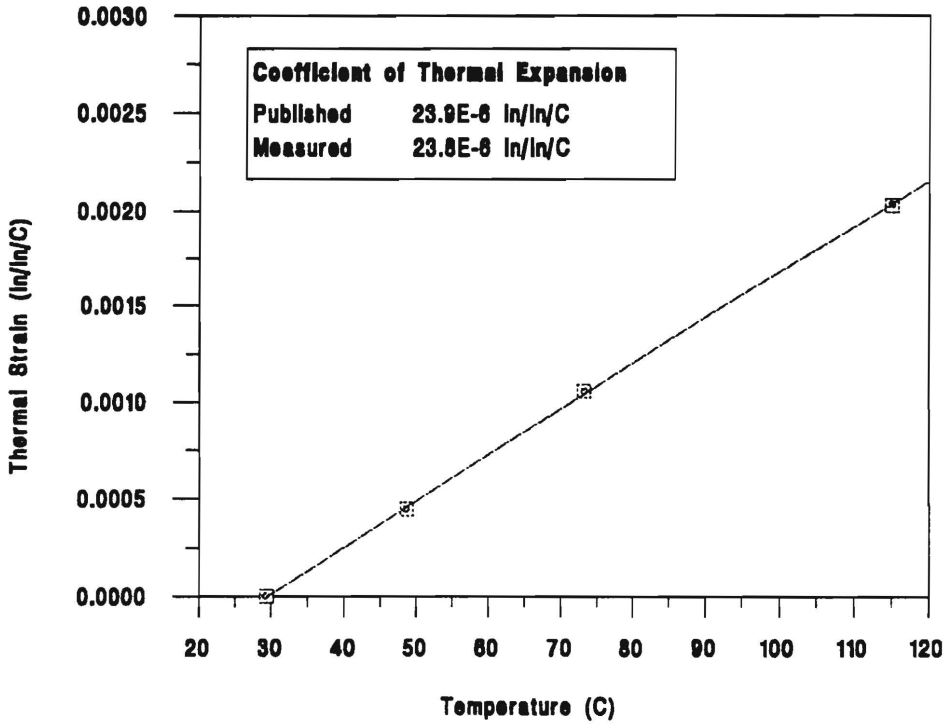

Figure 3.3 Thermal Strain vs. Temperature for Aluminum

Operating Procedure

Coupon Specifications

The test specimen geometry was determined based upon the ASTM standard test method for fiber-resin composites [20]. For the 0/90° ply fiber orientation, the specimen's recommended width and gage length were 1 and 5 inches respectively (See figure 3.4).

The gripping mechanism initially presented a problem during specimen loading. The edges of the grip 'teeth' cut through the thin specimen, causing failure at the grip with relatively low loads. To correct the problem, several tests were performed with varying torque applied to grip screws, to determine what torque is sufficient to prevent slipping without causing grip failure.

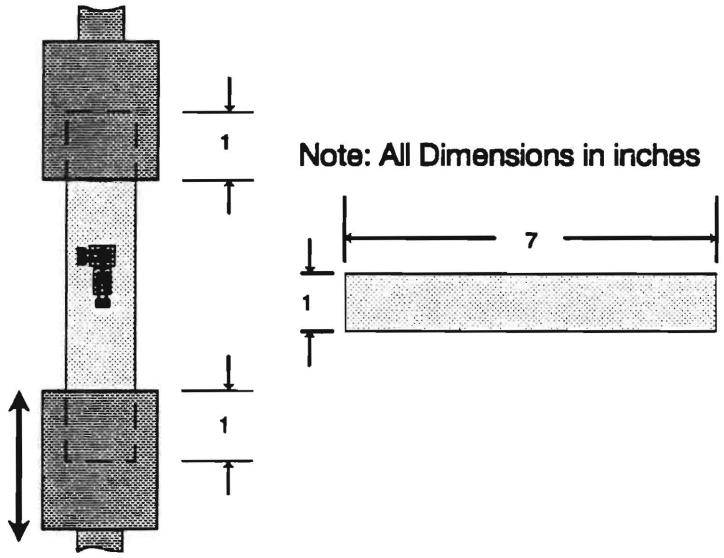

Figure 3.4 Coupon specification and grip configuration

CTE Measurement

The common method for measuring the thermal coefficient of expansion is to utilize a half-bridge circuit configuration (See chapter 2 for details), incorporating a material with a known CTE in one quarter of the bridge. For our system, titanium silicate was chosen because of its extremely low CTE value, approximately 0.05E-6 in/in/C° [15]. The half-bridge configuration provides a simple method for removal of thermal output effects. The thermal output of the gage can be expressed in terms of two factors: 1) Resistivity change of the gage grid alloy with temperature 2) Mechanical strain due to

difference in thermal expansions of the gage alloy and test material. Due to the fact that the half bridge configuration was used, two sources of thermal output existed. The first was thermal output of the gage with respect to the specimen or test material (Denoted by G/S), the second was the thermal output of the gage with respect to the reference material (Denoted by G/R). The thermal output with of the gage with respect to the specimen is written as [15]:

$$\varepsilon_{T/O(G/S)} = \frac{[\beta_G + (\alpha_S - \alpha_G)F_G]\Delta T}{F_I} \qquad (3.3)$$

where: $\varepsilon_{T/O(G/S)}$ = thermal output for grid alloy G on specimen material S

β_G = thermal coefficient of resistivity of grid material

$\alpha_S - \alpha_G$ = difference in thermal expansion coefficients between specimen and grid ` respectively

F_G = gage factor for strain gage

ΔT = temperature change from arbitrary initial reference temperature

The indicated strain due to a resistance change in the gage is:

$$\varepsilon_i = \frac{\Delta R / R}{F_I} \qquad (3.4)$$

where: F_I = instrument gage factor

$\frac{\Delta R}{R}$ = unit resistance change

The thermal output can then be expressed in strain units as follows:

$$\varepsilon_{T/O(G/S)} = \frac{[\beta_G + (\alpha_S - \alpha_G) F_G]\Delta T}{F_I} \qquad (3.5)$$

If the instrument gage factor is set equal to that of the strain gage, then equation (3.5) becomes:

$$\varepsilon_{T/O(G/S)} = [\frac{\beta_G}{F_G} + (\alpha_S - \alpha_G)]\Delta T \qquad (3.6)$$

The above equation can be rewritten for an identical type gage mounted on the reference material which is in the adjacent arm of the bridge and represents the thermal output of the gage with respect to the reference material. The equation becomes:

$$\varepsilon_{T/O(G/R)} = [\frac{\beta_G}{F_G} + (\alpha_R - \alpha_G)]\Delta T \qquad (3.7)$$

In equation 3.7, R denotes the reference material with a known CTE. Subtracting equation 3.7 from 3.6 and rearranging gives:

$$\alpha_S - \alpha_R = \frac{(\varepsilon_{T/O(G/S)} - \varepsilon_{T/O(G/R)})}{\Delta T} \qquad (3.8)$$

With equation 3.8, the procedure for calculating the CTE of the test material (α_S) becomes a simple task. The indicated strain from the system, represented by the numerator on the right hand side of equation 3.8, was plotted versus temperature. The slope of this plot represents the difference in CTEs of the specimen and reference material. The CTE of the reference material was then added to this value to produce the actual CTE for the test specimen.

The Testware-SX software test program used in CTE measurement contains a series of loops corresponding to the different temperatures for which strain data is taken. These loops represent the *steps* discussed earlier in this chapter. The first process for each step was the setting of the oven temperature through the use of the External command. The Honeywell Digital Controller was fitted with an input card which allowed for remote set point control of the process variable, which for this case was oven temperature. The input card accepted a +1-5 VDC signal, which was scaled according to controller configuration. For the current project, the range represented 0-400°C.

The next process was an Event Detector Command which triggered the data acquisition process discussed next. The process detected when the input temperature from the K-type thermocouple meter reached the remote set point temperature. The input temperature was taken from a thermocouple attached to the titanium silicate specimen (Material used as reference in half-bridge configuration) to assure that both the reference material and the test specimen were at the same temperature. Because of titanium silicate's low thermal conductivity, it was assumed to be the controlling factor in determining when to take strain data.

The Data Acquisition process recorded the values from user specified input channels. The channels used in CTE testing were temperature and the strains in both the transverse and longitudinal directions. A series of twenty readings were recorded for each

temperature, with the average value used in CTE calculation. Subsequent readings were appended to the bottom of the data file. A loop of the CTE test program is illustrated in figure 3.5.

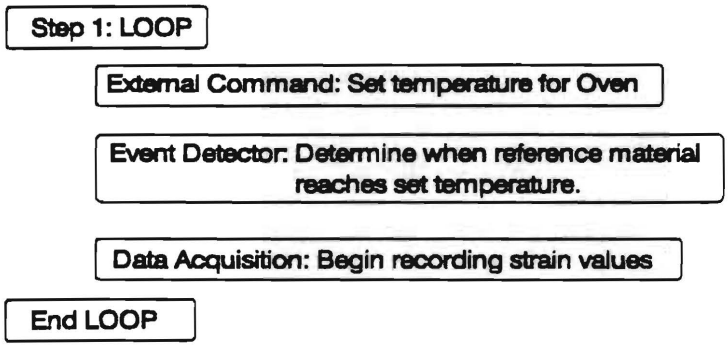

Figure 3.5 Representative loop of CTE test program

Limitations

One of the limitations of the CTE test process was the use of the reference material in the half bridge. Titanium silicate has an extremely low coefficient of thermal expansion which greatly increased the time steps between subsequent strain data readings. The effects due to prolonged exposure to temperatures above the glass transition temperature of the composite material merits further investigation, but was not within the scope of this research project.

Moduli (E_x, E_y), Poisson's ratios(ν_{xy}, ν_{yx})

The strain gage configuration for modulus testing was similar to that for CTE measurement discussed previously; however, the reference material used in the half-bridge configuration was replaced with a 'dummy' gage mounted on a coupon approximately identical to the test specimen. During a stress test at elevated temperatures, two effects contribute to specimen strain. The first is strain due to the applied load, the second is that

of strain due to thermal expansion with change in temperature. Incorporation of the dummy gage aids in eliminating thermal expansion effects from the strain readings of the test specimen [22].

Test procedures were based upon the ASTM standard test method for fiber-resin composites, designation D3039-76 [20]. Based upon this standard, the speed of testing for the prepreg was approximately 0.3 in/min. The speed of testing for copper was not as critical, so a value of 0.1 in./minute was chosen. The speed of testing for both copper and prepreg were set by constant cross-head speed. In accordance with ASTM test standards, the elastic modulus was calculated using the following equation [20]:

$$E = \frac{\Delta P/\Delta l}{l/bd} \qquad (3.9)$$

where: E = modulus of elasticity, MPa or psi

$\Delta P/\Delta l$ = slope of the plot of load as a function of deformation within the linear portion of the curve

l = gage length of measuring instrument , mm or in. (0.25 in. for gage used in research)

b = width of specimen, mm or in.,

d = thickness of specimen, mm or in.

Poisson's ratio was determined experimentally by the following equation [20]:

$$\mu = -\Delta\varepsilon_{\perp}/\Delta\varepsilon_{II} \qquad (3.10)$$

where: μ = Poisson's ratio

$\Delta\varepsilon_{\perp}/\Delta\varepsilon_{II}$ = slope of strain-strain curve in the linear region, $\perp$ denotes strain perpendicular to applied load, and II denotes strain parallel to applied load

To ensure accurate strain measurements, it was vital that the specimen be mounted correctly. Referring to figure 3.4, which illustrates the grip and specimen configuration, it can be seen that one requirement was the proper alignment of the specimen in the grip system to provide uniform loading. The failure of the specimen at the grip location was a major problem due to the thickness of the specimens (0.6 to 3.5 mil range). A close up of the grip 'teeth' is shown in figure 3.6.

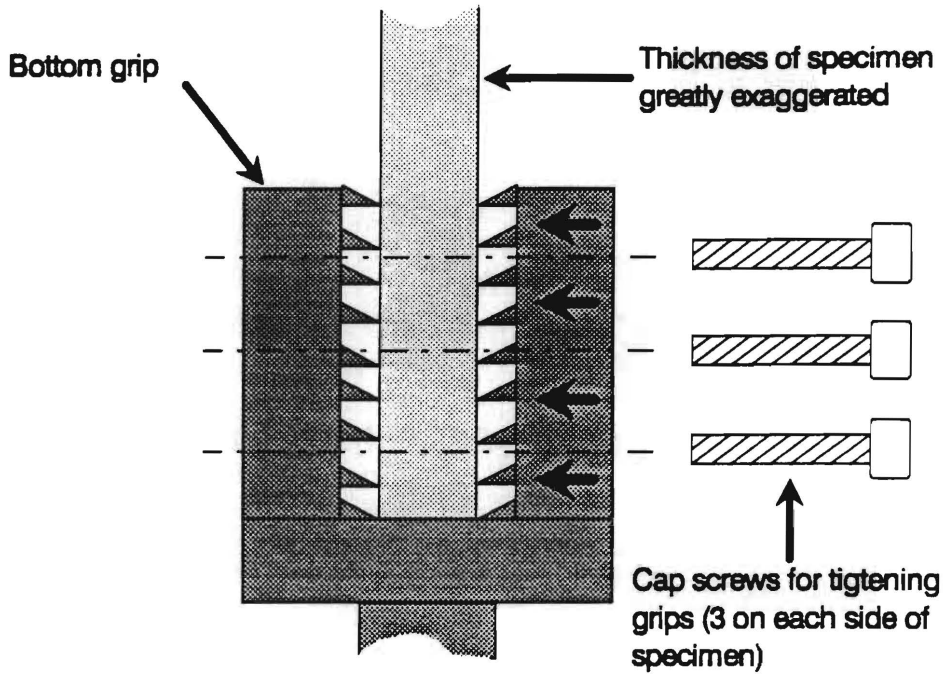

Figure 3.6 Close up of lower grip

Through trial and error, standard methods were developed for specimen mounting. For the case of the prepreg specimen, the grip screws shown in figure 3.6 were tightened using a beam type torque wrench with range of 100 lbf-in to a final torque of 5 lbf-in. With this torque, specimen slippage did not occur and grip failure was greatly reduced.

Copper foil specimens required slightly different preparation. With the 0.6 mil thickness of 0.5 oz. copper foil, the grip teeth cut through the specimen even with the lowest available torque use. To remedy this, small samples of prepreg were adhered to either side of the copper specimens using the same bonding procedure used for gage mounting. Figure 3.7 illustrates the configuration.

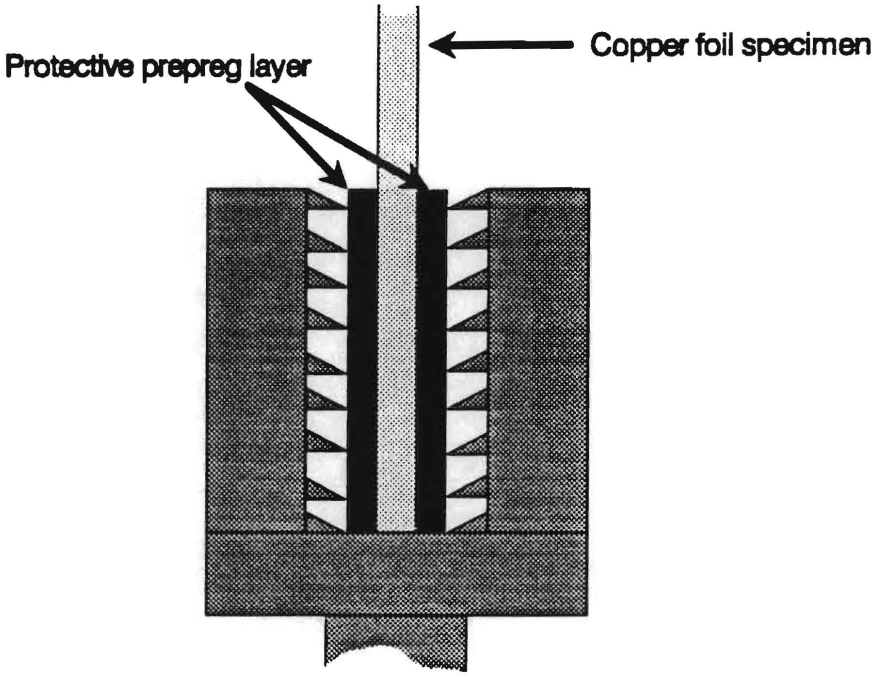

Figure 3.7 Grip configuration used for copper foil specimens

Several trial tests were performed at varying torque levels for the grip screws to eliminate slippage without producing grip failure. After a trial and error process, a torque of 30 lbf-in was determined to be sufficient.

Once the specimen was prepared and mounted, testing began. Unlike CTE measurements discussed earlier, the measurement of moduli and Poisson's ratio required load conditions. Therefore the Testware procedure also had to be modified. The main addition was the inclusion of control commands for the MTS load unit. To accomplish this, several new *steps* and *processes* were created.

Much like the CTE testing program, the modulus program contained several loops corresponding to the different temperature levels. The program began by initializing external control devices and querying the user for system readiness, utilizing a subset of the event detector process discussed earlier known as operator event detector. This

detector manifested itself in the form of a push button dialog box in Testware's window environment. The operator event detector asked the user if the Honeywell temperature controller is ready for remote set point operation, allowing for external control of oven temperature by the Testware software. If it was not ready, the user simply changed to remote set point operation by pressing the mode selection button on the Honeywell temperature controller, and then continued. Once the operator clicked the mouse on the 'ready' button, the program ran automatically until the test was completed.

Once initialization was complete, the actual testing process began. The test itself was a repetition of a combination of two *steps*. The first set the oven temperature and waited until the desired level was reached. The second was a servo-valve control loop which loaded and unloaded the specimen between an upper and lower limit load value. The upper load values for each type of test specimen are shown in table 3.1 The lower load value for all test materials was 5 lbf.

The first step contained two processes, 1) an external control command , 2) an event detector. The external control command set the oven temperature using the Honeywell controller. The event detector monitored the oven temperature measured by the K-type thermocouple meter, signaling the end of the first *step* when the temperature matched that of the set point. The second step was a loop command that contained five processes. The first was a monotonic command that used length control to increase the load on the specimen (See table 3.1 for maximum load values for each specimen).

Material	Maximum Load (lbf)
Copper 1.0 oz.	25
Copper 0.5 oz.	15
Prepreg, (Ex and Ey)	20
Prepreg, (Off-axis testing)	20

Table 3.1 Maximum Loads used for modulus testing for each type of specimen

The second process was an event detector which monitored the force channel of the system. The detector was triggered when the measured load exceeded the upper limit as specified by the tester. The completion of this maximum force detector then triggered the next process which also was a monotonic command process. However, this process decreased length at a specified rate, thus reducing the load on the test specimen. This process continued until another event detector was triggered when a minimum force or load was encountered. This value was set to 5 lbf. for all tests done for this project. The final process was a data collection command which was active during the execution of the four previous processes. This command stored data from the length channel, the force channel, and both strain channels (Transverse and longitudinal), in a data file which was stored in an optional Excel format allowing for later processing using the commercial spreadsheet. A representation of the two step combination is shown in figure 3.8. The loop shown in figure 3.8 was repeated two times for each temperature level, to allow for averaging.

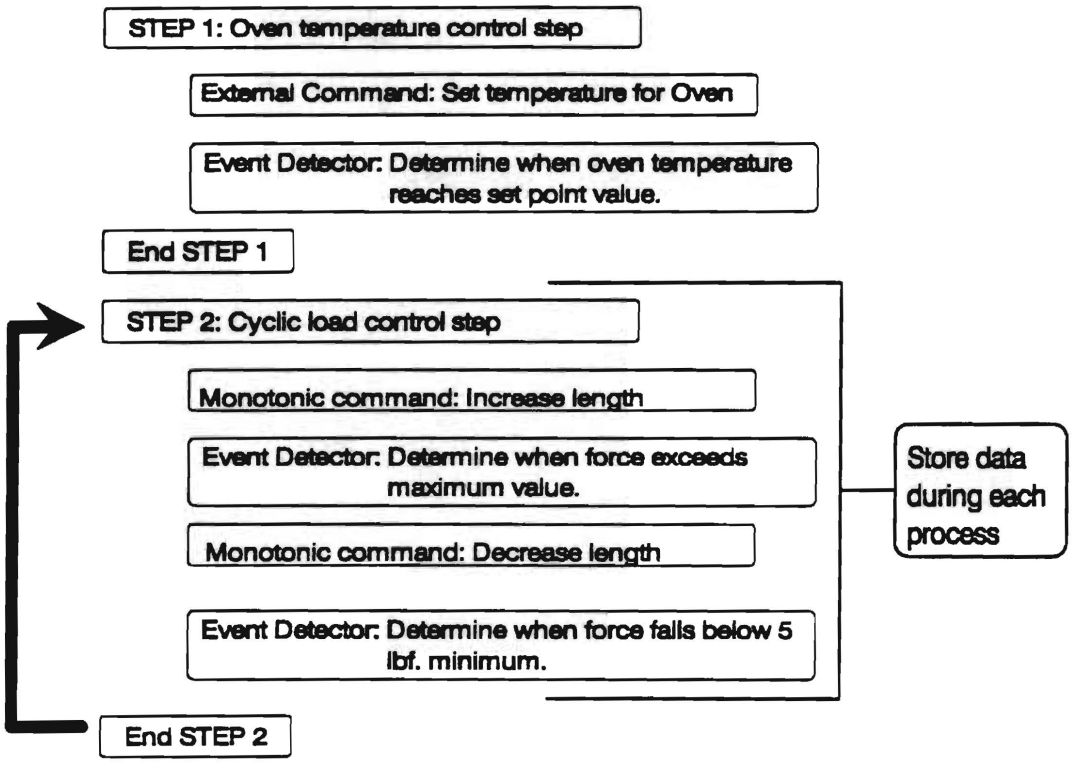

Figure 3.8 Representation of commands repeated for each temperature level for modulus testing.

The next phase of the properties testing process involved calculating the various mechanical properties based upon the strain and load values stored in the data file created by the Testware program and the physical geometry of the specimen. This process was both time consuming and tedious, requiring relatively large amounts of disk space for data storage. The Excel commercial spreadsheet was used to calculate moduli from stored data. The data was then plotted using Cricket Graph commercial software. Moduli testing results for the various materials are given in chapter 4 of this paper.

Shear Modulus (G_{xy})

Traditional shear modulus tests for isotropic materials are not applicable in the case of unidirectional composites due to the shear-coupling effect as a result of matrix-fiber interaction [3,10,4]. Instead, the off-axis coupon test is used to determine the shear modulus G_{12}. The actual specimen lay-up along with strain gage orientation is shown in figure 3.9. The lines in the figure represent the warp direction of the prepreg test specimens, which are woven fiber composites. However, the following analysis is also applicable to woven fiber composites [3].

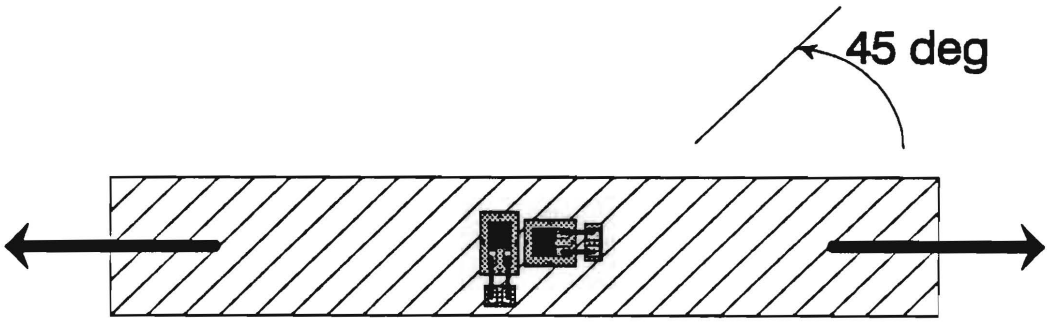

Figure 3.9 Specimen for 45° off-axis coupon test to determine shear modulus

The stresses in the 1 and 2 directions (see figure 3.10 for axes description) can be written as [3]:

$$\sigma_1 = \sigma_x \cos^2\theta$$

$$\sigma_2 = \sigma_x \sin^2\theta \qquad (3.11)$$

$$\tau_{12} = \sigma_x \sin\theta\cos\theta$$

The strains in the 1 and 2 directions (longitudinal and transverse direction or material axis system) are related to the strains in the x and y directions by the following relations:

$$\varepsilon_1 = \cos\theta(\cos\theta - \sin\theta)\varepsilon_x + \sin\theta(\sin\theta - \cos\theta)\varepsilon_y + 2\sin\theta\cos\theta\varepsilon_{45}$$

$$\varepsilon_2 = \sin\theta(\cos\theta + \sin\theta)\varepsilon_x + \cos\theta(\sin\theta + \cos\theta)\varepsilon_y - 2\sin\theta\cos\theta\varepsilon_{45} \qquad (3.12)$$

$$\gamma_{12} = -(\cos^2\theta + 2\cos\theta\sin\theta - \sin^2\theta)\varepsilon_x - (\cos^2\theta - 2\sin\theta\cos\theta - \sin^2\theta)\varepsilon_y + 2(\cos^2\theta - \sin^2\theta)\varepsilon_{45}$$

By measuring the strains ε_x , ε_y , andε_{45} with a three-element strain gage configuration, equation 3.12 allows for the calculation of strains in both the fiber and matrix direction, as well as the shear strain in the material axis system. The off-axis coupon tests conducted as part of this research project used specimens with θ = 45°, which allow the shear stress and strain equations to be rewritten as:

$$\tau_{12} = \frac{1}{2}\sigma_x \qquad (3.13)$$

$$\gamma_{12} = \varepsilon_y - \varepsilon_x \qquad (3.14)$$

It can be shown that by combining equations 3.13 and 3.14 and then using the stress-strain relations the following result can be found.

$$G_{12} = \frac{E_x}{2(1+\nu_{xy})} \qquad (3.15)$$

Equation 3.15 was used to determine the shear modulus of the woven fiber composite prepreg. The equation shows that the two gage configuration illustrated in figure 3.9 is sufficient for determining the shear modulus when the off-axis angle is 45°.

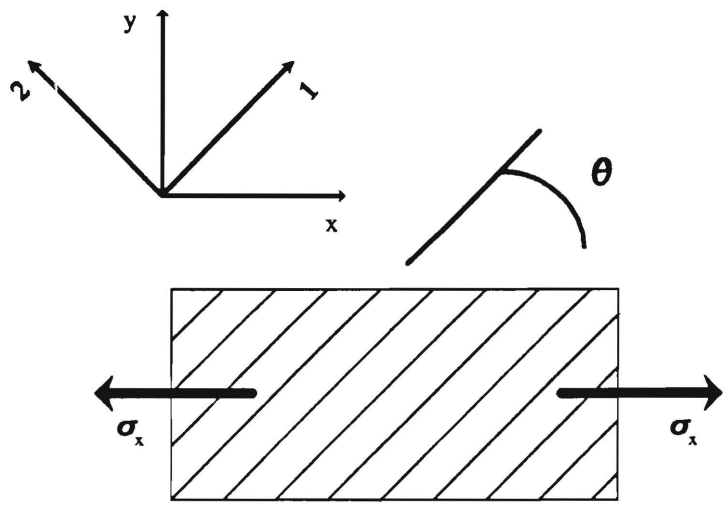

Figure 3.10 Diagram of off-axis coupon test with axes-system and notation

The Testware-SX program for shear modulus testing was similar to the test discussed in the previous section for E_x. The only difference between the two tests was the configuration of the test specimen for the case of prepreg.

Chapter Conclusion

The current system setup allowed the user to perform properties testing with some amount of initial system calibration. Prior to testing, the analog signal processor was tuned to maintain zero offset for the initial strain signal. Data was then be read directly without modification for offset, however; it was not necessary for accuracy of results. Future improvements include the addition of strain modules for the MTS Digital Controller. The modules would perform initial system calibration (Including shunt calibration of the bridge) as well as signal processing, thus eliminating the need for the analog signal processor. Once the modules are in place, the user only has to prepare the specimen and then press a button.

An additional benefit of the strain modules would be the ability for strain control, which is generally used in properties testing. At the time of testing , the strain modules were not available, and length control was used instead.

Perhaps the greatest improvement in the performance of the automated testing system would come from the incorporation of a laser extensometer. The extensometer would eliminate the extensive amount of time required for mounting of strain gages on the specimens, up to 2 hours per lot. The use of the extensometer would also decrease the amount of error due to gage mounting as well as gage variability. Though the first time cost of the extensometer is large (approximately $50,000), over time it will pay for itself by ending the need for strain gages which are not reusable. For this project, EA-13-250AE-350 open face foil strain gages are used costing about $37.00 for a pack of five gages. For the test conducted for this research alone, the gage cost totaled more than $500.

CHAPTER IV

PROPERTY DATA

As stated in the introduction of the thesis, the main objectives of this research was the determination of the temperature dependent thermo-mechanical properties of the printed wiring board's constituent materials, as well as the automation of said process. The following chapter details the experimental results of the properties testing for the PWB's core materials: prepreg, 1.0 oz. copper foil, and 0.5 oz copper foil. The chapter is divided into two sections, the first containing test data for prepreg, the second for copper, both 1.0 and 0.5 oz. styles. Included in the sections is a comparison with related temperature dependent test data found in the literature. Located on each graph of material properties is information indicating both material data from the literature, as well as the values measured in the course of the research. The measured values are given at the first data point temperature level (Between 25°C and 30°C) to allow comparison with published data, which is given for room temperature. Values for the first data points range between 25°C and 30°C due to the fact that after the completion of one test, the oven must be allowed to cool before another test can begin. For some tests, the oven did not completely cool to room temperature.

Data Preparation

All experimental data originated from the MTS Testar system, in particular, the Testware SX application program . Strain measurements were stored in data files using an Excel spreadsheet format, allowing for later manipulation by the Excel software package.

For each material property, a series of tests were conducted, with the average value used to create the plots which follow. CTE calculations used the average of five tests, while all other property plots were based upon the average of three tests. In addition to the average data points, error bars are also shown for each data point. These error bars indicate the *estimated standard error* of the test samples. This estimated standard error is included to indicate the relative level of dispersion for the data points obtained for the 3/5 different trials at each temperature level. The method of calculating the error follows[11]. First, the sample variance was determined by the following equation:

$$s^2 = \frac{\sum_{i=1}^{n} x_i^2 - \left(\sum_{i=1}^{n} x_i^2\right)^2 \Big/ n}{n-1} \qquad (4.1)$$

where: s^2 = sample variance

x_i = sample measurement

n = number of samples

From the sample variance, the sample standard deviation was calculated by simply taking the positive square root. The sample variance calculation was used in place of the

standard variance calculation due to the relatively low number of samples (n=3 for most tests). The estimated standard error was then calculated from the sample standard deviation (s) and the number of samples using the following equation:

$$e = \frac{s}{\sqrt{n}} \qquad (4.2)$$

where: e = estimated standard error

Prepreg Property Data

The material properties tested for the prepreg included CTE, Young's moduli, shear modulus, and Poisson's ratio. The prepreg material tested is a woven fiberglass/epoxy composite with a fiber count of 60 in the warp direction, and 47 in the fill direction (See appendix E for manufacturer information). Because the prepreg is a fiberglass/epoxy composite with orthotropic properties, Young's modulus is shown for both warp and fill directions. Warp direction is labeled the 'X' direction, with fill corresponding to the 'Y' direction. Figures 4.1-4.6 illustrate how material properties varied with temperature over an approximate range of 25°C to 170°C.

CTE Testing Data for Prepreg

Each of the data points shown in figures 4.1 and 4.2 are the average of five tests of thermal strain versus temperature. The slopes of the plots represent the coefficients of thermal expansion (See chapter 3 for equation derivation) for both warp and fill directions. As seen in the figures, the CTE for prepreg in the warp and fill direction was 20.1E-6 in/in/C° and 21.7E-6 in/in/C° respectively. The error bars indicate that sample variance was very small for CTE data measurement in both warp and fill directions. The measured values of CTE were in the mid-range of published values.

Moduli and Poisson's Ratio Testing Data for Prepreg

The review of related literature produced a paper by Haque et. al. [8] in which temperature and moisture dependent properties testing was conducted on kevlar-graphite/epoxy composite laminates. In conclusion, the investigators found that over the temperature range of 25-150°C, Young's modulus decreased while Poisson's ratio increased for dry specimens. These results are similar to the results of testing done for the current paper. As seen in figures 4.3 and 4.4, Young's moduli decreased with temperature, while figure 4.6 shows how Poisson's ratio increased. Figure 4.7 indicates the percent change in the material properties for prepreg over the test temperature range. The figure shows the greatest percent change in Poisson's ratio, which increased by approximately 106%. The percent change in Young's modulus was greater in the fill direction than in the warp direction, with values of 33% and 20% respectively. This is to be expected due to the fact that the fiber count was higher in the warp direction (See appendix E for manufacturer information for prepreg). The shear modulus increased by 76%. Table 4.1 indicates both published values and measured values for the material properties of prepreg.

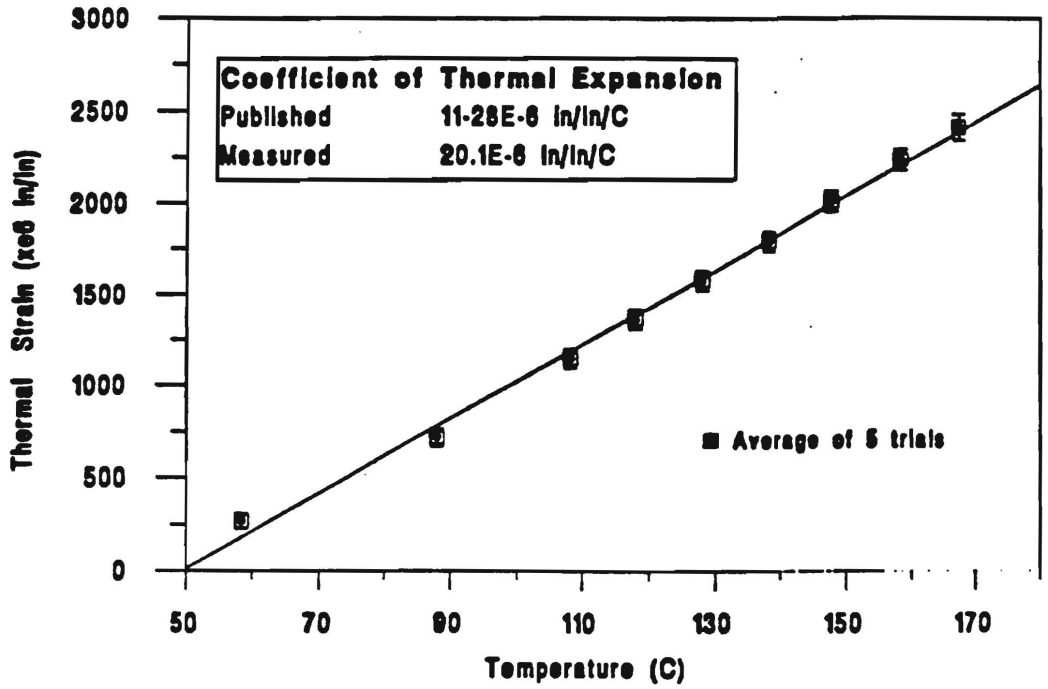

Figure 4.1 Thermal strain vs. temperature for prepreg in warp direction

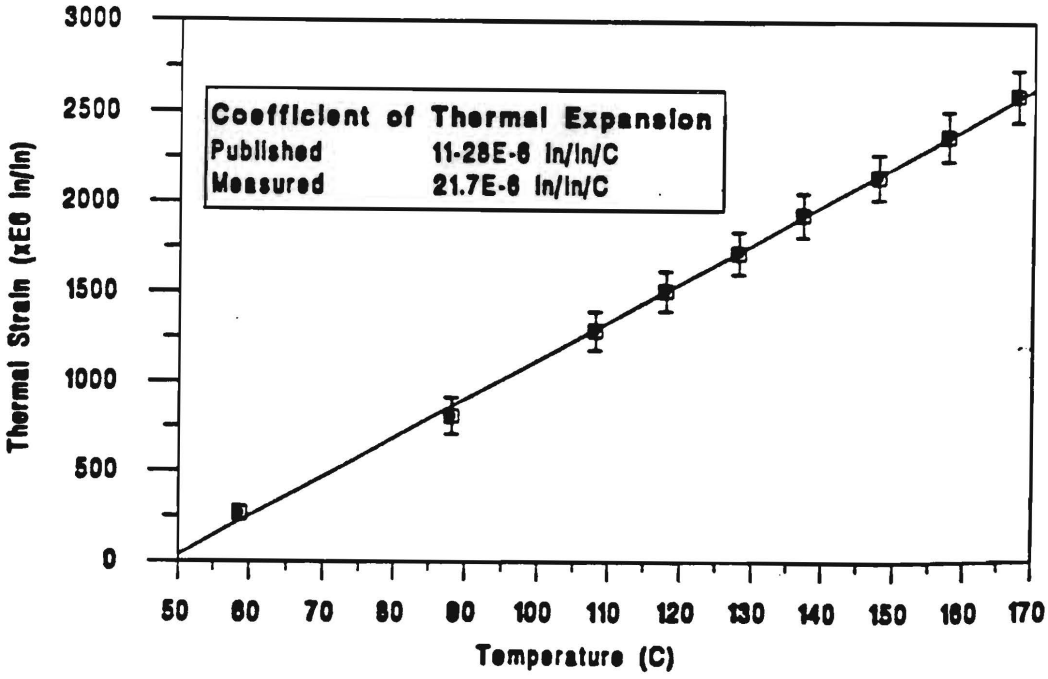

Figure 4.2 Thermal strain vs. temperature for prepreg in fill direction

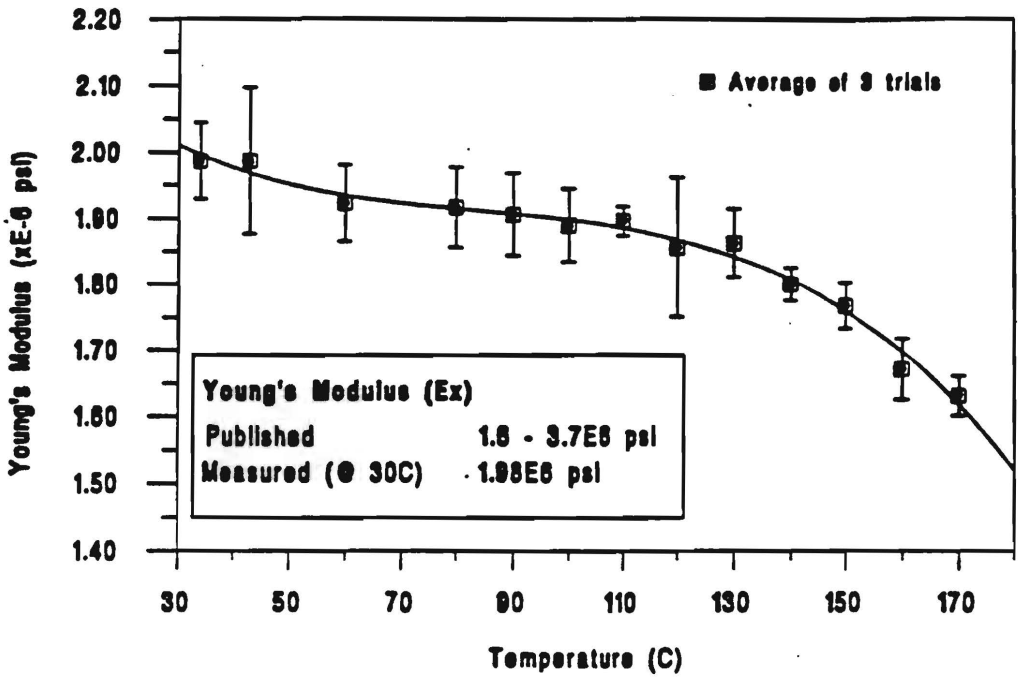

Figure 4.3 Young's Modulus vs. temperature for prepreg in warp direction

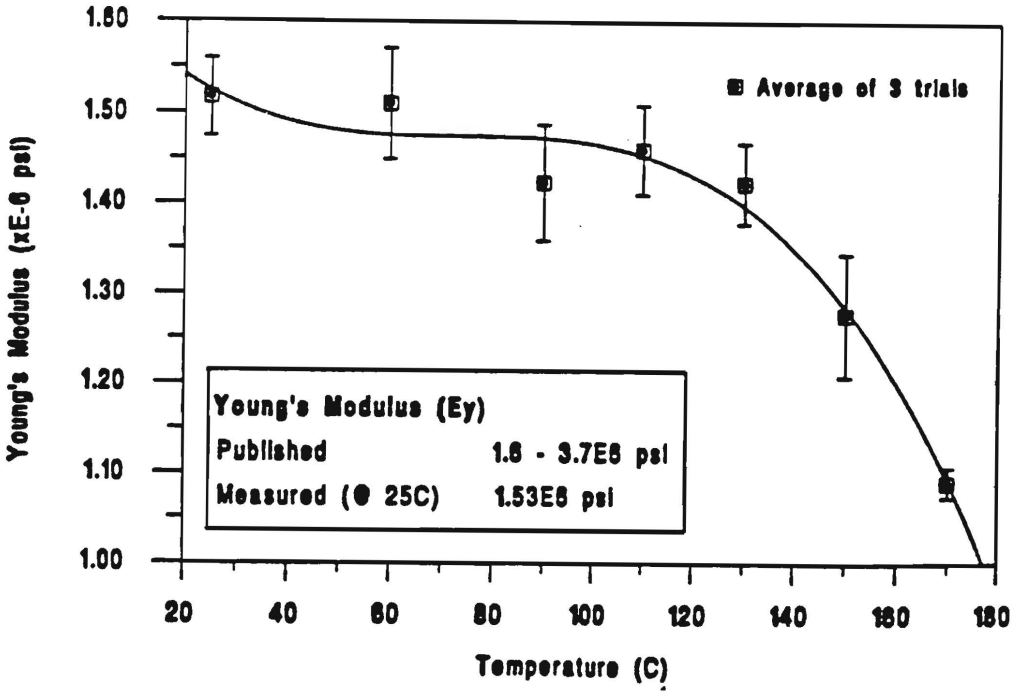

Figure 4.4 Young's Modulus vs. temperature for prepreg in fill direction

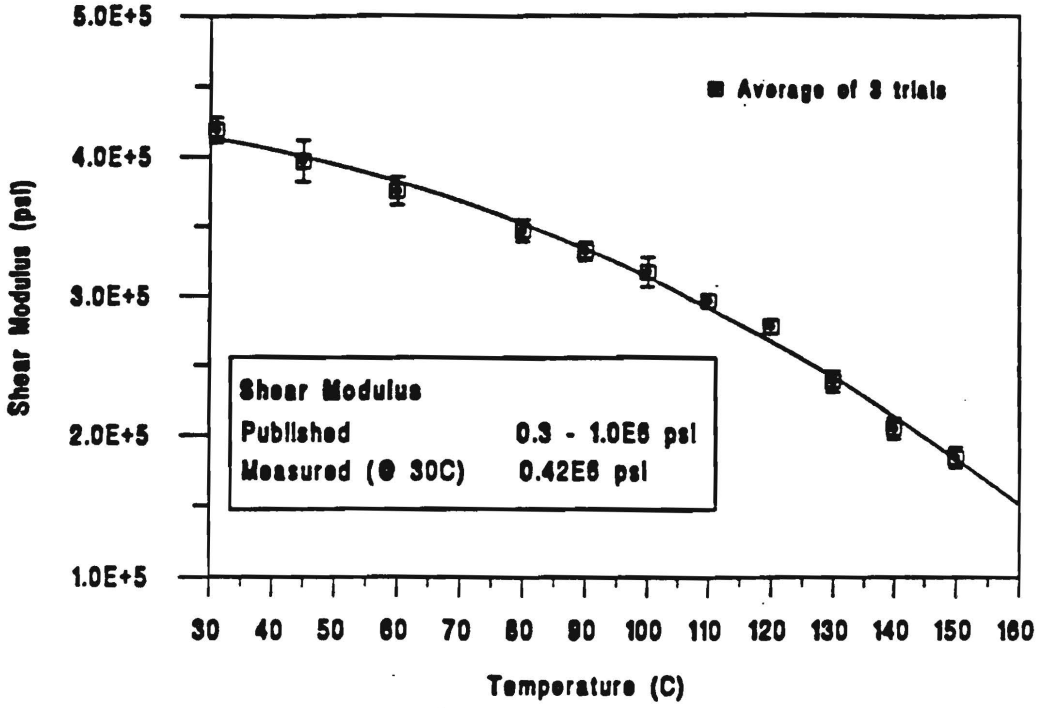

Figure 4.5 Shear modulus vs. temperature for prepreg

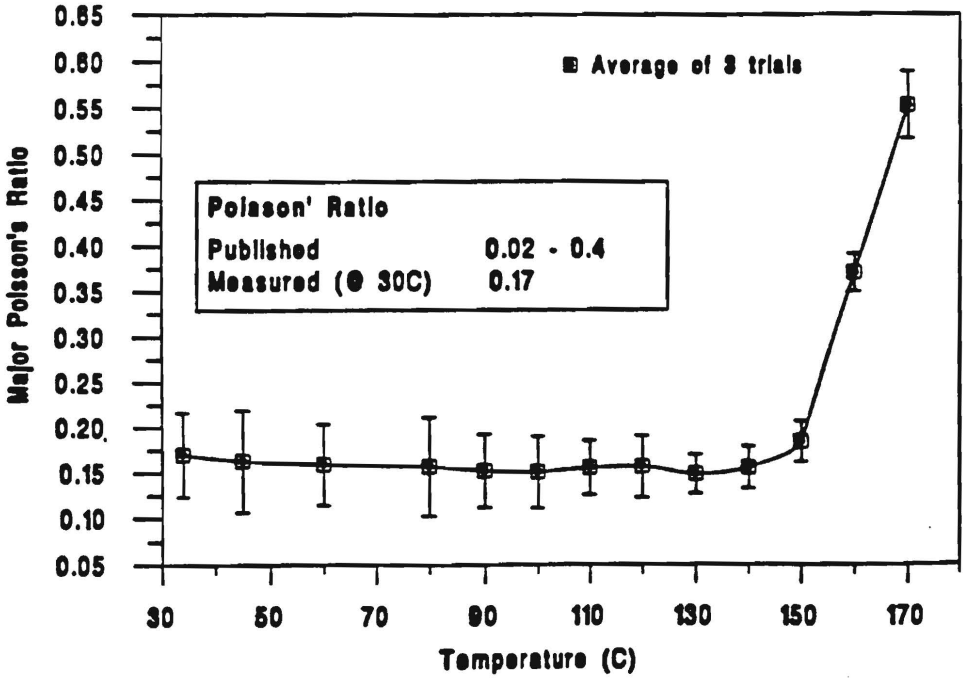

Figure 4.6 Major Poisson's Ratio vs. temperature for prepreg

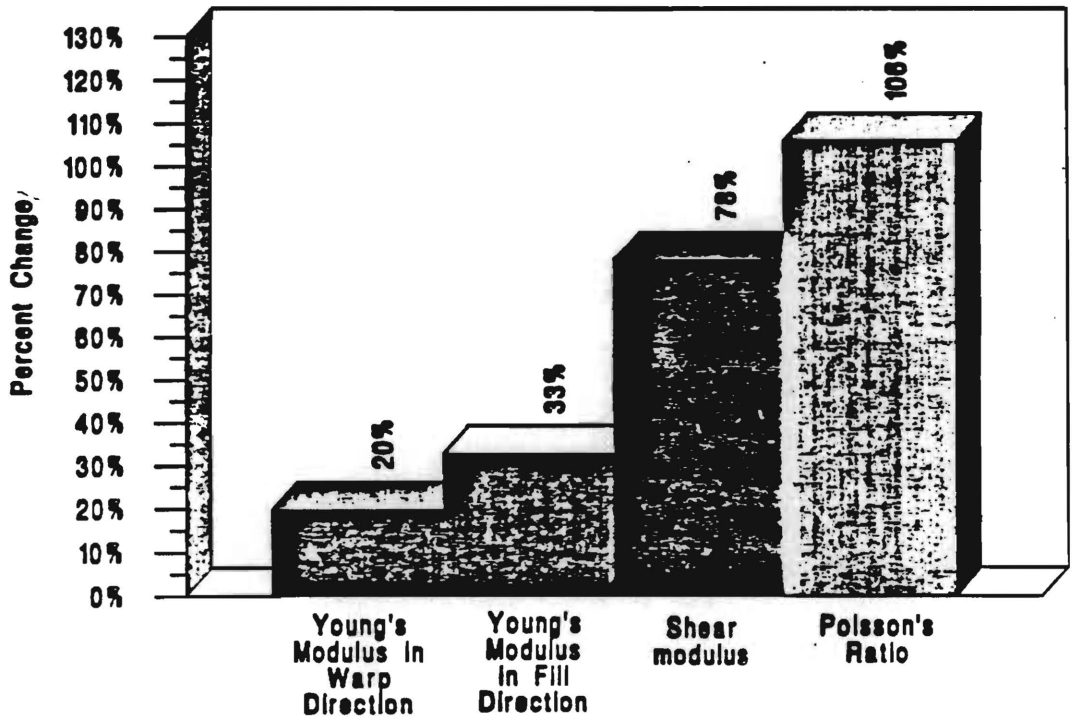

Figure 4.7 Percent change in material property over test temperature range for prepreg

Material	Property	Published (25°C)	Measured(25-30°C)
Prepreg	Ex (psi)	1.6-3.7E6	1.98E6
	Ey	1.6-3.7E6	1.53E6
	Gxy (psi)	0.3-1.0E6	0.42E6
	vxy	0.02-0.04	0.17
	αx (in/in/C°)	11-28E-6	20.1E-6
	αy (in/in/C°)	11-28E-6	21.7E-6

Table 4.1 Published and measured properties for prepreg

Copper Foil Property Data

The properties tested for 1.0 and 0.5 oz. Copper foil include CTE, Young's and shear modulus, and Poisson's ratio. As is the case for prepreg, three samples were tested for each tensile property, and 5 samples for CTE, with the average value shown in the following figures.

CTE Testing Data for Copper

The average measured coefficient of thermal expansion for 1.0 oz. copper foil (thickness approximately 0.0012 inches) was 20.4E-6 in/in/C°, as shown in figure 4.9. The measured value is slightly greater than the upper bound of published data, which ranges from 15 to 20E-6 in/in/C°. The average CTE for 0.5 oz. copper foil (Thickness approximately 0.0006 inches) was 17.7E-6 in/in/C° (see figure 4.14), which is approximately in the mid range of published data. The error bars indicate relatively little

dispersion of data points for each temperature level, increasing the confidence in measurement values.

Moduli and Poisson's Ratio Testing Data for Copper

In reviewing the literature, temperature dependent properties testing has previously been conducted on several samples of copper and copper-base alloys by a joint ASTM-ASME committee [25]. The results of the investigation for the annealed 0.07 mm copper specimen are duplicated here for comparative purposes. The specimens for the current paper differ from the aforementioned investigation in that current specimens were produced through an electro-depostion process, and ranged in thickness from 1.2 to 0.6 mils as compared to approximately 18 mils for the ASTM project. However, similarities are seen in property behavior.

Figure 4.8 shows a plot of Young's modulus versus temperature for the ASTM study. The plot shows a decrease in modulus as temperature increases. The same general trend is found in modulus testing for copper foil specimens for the current project, of which 1.0 oz. copper foil is first discussed. Figure 4.10 shows a decrease in Young's modulus as temperature increases over the test range. The measured value of Young's modulus at 30°C, 14.8E-6 in/in/C°, lies in the mid range of published values of 12-17.9E-6 in/in/C°. Shear modulus also decreased over the test range (see figure 4.11), while Poisson's ratio increased (see figure 4.12). The measured value of shear modulus at 30°C is 5.7E6 psi, while the published value for copper is 5.6E6 psi. The measured value of Poisson's ratio at 25°C and published values are 0.35 and 0.3-0.35 respectively. The estimated sample error for Young's modulus and shear modulus show moderate sample dispersion, while Poisson's ratio is somewhat larger than both. While noise effects were moderate for each channel of strain measurement for the test system, the combination of

the effects as required by the computation of Poisson's ratio, probably magnified the effects of signal noise, increasing sample variance, and thus the estimated sample error. Several methods of decreasing noise effects are discussed in the conclusions of the chapter. Figure 4.13 illustrated the total percent change over the test temperature range for 1.0 oz. copper foil. Young's modulus decreased by 43%, while Poisson's ratio increased by 31%. The largest change is seen in the shear modulus, which decreases by approximately 52%.

The trend seen in the behavior of material properties with temperature for 1.0 oz. copper foil was also found in the copper 05. oz copper foil specimens. Young's modulus decreased as temperature increased, as did the shear modulus, as shown in figures 4.15

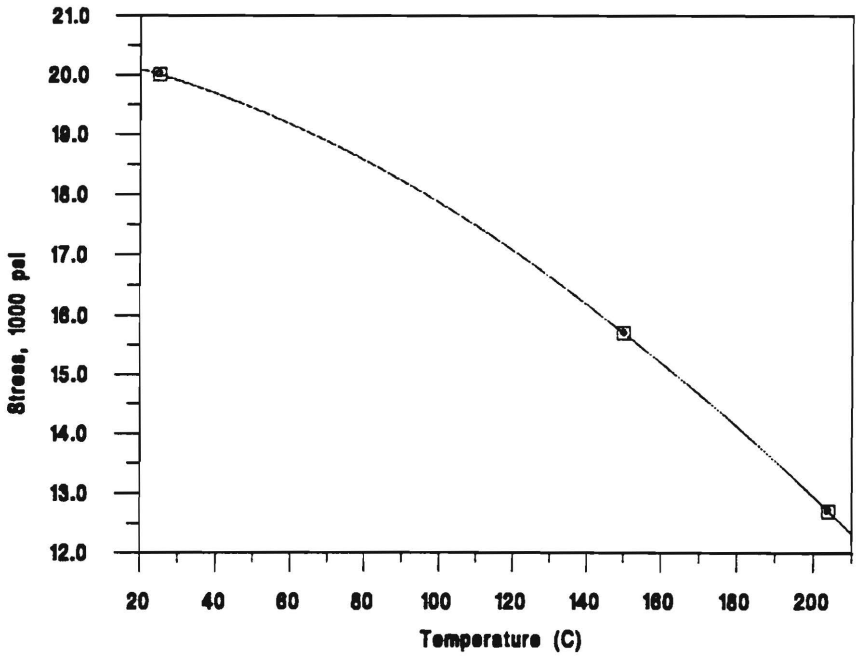

Figure 4.8 ASTM-ASME joint committee study on elevated temperature properties for annealed copper [25].

and 4.16. However, Poisson's ratio appeared to remain constant, with error bars indicating fairly large sample variance for several data points (see figure 4.17). The author refers the reader to the noise effects alluded to previously in the chapter. These effects were even more pronounced for the 0.5 oz. specimens due to the fact that the maximum load during testing was lower than that for 1.0 oz. copper, thus decreasing strain measurement resolution. Again, proposed solutions are discussed in the chapter conclusion. Table 4.2 compares published values of material properties at room temperature with measured values at approximately the same temperature.

The total percent change for 0.5 oz. copper foil material properties over the test temperature range is shown in figure 4.18. Young's modulus and shear modulus decreased by 39% and 32% respectively, while Poisson's ratio shows just a 4 % drop.

Material	Property	Published (25°C)	Measured(25-30°C)
Copper, 1.0 oz.	Ex (psi)	12-17.3E6	14.8E6
	Gxy (psi)	5.6E6	5.7E6
	vxy	0.3-0.35	0.35
	αx (in/in/C°)	15-20E-6	20.4E-6
Copper, 0.5 oz.	Ex (psi)	12-17.3E6	17.8E6
	Gxy (psi)	5.6E6	6.6E6
	vxy	0.3-0.35	0.37
	αx (in/in/C°)	15-20E-6	17.7E-6

Table 4.2 Published and measured properties for copper (1.0 and 0.5 oz. styles)

Table 4.2 indicates published values for copper at room temperature as well as measured values ranging from 25 to 30°C.

Chapter Conclusion

Tables 4.1 and 4.2 contain both measured and published values for all tests conducted for the thesis. Graphs showing the relationships between material properties and temperature over the test range of 25-170°C are presented. Each plot includes error bars representing the estimated sample error for each set of data points for the corresponding temperature level. Figure 4.7, 4.13, and 4.18 illustrate the total percent change in the material property over the test range of temperatures. The results of related research studies appear to correspond well with current research results, increasing the authors confidence in experimental data.

The results for Poisson's ratio for 0.5 oz. copper may be improved by changing the load cell on the MTS Load Unit. For the current project, a 5000 lbf. load cell was used. The maximum load placed on the 0.5 oz. copper specimen was 15 lbf. (see table 3.1), which is approximately 0.3% of the load cells range. However, with a smaller load cell, such as 500 lbf., load data resolution would increase. As a result, more accurate load measurements could be made, producing more accurate property calculations.

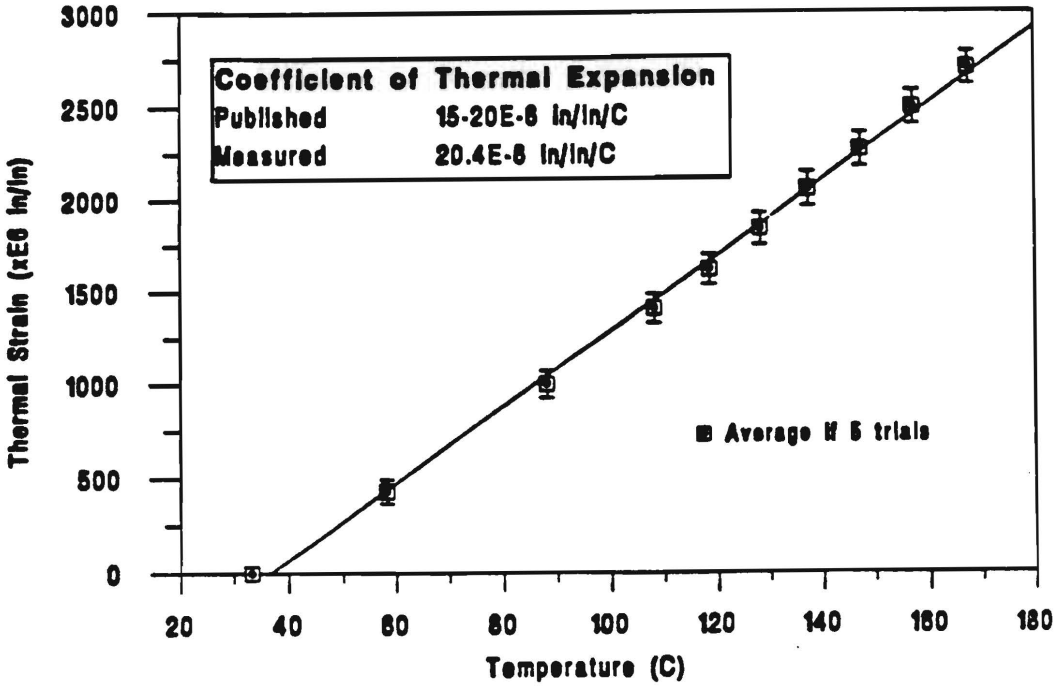

Figure 4.9 Thermal Strain vs. temperature for 1.0 oz. copper foil

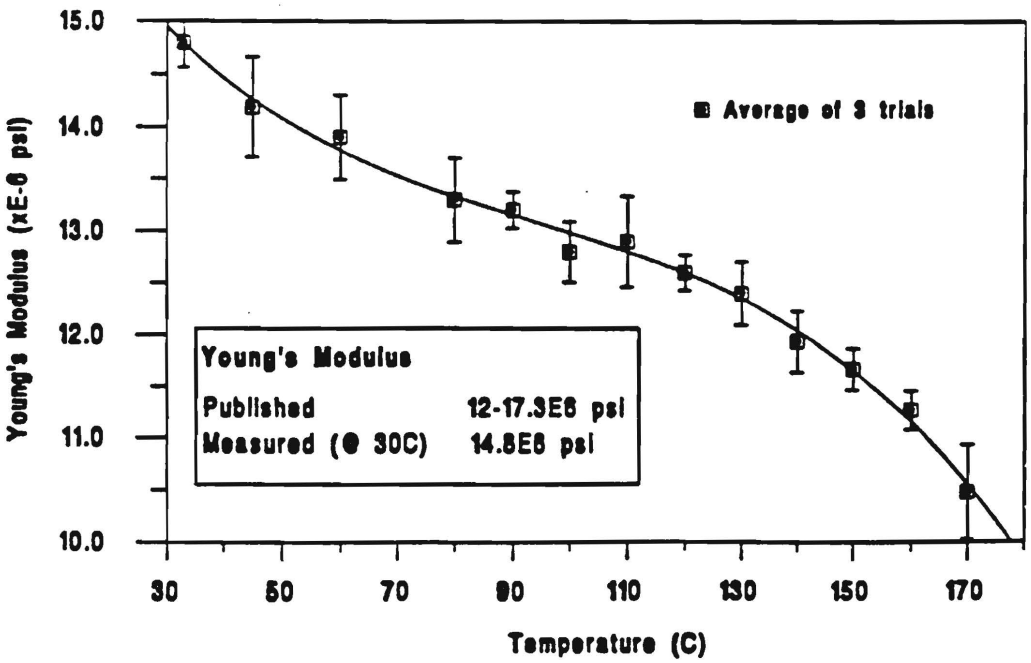

Figure 4.10 Young's Modulus vs. temperature for 1.0 oz. copper foil

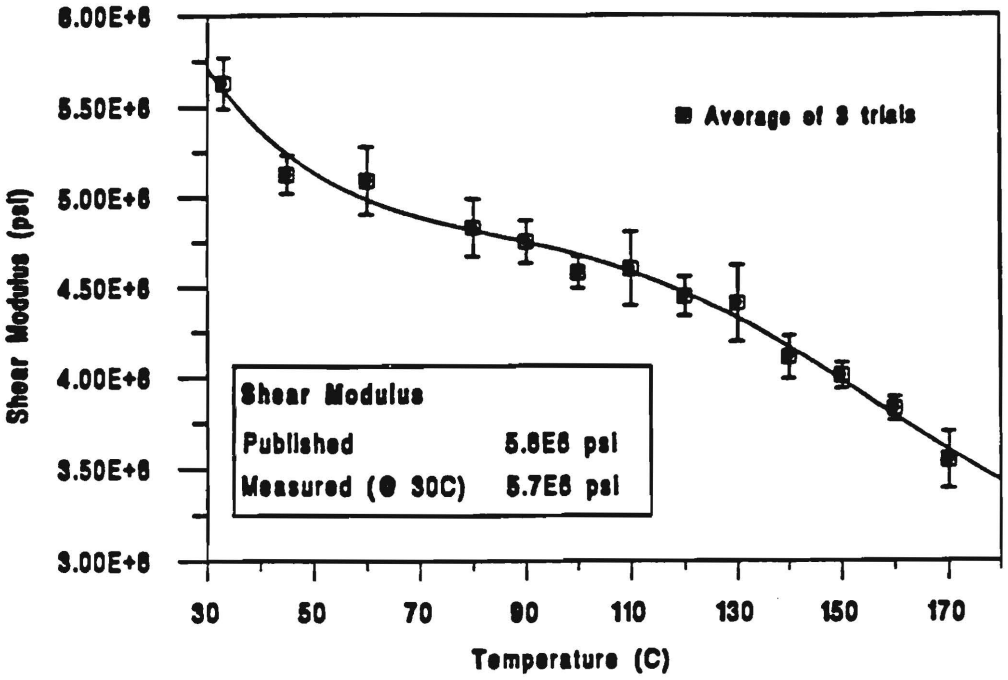

Figure 4.11 Shear Modulus vs. temperature for 1.0 oz. copper foil

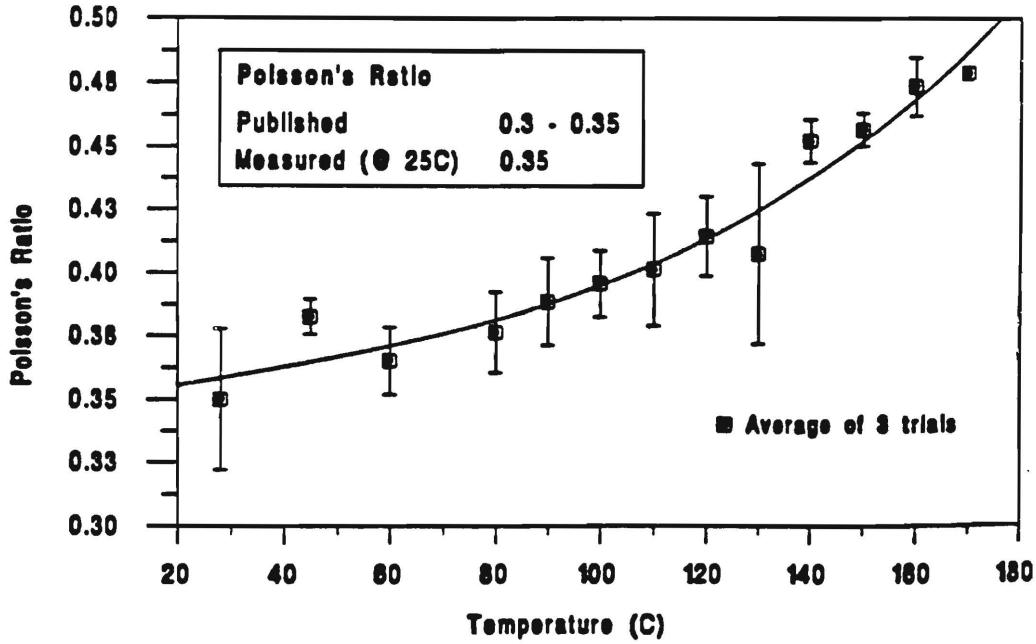

Figure 4.12 Poisson's Ratio vs. temperature for 1.0 oz. copper foil

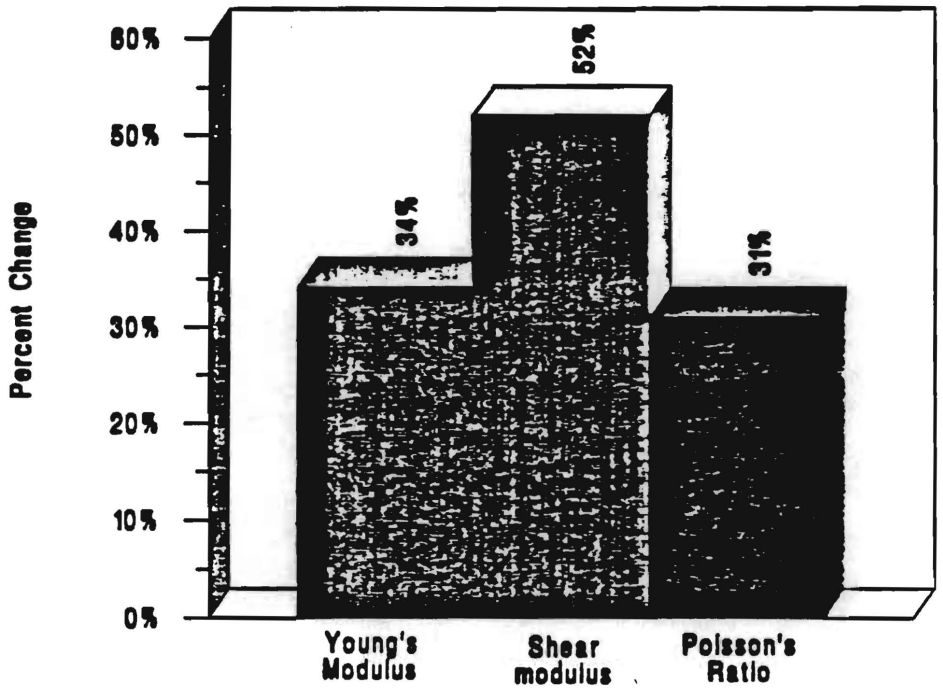

Figure 4.13 Percent change in material property over test range for 1.0 oz. copper foil

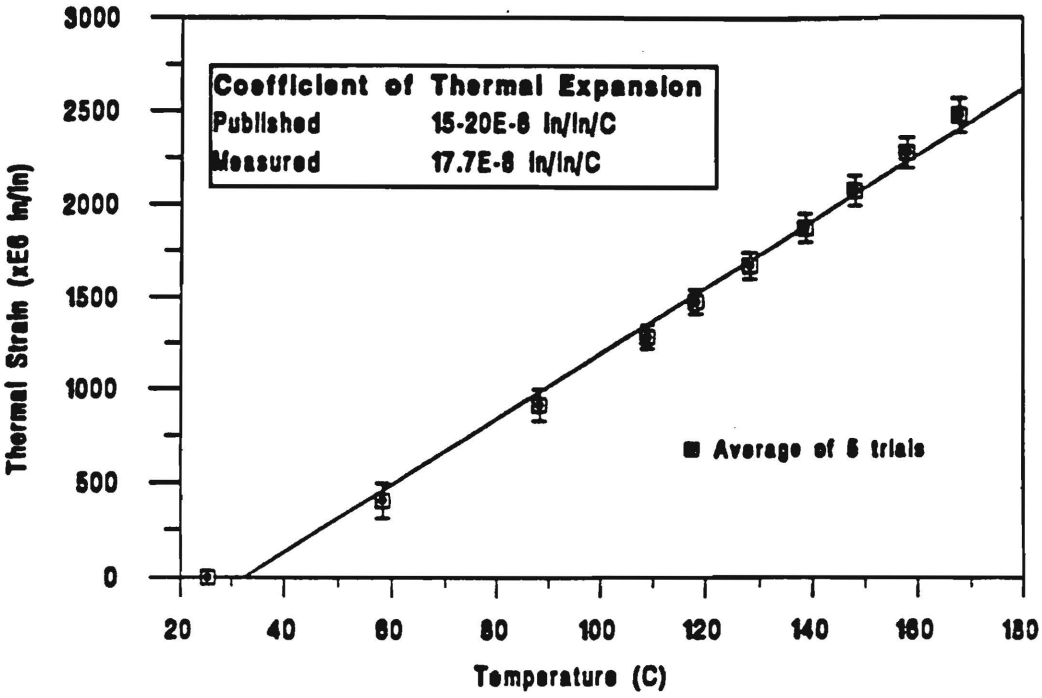

Figure 4.14 Thermal Strain vs. temperature for 0.5 oz. copper foil

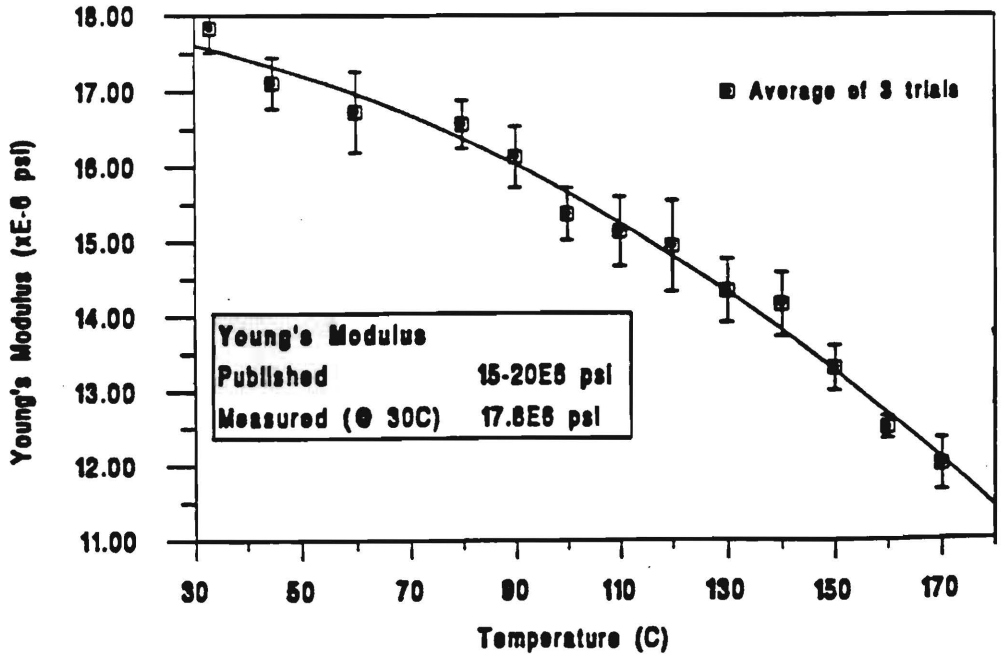

Figure 4.15 Young's Modulus vs. temperature for 0.5 oz. copper foil

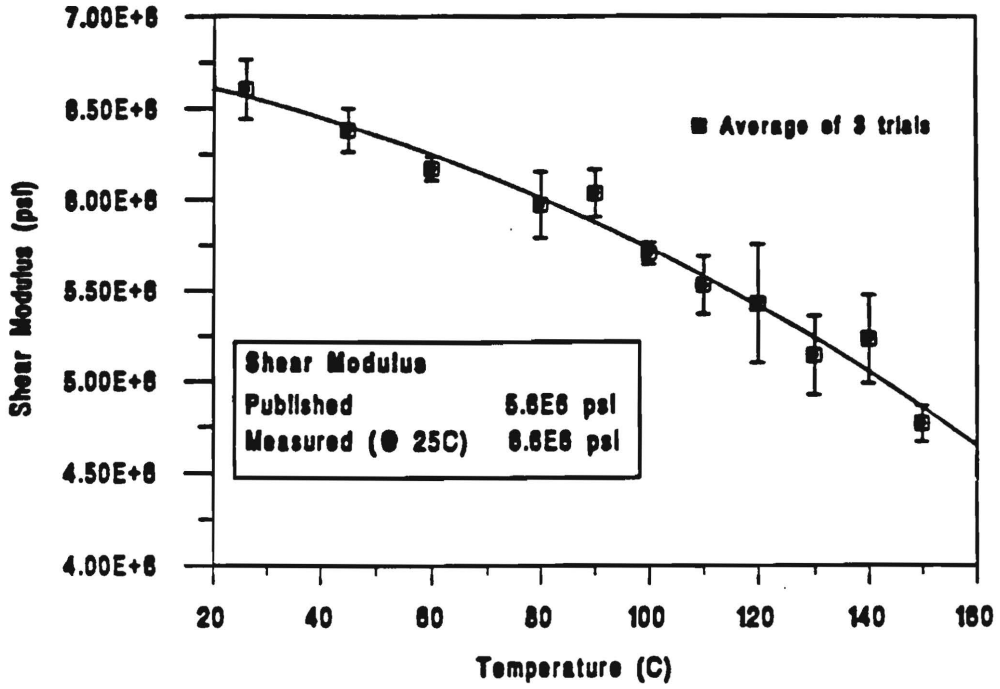

Figure 4.16 Shear Modulus vs. temperature for 0.5 oz. copper foil

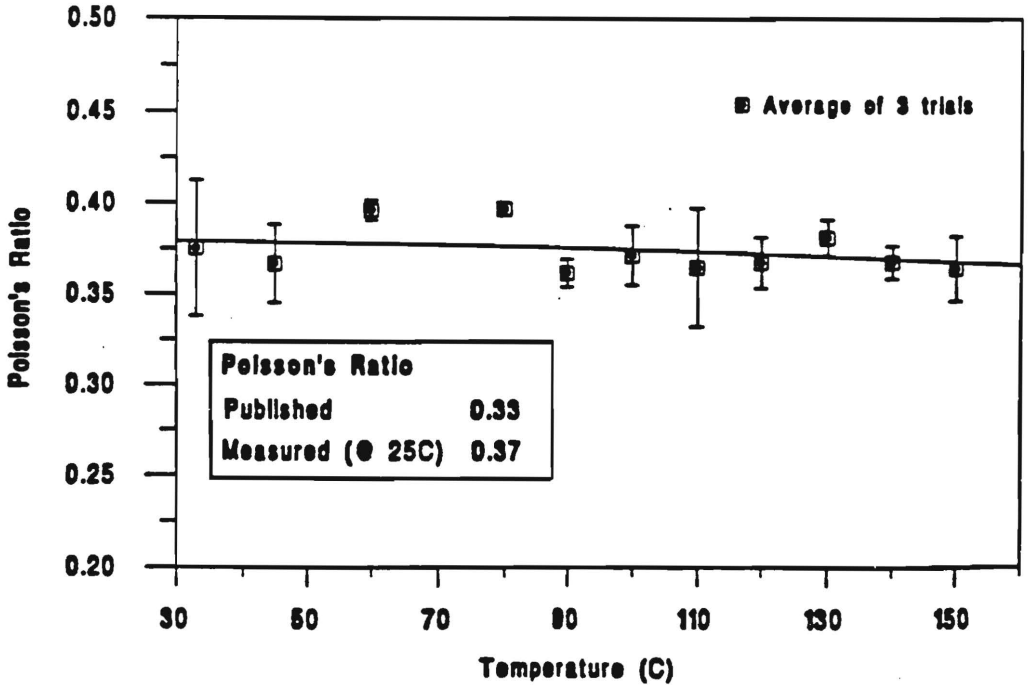

Figure 4.17 Poisson's Ratio vs. temperature for 0.5 oz. copper foil

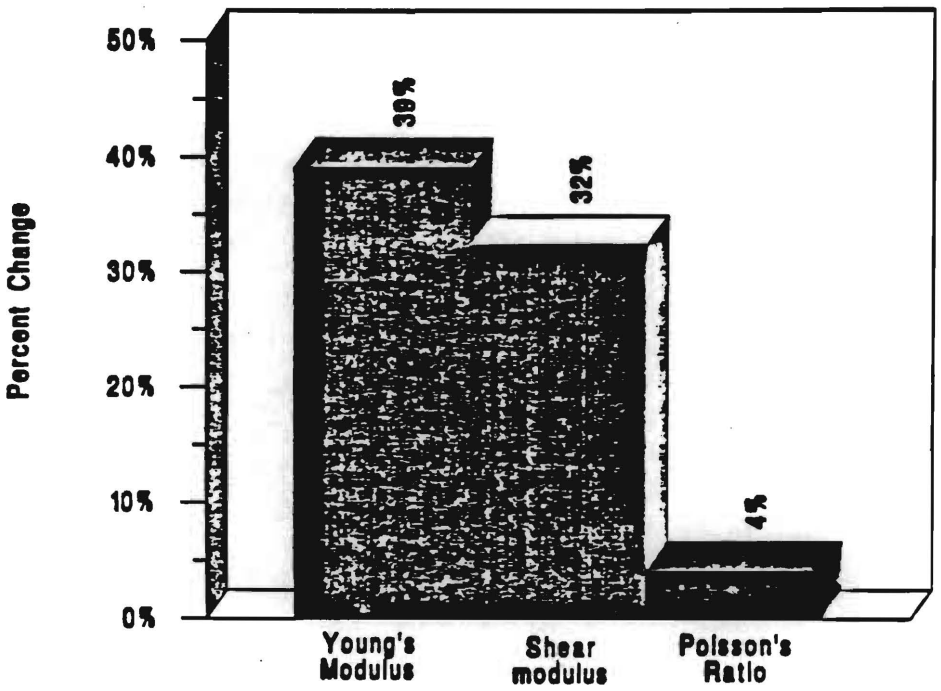

Figure 4.18 Percent change in material property over test range for 0.5 oz. copper foil

CHAPTER V

FINITE ELEMENT ANALYSIS

This chapter represents the analytical portion of the paper, as opposed to chapters 2,3,4, and 6, which are experimental in nature. The methods and results presented in this chapter form the impetus for the three previous chapters. The results of the rigorous temperature dependent properties testing detailed in chapter four are now applied to the application of predicting out-of-plane deflection of a sample printed wiring board subject to thermal loading, simulating the wave soldering process (See chapter 1 for description of wave soldering process). Analytical predictions are also made using both the maximum and minimum values of published property data for the tested materials. These values provide an upper and lower bound to demonstrate the variance in warpage prediction that can be obtained using published data.

A brief description of the sample board lay-up, or physical geometry, is first given, followed by a discussion of methods used for PWB manufacture. The discussion provides information which is key to understanding the reasoning behind assumptions made in the creation of the finite element model. In keeping with the objective of the research, i.e., automation of the entire testing/modeling process, the chapter also contains a discussion of a computer program written by the author to act as an interface between the tester and the Ansys software package. The experimental technique for measuring the sample board's warpage, Shadow Moiré, is discussed and the experimental setup is shown. Results from analytical warpage prediction are given for the following cases using: 1)

measured temperature dependent property data, 2) maximum published property data, 3) minimum published property data. Experimental warpage measurement results using the Shadow Moiré technique are shown for illustrative purposes only, to demonstrate the method by which future analytical predictions will be evaluated.

PWB Lay-up

The printed wiring board (PWB) is a *laminate*, which is defined as any material made up of multiple layers bonded together [9]. Most PWBs are composed of layers of fiberglass epoxy and copper. These *core materials* were the subject of properties testing discussed in chapter three. In this chapter, the focus will be on utilizing the previously determined thermo-mechanical properties to predict the out-of-plane warpage of the laminate. Figure 5.1 illustrates the sample PWB configuration.

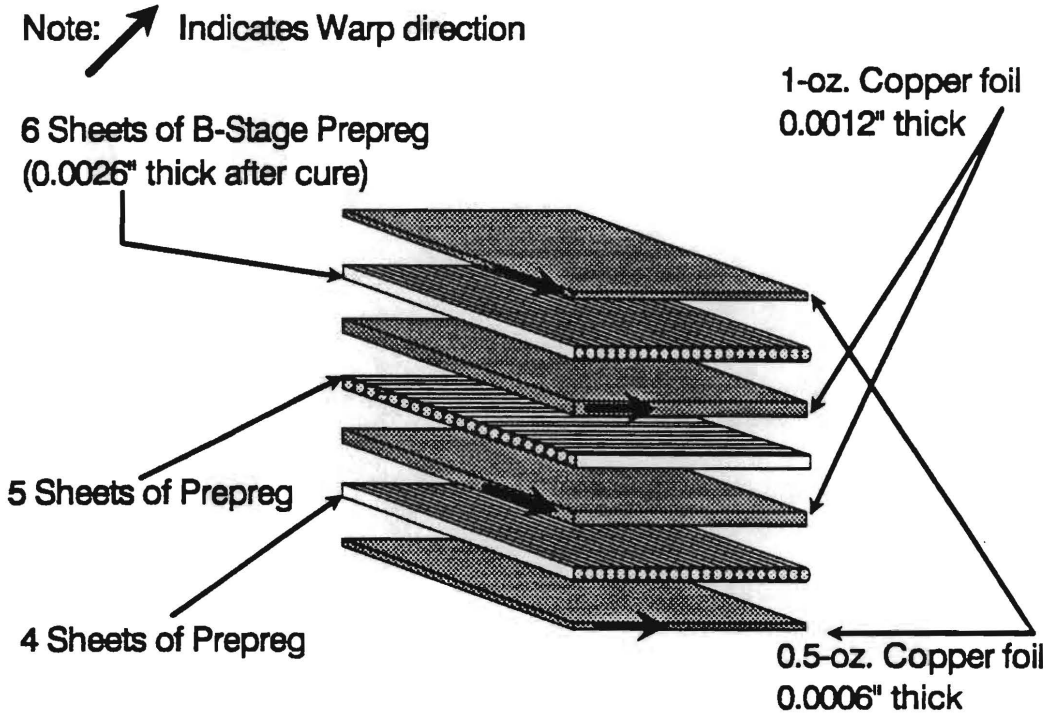

Figure 5.1 Sample PWB

PWB Manufacture

Materials

Traditional multi-layer printed wiring boards are made of conductive copper layers separated by non-conductive or dielectric layers bonded together through a heat treatment or 'baking' process.

The copper layers are chosen from standard sizes which are specified in oz/ft^2, and are typically available in 0.5, 1, 2, and 3 oz/ft^2. The layers of copper are either designated as *power* or *signal* planes. Power planes provide necessary voltages for board components, while signal planes provide the circuitry for transporting device signals. For this project, 0.5 and 1 oz/ft^2 sheets of copper foil were used in the production of the sample PWB.

The dielectric material used for this project is glass-reinforced epoxy. It is widely used due to its relatively low cost and desirable mechanical properties such as stiffness, flexibility, and dimensional stability [13]. The material is a epoxy-glass composite, comprised of woven fiberglass cloth 'impregnated' with an epoxy resin. The composite is then partially cured to what is called B-stage prepreg. This is generally the form most PWB manufacturers receive the dielectric material. The process by which the prepreg and copper foil are bonded to form the actual board is given below.

Process

Multi-layer PWBs are usually produced through a combination of three processes: 1) Imaging, 2) Chemical , and 3) Mechanical [13]. For the case of four layer (Four referring to the number of copper layers) boards such as those used in this project, the manufacturing process usually occurs in two steps. First the inner layer is produced by placing several sheets of B-stage prepreg together, then 'sandwiching' them together

between sheets of copper foil. The laminae are then placed in a hydraulic press and 'baked' or heated in an oven at approximately 135 to 150°C for 8 to 16 hours. The boards must be placed on a flat surface to prevent deformation due to their own weights because the baking temperatures are above the glass transition temperature for the prepreg, which is approximately 125°C (See appendix for lamination process for boards used in this project) . The inner layers of a multi-layer PWB are baked for such a long time, to improve dimensional stability in subsequent heat treatments of outer layers [13].

The manufacture of PWBs can be either through Additive technology, or Subtractive technology. In Additive technology, the manufacturer begins with the dielectric substrate and adds conductive strips to the panel in some pre-defined pattern. All necessary drilling is performed first, followed by catalyzing, and printing. The final step is to deposit the copper strips through either electroless or electrolytic plating.

In the Subtractive process (Used for sample PWB manufacture, see figure 5.2), copper foil is bonded with the dielectric substrate, then portions are removed, leaving behind the desired circuitry pattern. The copper removal, or *etching* is achieved by first coating the copper layer with *photoresist*, then curing the 'resist' by exposing it to ultraviolet light using the circuit pattern. Then imaging techniques known as *printing* are used to create the circuit pattern, a process which removes the resist from portions of the board, exposing the copper to be removed by the etching process.

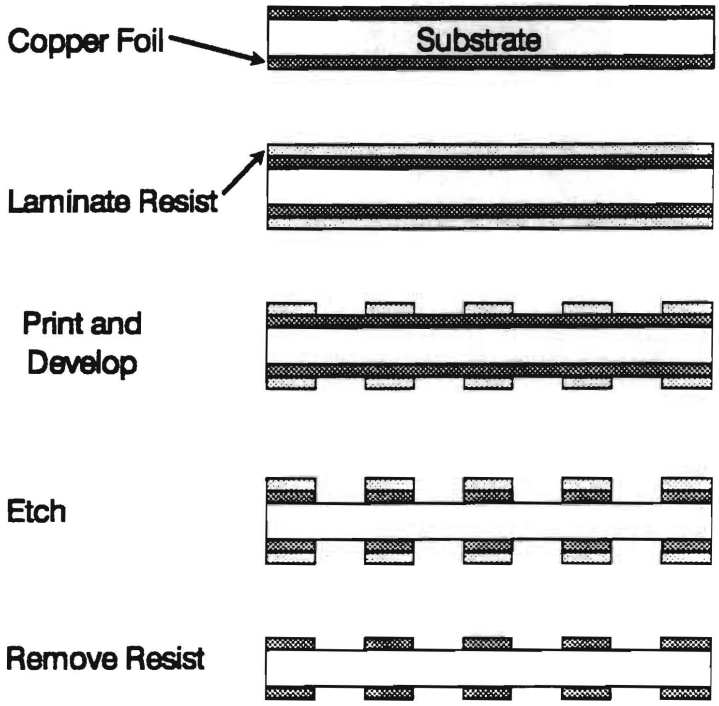

Figure 5.2 Subtractive technology etching process [13]

Element Choice

The modeling of the PWB out-of-plane warpage was done using Ansys 4.4A on an IBM 486 PC. The element chosen was STIF 99, an 8-node layered shell element. The element is a version of the 8-Node Isoparametric shell element and allows up to 100 different material layers [23]. Each node has six degrees of freedom, translations in x, y, z and rotations about each of these axes.

Several assumptions were made to facilitate the analysis. It was assumed that no slippage occurs between the layers. Shear deflection was accounted for in the element, but lines normal to the center plane prior to loading remain normal afterwards [23]. The layers of B-stage prepreg used in the manufacture of the test PWBs, were treated as separate layers in the finite element model of the sample PWB.

Assumptions

Board Symmetry

The first assumption was the warpage of the PWB has two lines of symmetry as shown in figure 5.3. Under this assumption, only one quarter of the board was necessary to calculate warpage for the entire board, which greatly reduced computation times for the numerical analysis.

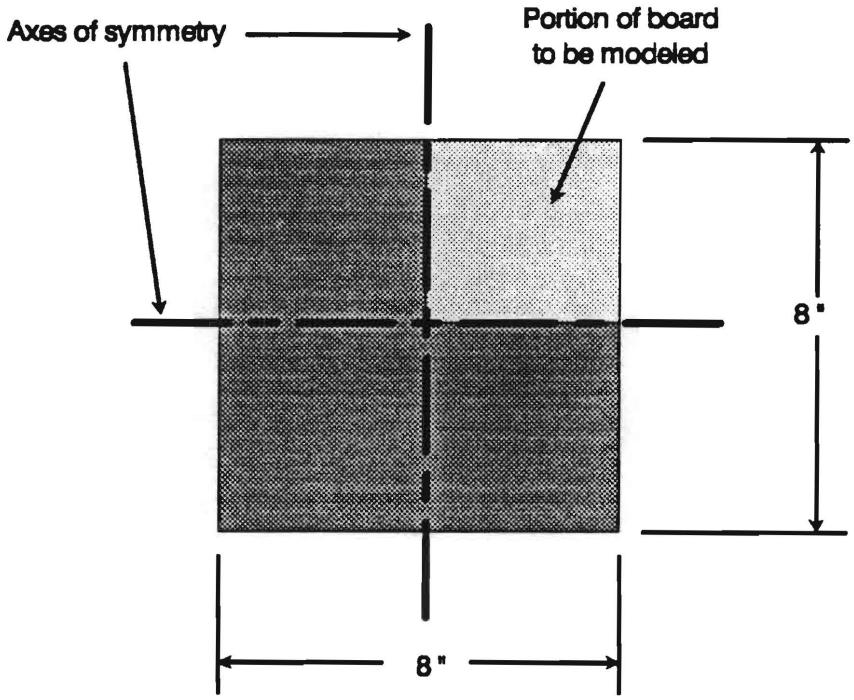

Figure 5.3 Portion of board to be modeled in FEA

Modeling Internal Copper Layers

One of the difficulties encountered during the finite element analysis was the modeling of the copper traces. The copper layers located within the PWB itself were treated as a fiber-reinforced composite. This assumption stemmed from the fact that during the manufacture of the printed wiring board, the outer layers of copper are bonded

to the internal layers by use of prepreg. During the final lamination process, temperatures reach approximately 175°C with pressures up to 10.3 MPa. As a result, the resin in the B-stage prepreg melts and flows, removing air cavities [13]. After curing, the resin solidifies into its final form known as C-stage. The process is illustrated in figure 5.4

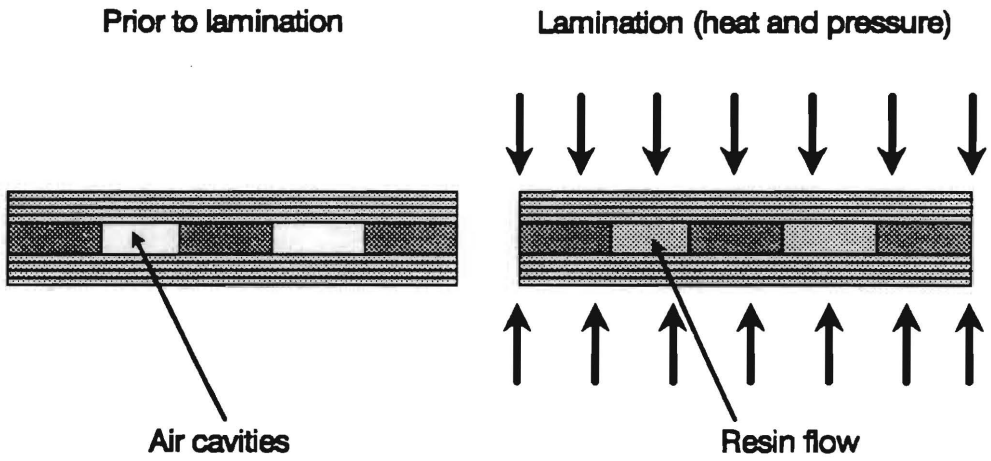

Figure 5.4 Resin flow during lamination process

The composite assumption for the inner copper layers required the use of analytic property calculations. The modulus in the fiber or warp direction, which in this case represents the direction in which the copper traces run, can be found from the following [1]:

$$E_1 = E_{1f}V_f + E_{1m}(1-V_f) \qquad (5.1)$$

where: E_1 = Young's modulus in trace direction

E_{1f} = Young's modulus of fiber (copper)

V_f = fiber volume fraction

E_{1m} = Young's modulus of matrix (epoxy)

Young's modulus in the transverse direction is determined by:

$$E_2 = \frac{E_{2m}(1+\xi\eta_2 V_f)}{(1-\eta_2 V_f)} \qquad (5.2)$$

where: E_{2m} = transverse Young's modulus of matrix (epoxy)

ξ = 2 for square packing (chosen)

= 1 for hexagonal packing

$$\eta_2 = \frac{(E_{2f}/E_{2m}-1)}{(E_{2f}/E_{2m}+\xi)} \qquad (5.3)$$

Major Poisson's ratio can be written as:

$$\nu_{12} = \nu_{12f} V_f + \nu_{12m}(1-V_f) \qquad (5.4)$$

where: ν_{12f} = Poisson's ratio of fiber

ν_{12m} = Poisson's ratio of matrix

The shear modulus for a continuos fiber composite is calculated from:

$$G_{12} = G_{12m}\frac{G_{12f}(1+V_f)+G_{12m}(1-V_f)}{G_{12f}(1-V_f)+G_{12m}(1+V_f)} \qquad (5.5)$$

where: G_{12m} = shear modulus of matrix

G_{12f} = shear modulus of fiber

Coefficients of thermal expansion can be estimated by the following equations:

$$\alpha_1 = \frac{\overline{E\alpha}}{\overline{E}} \qquad (5.6)$$

where: $\overline{E\alpha} = E_f \alpha_f V_f + E_m \alpha_m (1 - V_f)$

$\overline{E} = E_f V_f + E_m (1 - V_f)$

α_f = Coefficient of thermal expansion for fiber

α_m = Coefficient of thermal expansion for matrix

$$\alpha_2 = \alpha_f V_f (1 + V_f) + \alpha_m (1 - V_f)(1 + \nu_m) - [\nu_f V_f + \nu_m (1 - V_f)] \frac{\overline{E\alpha}}{\overline{E}} \qquad (5.7)$$

where: ν_m = Poisson's ratio for matrix

ν_f = Poisson's ratio for fiber

Using the equations 5.1-7, all of the necessary material properties for the finite element model are found (See FEA model files in appendix B for values).

The copper traces on the outer faces of the completed printed wiring board posed a more difficult problem than the inner layers. These traces could not be modeled as a composite layer due to the lack of a matrix material (see figure 5.5).

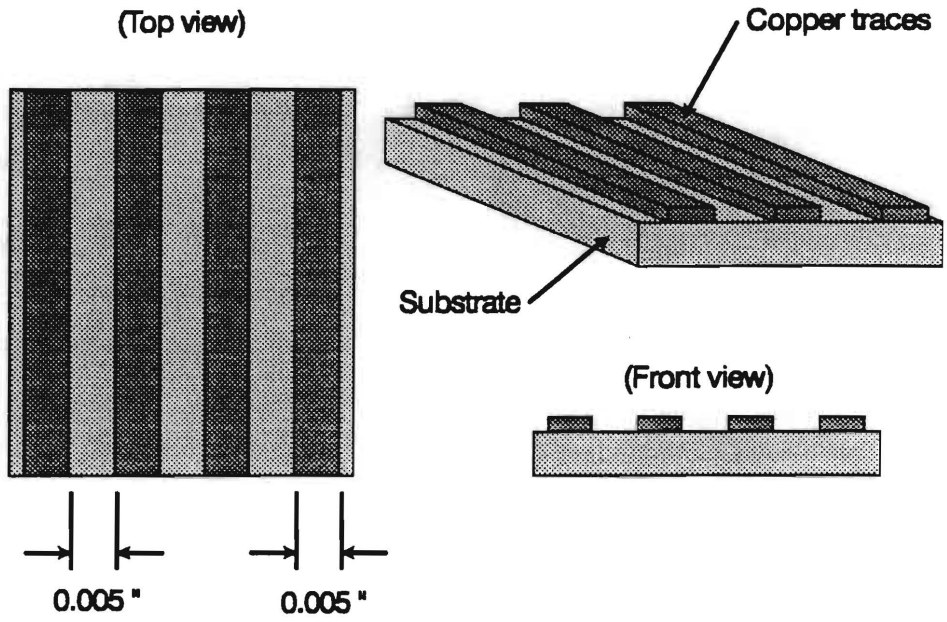

Figure 5.5 Illustration of PWB outer layer traces

Modeling External Copper Traces

The method for modeling the external layers of copper foil was developed in conjunction with fellow project member Wen Zhou [27]. Referring to figure 5.5, the traces on the surface of the board were approximately 5 mils in width, with 5 mils spacing. The approach simplified the finite element analysis by substituting for the outer traces, a uniform solid layer of copper with modified properties. The modification was necessary due to the fact that the representative layer will have orthotropic property characteristics as a result of the material discontinuities. The stiffness perpendicular to the trace direction would be much lower than that parallel with the trace direction. Since the thrust of the analysis was to predict out-of-plane warpage, the bending characteristics of the outer copper traces was of primary concern. It was with this emphasis that the modeling methods were developed.

Considering the copper traces as uniform cantilever beams under pure bending, and utilizing the symmetry boundary conditions, the equation for the maximum deflection of a beam is:

$$v = \frac{Ml^2}{2EI} \qquad (5.8)$$

where: M = Applied Moment
l = Length of beam
E = Young's Modulus
I = Moment of Inertia

To maintain the behavioral characteristics of the copper traces under bending in the trace direction, the stiffness (EI/l) of the representative uniform copper layer must be similar to that of the traces. This was achieved by making the thickness of the uniform layer one half the thickness of the copper trace. Referring to figure 5.6, the area moment of inertia for one trace is given by the following equation:

$$I_{trace} = \int_{y_i}^{y_o} w y^2 dy \qquad (5.9)$$

where: I_{trace} = area moment of inertia for trace
w = width of traces (5 mils)
y = vertical distance from stress free axis
y_o = distance from stress free axis to outer surface of external copper trace
y_i = distance from stress free axis to inner surface of external copper trace

The solution of equation 5.9 is:

$$I_{trace} = \frac{w\left(-y_i^3 + y_o^3\right)}{3} \qquad (5.10)$$

The equation for the area moment of inertia for a representative uniform copper layer is given as:

$$I_{unif} = \int_{y_i}^{\left(\frac{y_o+y_i}{2}\right)} 2wy^2 dy \qquad (5.11)$$

the solution becomes:

$$I_{unif} = \frac{-2wy_i^3}{3} + \frac{w(y_i + y_o)^3}{12} \qquad (5.12)$$

To solve these equations, it was assumed that the stress free axis lies approximately in the middle of the board, which had an overall thickness of 43 mils. The percent difference between the area moments of inertia values is approximately 1.5%. Thus, the use of the uniform copper layer with half the thickness of the copper trace seemed reasonable. However, additional modifications were required to model material behavior in the transverse direction (Perpendicular to the trace direction). Finite element modeling methods were used to match the representative uniform layer's behavior in the transverse direction with that of the traces. An finite element analysis was done using chosen property values for the uniform layer. Then an analysis is made of the actual traces, with both cases subject to identical thermal load conditions and boundary conditions. The results of both were compared, and new values for the representative uniform layer were chosen. The process was repeated until the behavior of the representative uniform layer and the actual traces was approximately the same. The results indicated the use of a

transverse modulus equal to one tenth that of the trace direction, and a Poisson's Ratio of 0.1 for the uniform copper layer model.[27].

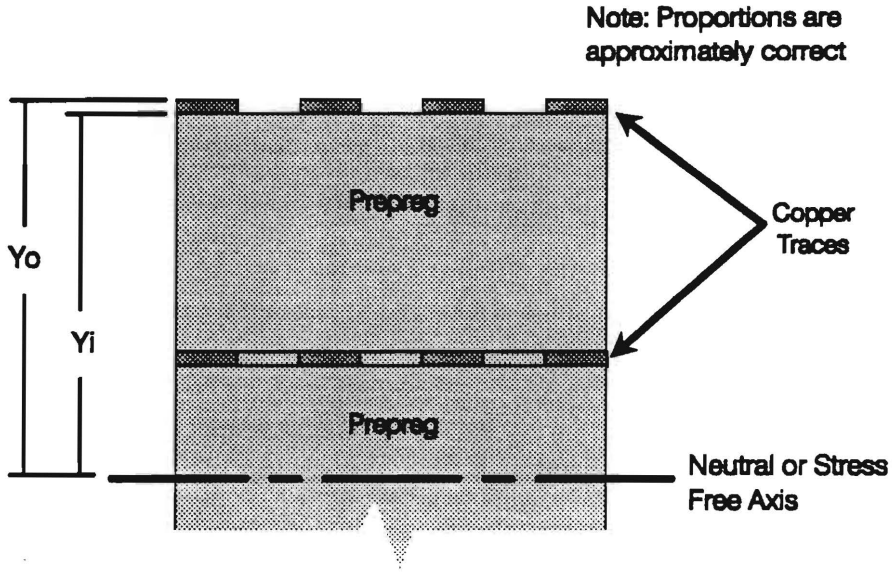

Figure 5.6 Cross-sectional view of PWB

Automation of Finite Element Analysis Modeling Process

In keeping with the thrust of this research project, rapid determination of printed wiring board thermo-mechanical behavior, efforts towards improving the efficiency of the analytical procedures are discussed. Though the time required to perform the material testing was reduced significantly as a result of measures outlined in chapter three, the calculations of predicted board warpage using the ANSYS 4.4A finite element analysis package were both time consuming and prone to user input error. To reduce both the time required to input preprocessor data as well as the errors involved in this activity, a computer program to act as a 'front end' between the user and the ANSYS program written by the author is described.

The program is a prototype for a system which will automatically generate the input file for the ANSYS preprocessor module based upon user supplied answers to questions about the test board's lay-up. The input file contains geometrical properties

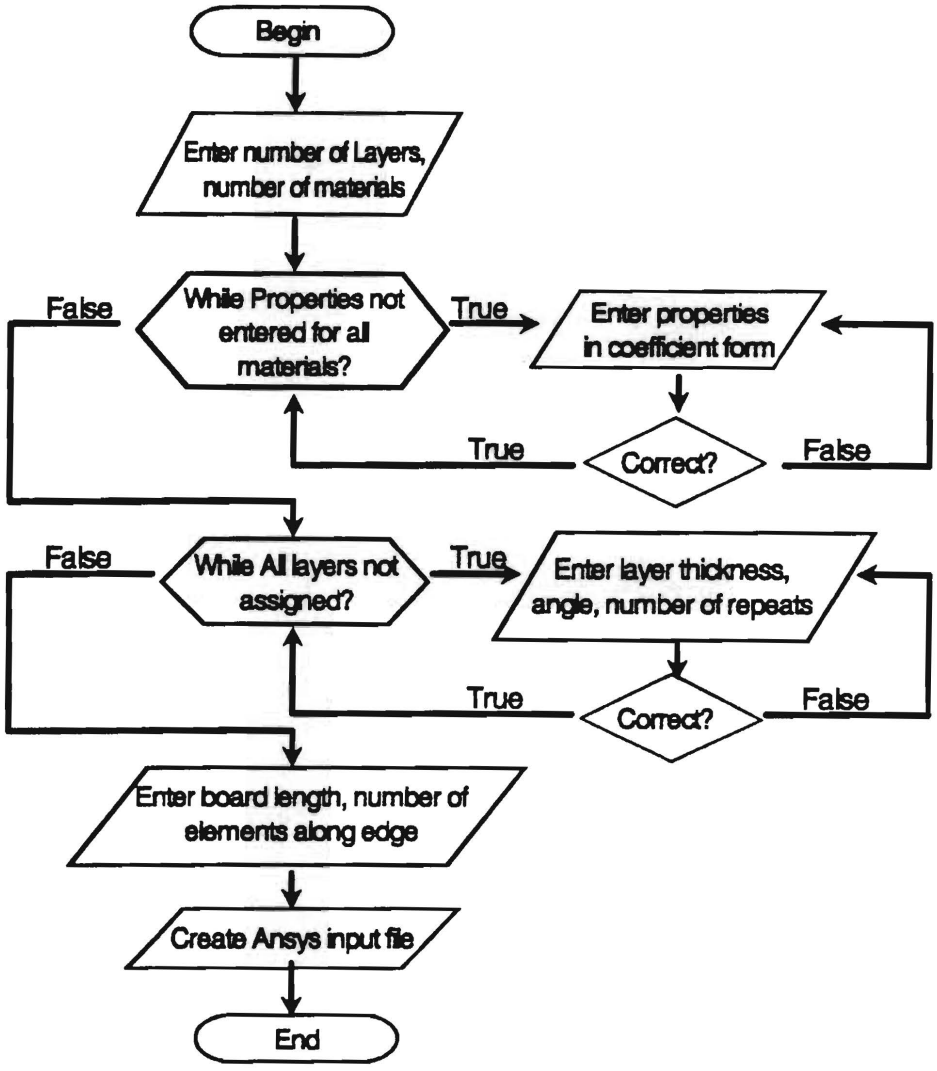

Figure 5.7 Flowchart for Ansys input file creation program.

of the test board, as well as the thermo-mechanical properties data determined from the materials testing system. A program flowchart is shown in figure 5.7.

The program begins by asking the user for the number of individual layers making up the printed wiring board, as well as the number of different materials. For the current project, 19 layers were used (See figure 5.1 for layer description), with three different materials. The materials were: 1) uniform copper layer representing the outer surface traces, 2) prepreg , and 3) hybrid layer of copper and epoxy. The user is then asked to input the name of the first material, along with its properties in coefficient form. These coefficients are used by Ansys in a third order polynomial to determine properties at various temperatures. Once this information has been entered for each material, then the program begins a sequence which assigns a material to each layer of the board. Once the layer material is assigned, then the user is asked to input the thickness, element angle, and the number of times the layer repeats (Excluding the current layer). Once this information is completed for each layer of the board, the user is asked to enter the length of one side of the board, assuming a square specimen. Then the number of elements along one edge is entered, allowing for control of the finite element mesh size.

Once the input process is completed, the program automatically creates the input file required by Ansys' preprocessor module. The mesh is generated along with specified boundary conditions and the property tables for each material. The mesh generation is conducted in a specific manner to allow for the output of the Ansys post processor to be used for three dimensional surface plot generation using the Mathematica software package (See appendix for Mathematica plot routine). This method was chosen to allow for direct comparison of predicted warpage shapes with those measured using experimental techniques which are discussed in chapter 6.

Finite Element Analysis Results

Moiré Test Setup

The experimental setup for the Shadow Moiré test system was made up of a CCD camera, light source, oven, and a glass grating plate. A schematic of the setup is shown in figure 5.8. The Shadow Moiré method is well developed, and has been utilized for many years for the determination of out-of-plane displacement [2].

The experimental method for simulating the wave soldering process has been extensively investigated by previous project members [25]. This same technique was used for the sample printed wiring board used for this research. The temperature profile for both sides of the sample board are shown in figure 5.9. From the figure, it can be seen that a large temperature gradient exists across the thickness of the board. Referring to figure 5.8, the surface with the higher temperature value corresponds to the side which is facing the ceramic heat source. The ceramic heat plate was used to give the board a thermal shock to simulate the wave soldering process. The lower temperature surface faces the glass grating. The finite element analysis simulated the gradient condition during warpage measurement (See appendix for Ansys input files). Due to the thickness of the board (43 mils), the gradient was approximated using linear interpolation based upon the boundary surface temperatures.

Results of the experimental displacement measurement using the Shadow Moiré technique are shown in figure 5.10. The figures contain fringe patterns which are used to calculate out-of-plane displacements as a result of thermal stresses. Fringe patterns are shown for several temperature levels corresponding to the temperatures used for the finite element analysis. Though the sample board was already warped, these values were used

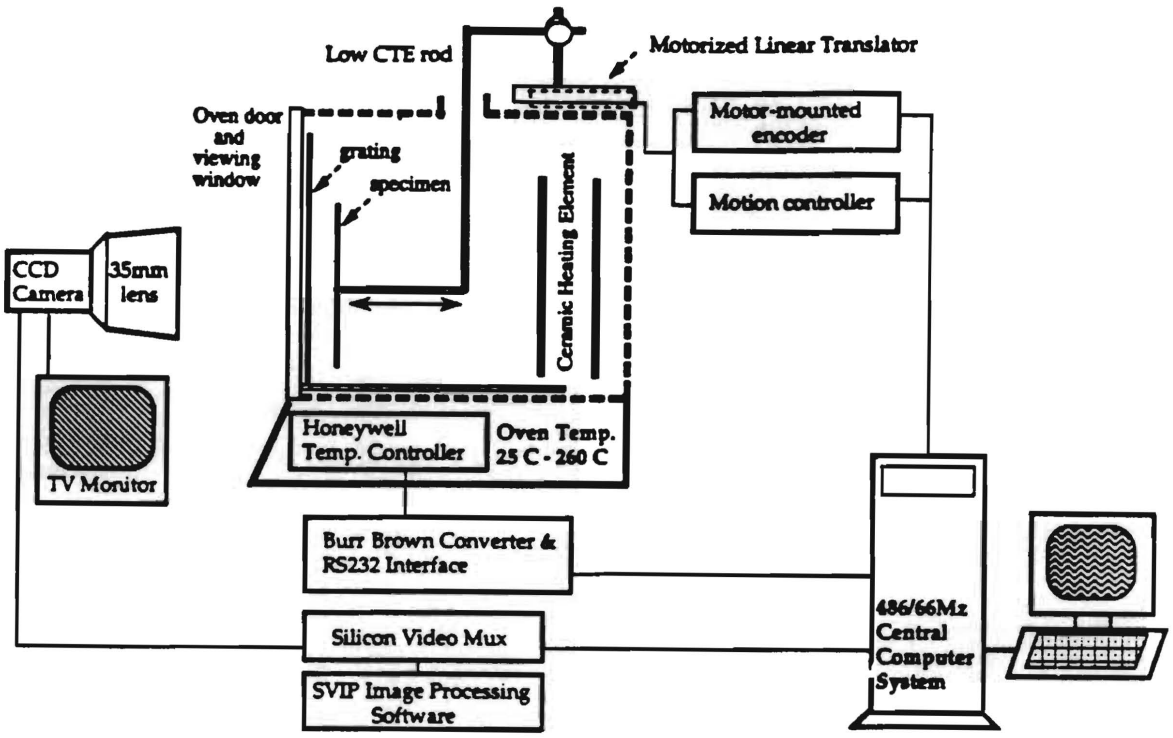

Figure 5.8 Experimental setup for Shadow Moiré testing

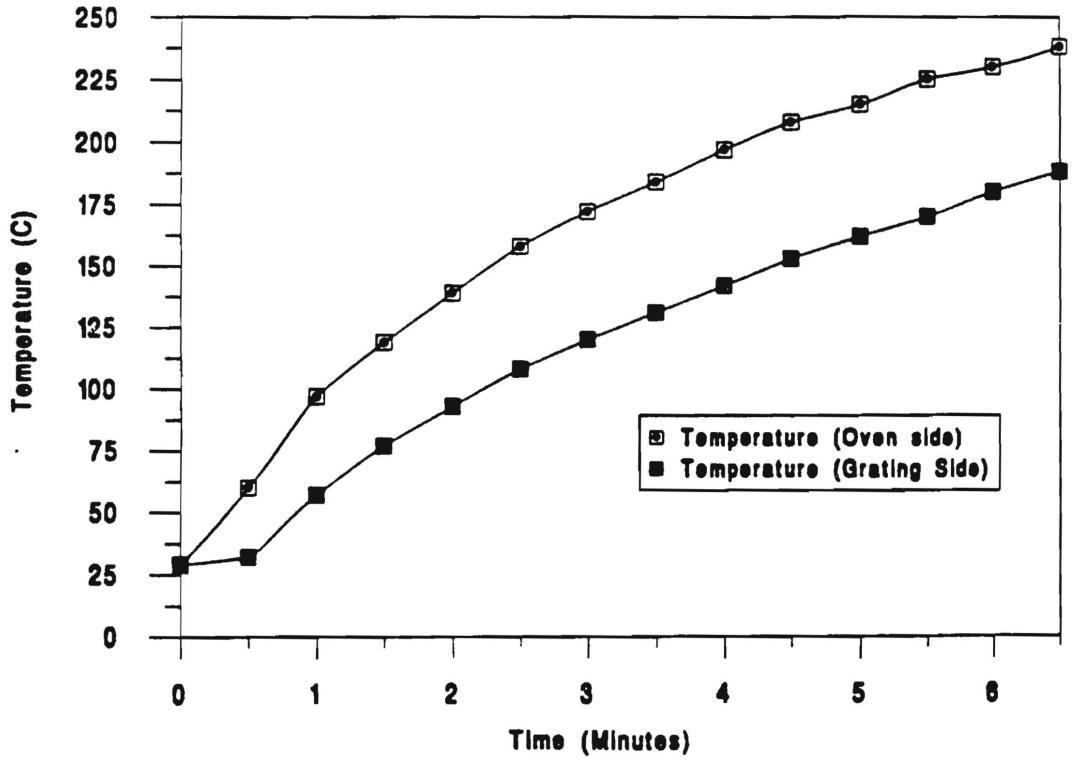

Figure 5.9 Temperature vs. time for board surfaces

as reference points, and thus represent zero displacement for comparative purposes. Thus these initial values were subtracted from subsequent fringe order calculations, to determine the net warpage.

Comparison of Warpage Prediction Results

Warpage predictions based upon measured property values, maximum published values, and minimum published values are shown in figures 5.11 and 5.12 along with the experimental displacement measurements from the Shadow Moiré test. Displacements are compared for two points on the sample printed wiring board. The first point shall be referred to as the 'top-mid' point, which is illustrated in figure 5.13. The second point is termed 'side-mid'. During the simulated wave soldering process, the PWB was oriented so that the surface facing the heat source directly had copper traces running horizontally. The dielectric layer beneath it was then composed of six sheets of prepreg, with the warp direction corresponding to the horizontal also. The opposite side of the board faced the glass grating used to produce the fringe patterns necessary for the Shadow Moiré technique.

The results of predicted warpage and experimental values for the top-mid point are shown in figure 5.11. Positive values indicate displacement in the direction of the ceramic heat source, while negative represent displacement towards the glass grating. The values for the displacements for the experimental case show a large initial negative displacement, which continued until a maximum negative displacement of approximately 45 mils was reached at 150°C, then a slight decrease in warpage was seen. The results for the case using maximum published property values resembled that of the experimental case, except

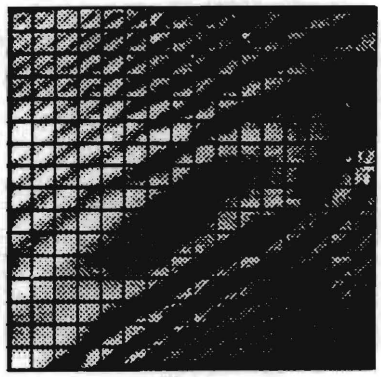

25 °C

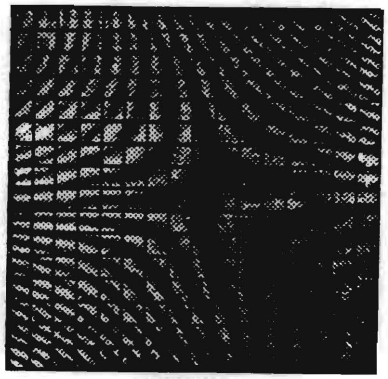

119 °C

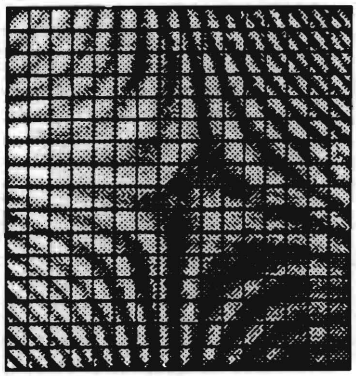

54 °C

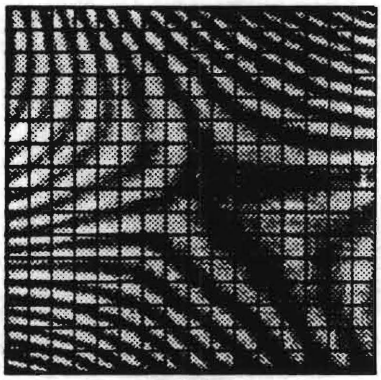

152 °C

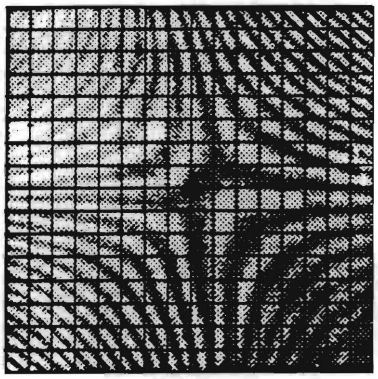

97 °C

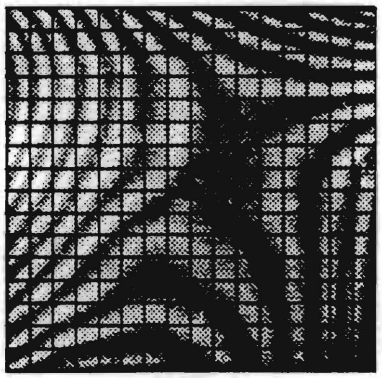

178 °C

Figure 5.10 Fringe patterns from Shadow Moiré testing of sample PWB

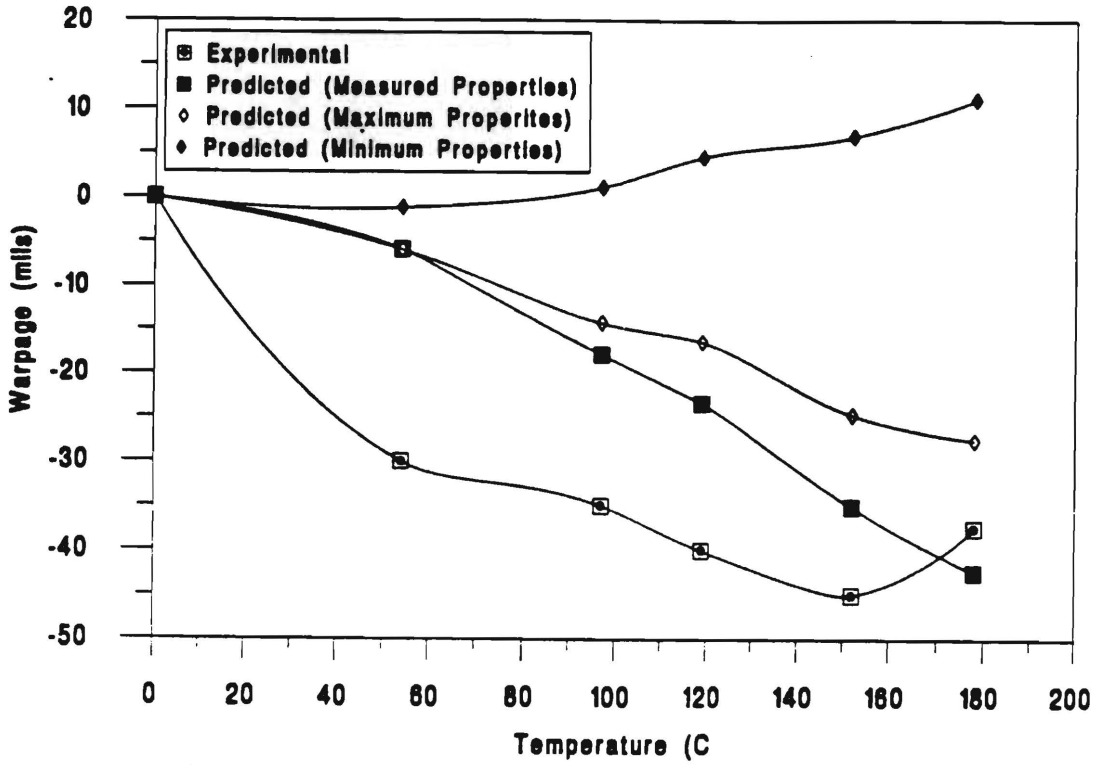

Figure 5.11 Warpage vs. temperature for top-mid point of PWB

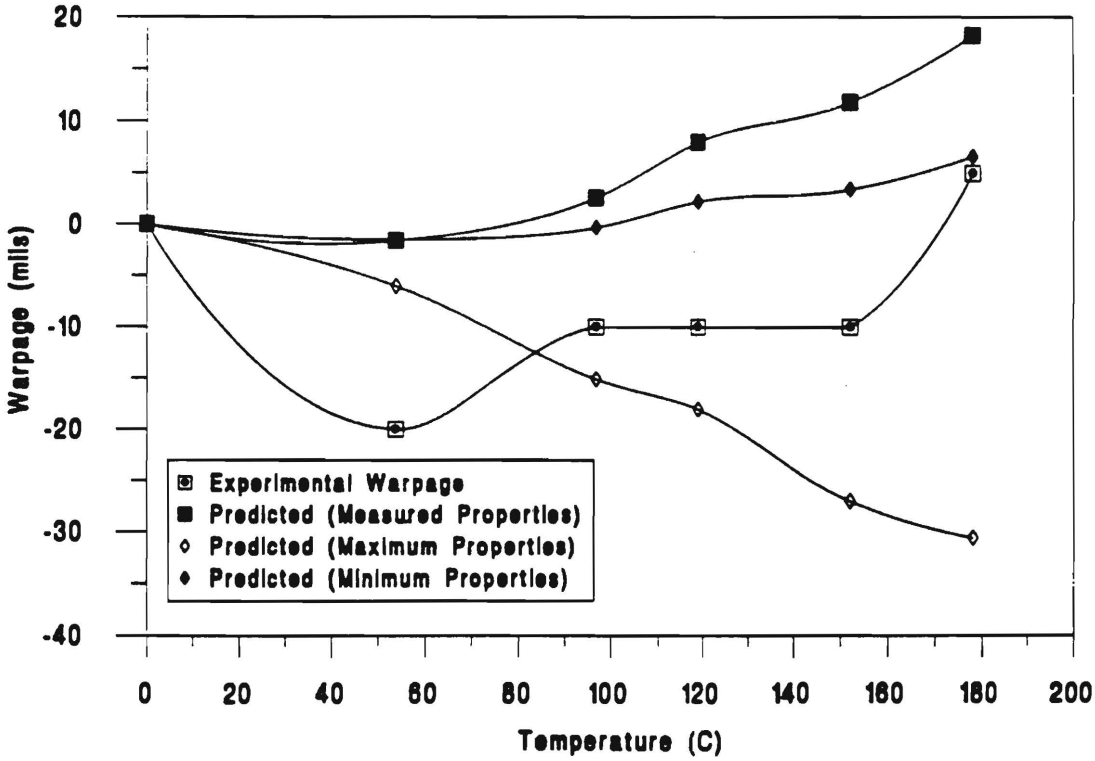

Figure 5.12 Warpage vs. temperature for side-mid point of PWB

with less magnitude. The largest negative displacement was 30 mils. The minimum published property case had an initial small negative displacement, then warped in the positive direction (i.e., away from glass grating, towards the heat source). The final

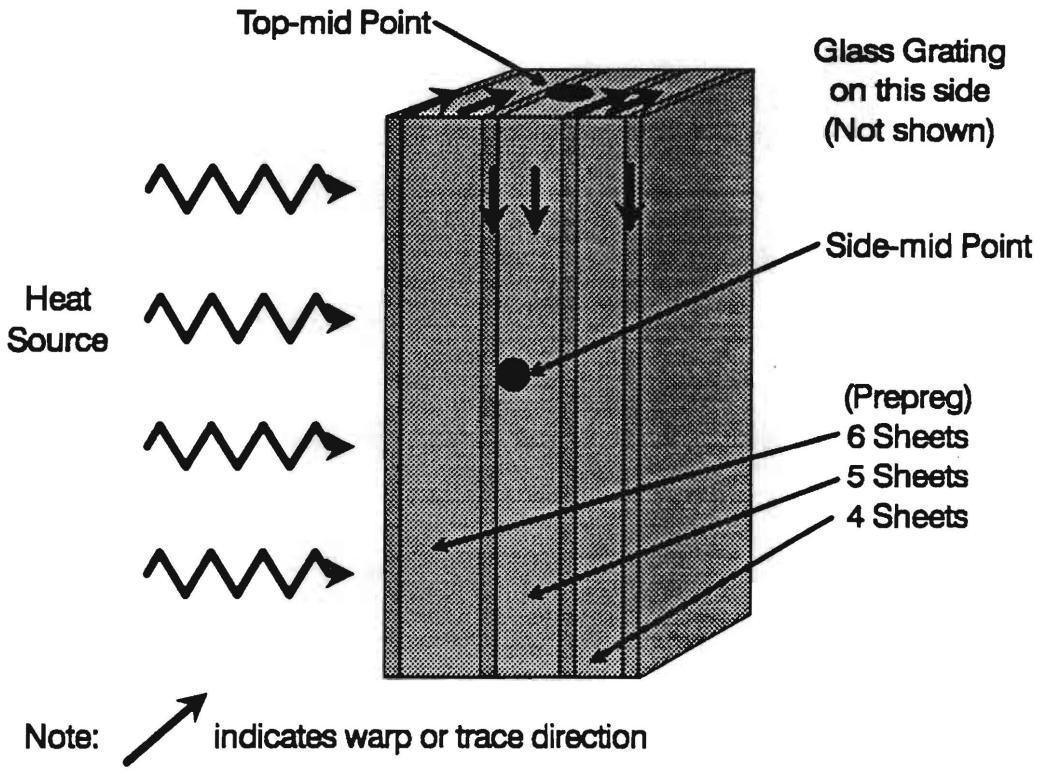

Figure 5.13 Configuration of Sample Board during Simulation of Wave Solder Process, Top-mid and Side-mid points indicated.

displacement was positive 10 mils. The measured temperature dependent properties case also warped in the negative direction, continuing the trend throughout the temperature range.

The side-mid point warpage results are shown in figure 5.12. The experimental measurements again showed a large initial negative deflection, then began to become more positive as the temperature increased. The final value was approximately positive 5 mils.

The predicted warpage using maximum published data initially showed negative deflection, and continued to become more negative as the temperature increased. The final deflection was -32 mils. The minimum published value case initially deflected in the negative direction, then became more positive as the temperature increased. The final value was approximately 6 mils. The results using measured properties initially were negative, then became positive as temperature increased. The final magnitude was approximately 17 mils.

Chapter Conclusion

Results for the prediction of warpage were calculated using property data as described below:

- Measured temperature dependent property data
- Maximum values of published property data
- Minimum values of published property data

Figures 5.14 and 5.15 show three dimensional surface plots of the predicted displacements for the three cases highlighted above. The plots show the final configurations corresponding to the 178°C temperature level (Note: surface temperature for side facing heat source). The three surface plots illustrate the large variance in PWB warpage prediction that can result from using published property data for the PWB core materials.

The variance in the predictions can be explained by considering each case individually. For the case of using maximum published property data (See table 4.1 and 4.2), the CTEs for copper and prepreg are 17.3E-6 in/in/°C and 28E-6 17.3E-6 in/in/°C respectively, while the Young's moduli are 17.3E6 psi and 3.7E6 psi respectively.

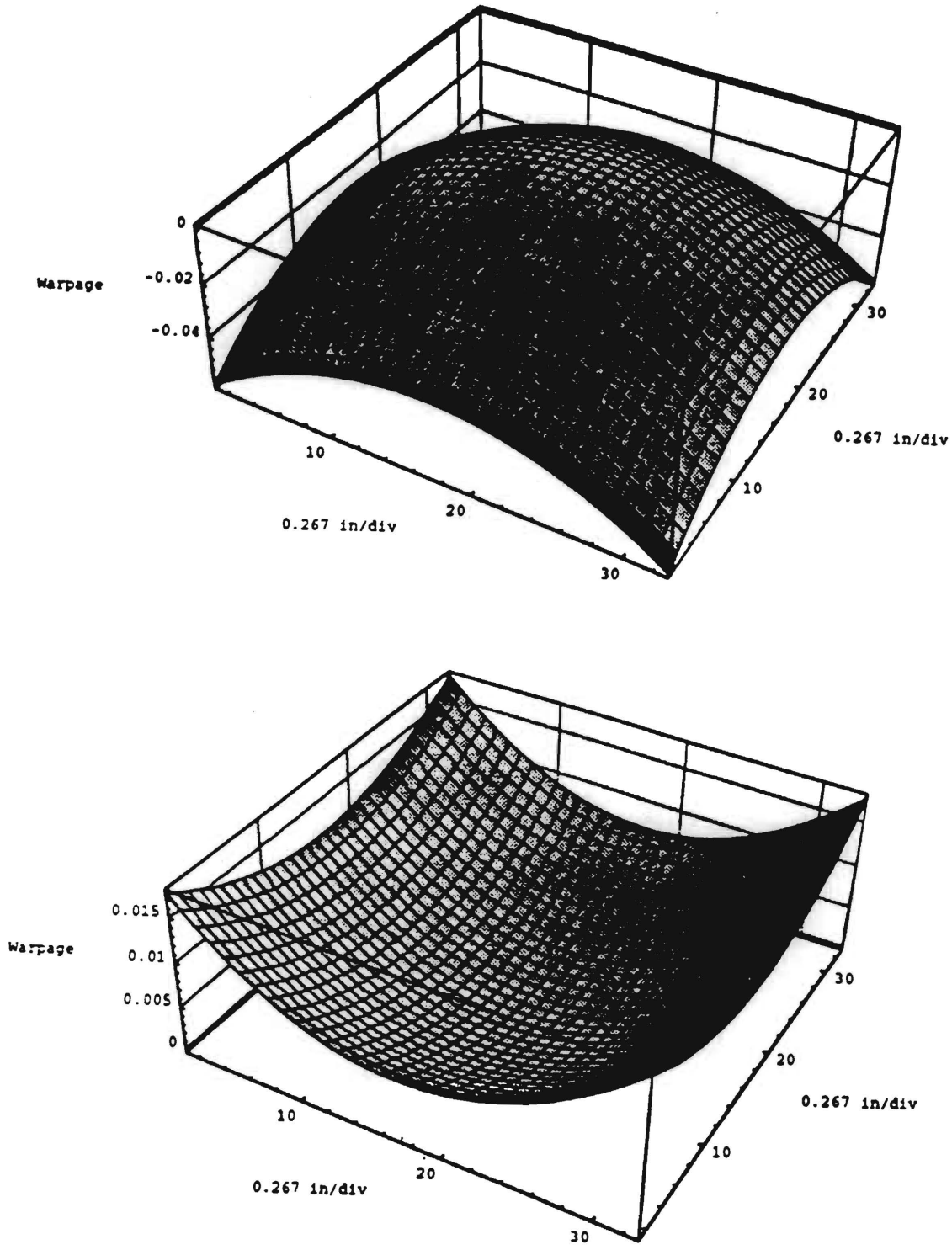

Figure 5.14 Three dimensional surface plots of predicted board warpage when upper surface (Side facing heat source) is at 178°C using maximum property values (top) and minimum property values (bottom).

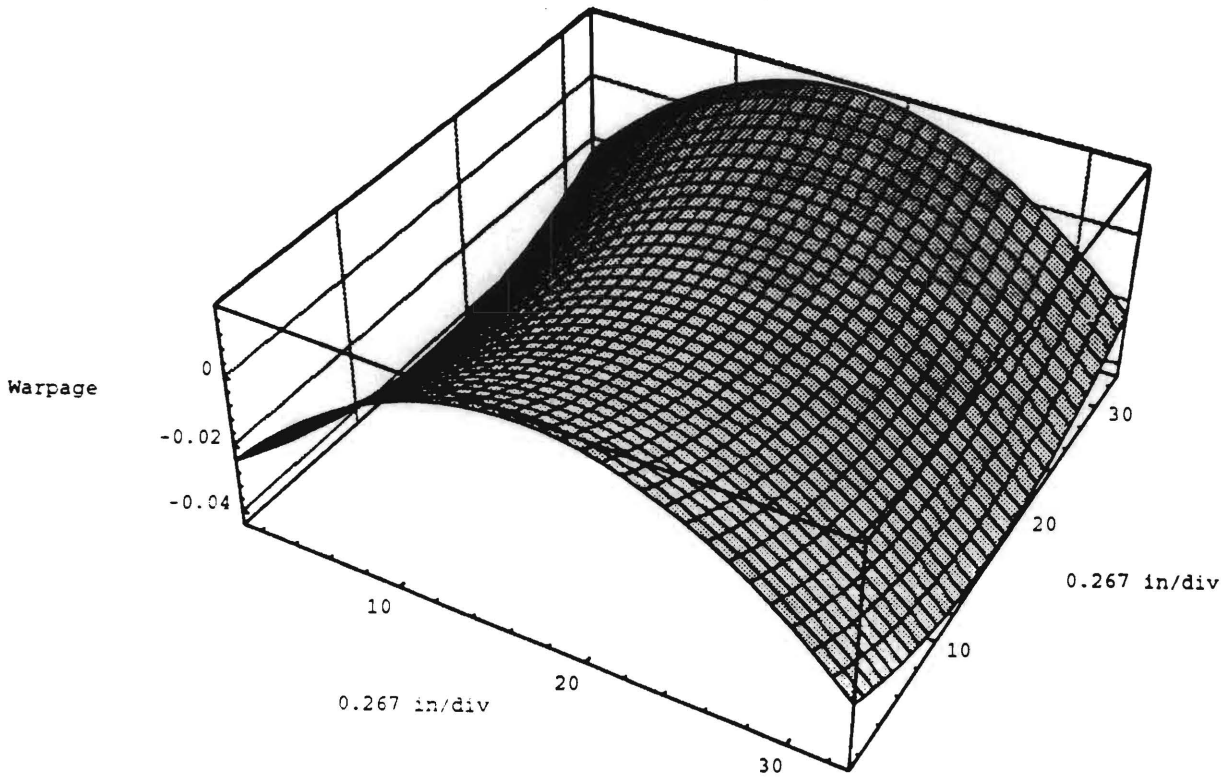

Figure 5.15 Three dimensional surface plots of predicted board warpage when upper surface (Side facing heat source) is at 178°C using measured property values.

Referring to figure 5.16, with the much larger coefficient of thermal expansion for the prepreg and the higher temperature of the upper surface , it is reasonable to expect the PWB to bow away from the heat source.

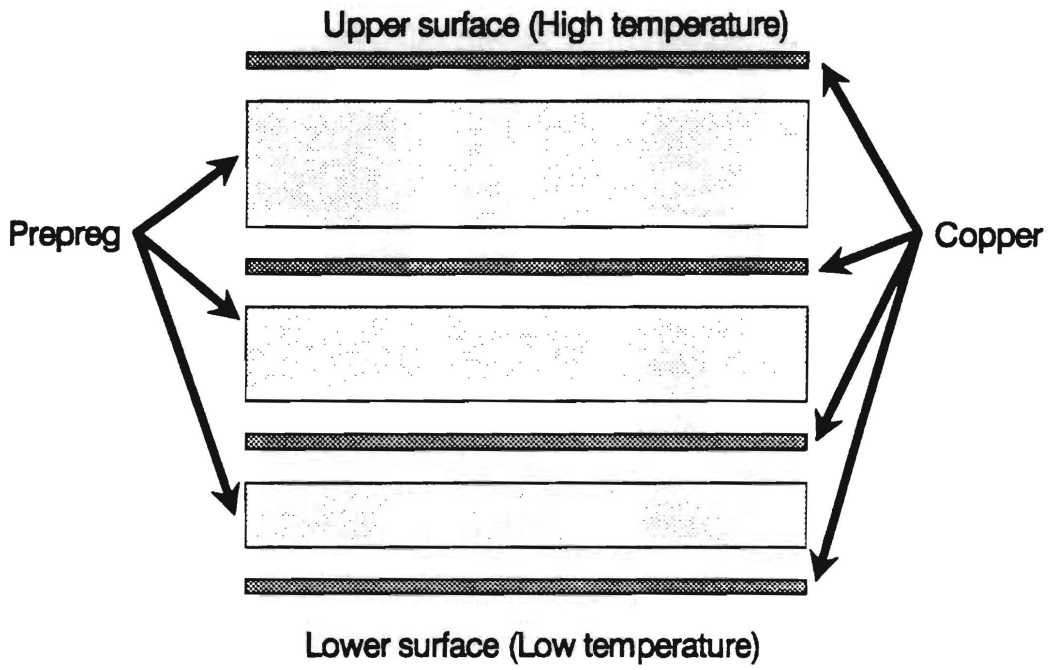

Figure 5.16 Schematic of sample board layup

The minimum published value property data case is slightly less intuitive. Using the minimum published property values from tables 4.1 and 4.2, the CTEs for copper and prepreg are 15E-6 in/in/°C and 11E-6 in/in/°C respectively, with Young's moduli of 12E6 psi and 1.6E6 psi respectively. Referring again to figure 5.16, the upper surface was at a higher temperature than the lower, and the CTE for copper is much higher than prepreg for this case. The copper on top was trying to expand, but was restrained by the 6 layers of prepreg just below it, due to the prepreg's smaller CTE. Even though the copper on the lower surface was at a lower temperature, it expanded more due to the fact that their were

less layers of prepreg to restrain its expansion. Therefore, the board bowed towards the heat source.

The measured temperature dependent property data case can be explained by the fact that the measured values of CTE for both copper and prepreg were relatively close (See figures 4.1,4.2,4.9,4.14). Therefore, the effects of the traces became evident. It was the traces which produced the saddle shape shown in figure 5.15.

From these three cases, it is evident that the range of property values provided by the literature can produce warpage predictions that vary greatly. These predictions not only vary in behavior, as shown in the surface plots, but also in magnitude. The maximum predicted warpage from the maximum and minimum published data cases were 32 mils and 12 mils respectively. However, the maximum predicted warpage using the measured properties data was 43 mils. This is important due to the fact that the maximum warpage is the primary interest of the PWB manufacturer. Determination of the maximum warpage incurred during the wave soldering process will allow the manufacturer to determine if the PWB lay-up requires alteration to reduce this value, to prevent excessive stresses in solder joints which can lead to solder joint failure.

A comparison of experimental warpage with predicted results indicated the latter under predict the initial negative displacements. This may be a result of the temperature profile assumption for the gradient across the board thickness. The current results were based upon the assumption that the temperature varies linearly through the thickness of the board. However, with the low thermal conductivity of the prepreg material, the profile probably is better represented by that shown in figure 5.17. With this profile, initial warpage in the negative direction would be larger due to the greater expansion of the side closest to the heat source. Further investigation of the actual temperature profile across

the thickness of the board should produce finite element predictions which are closer to experimental results.

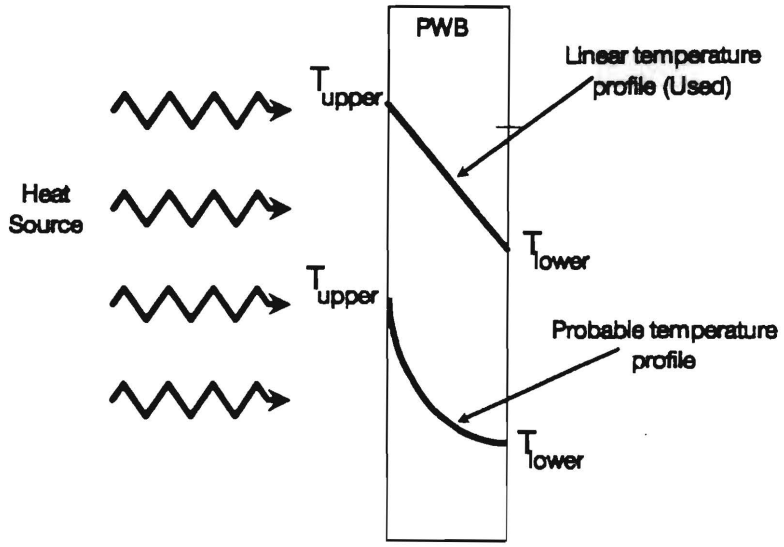

Figure 5.17 Assumed linear temperature profile, and more probable profile.

CHAPTER VI

CONCLUSIONS AND RECOMMENDATIONS

Current Status of the Project

The purpose of the project, as stated in the introduction, was the development of a system for the rapid determination of the thermo-mechanical behavior of printed wiring boards. In particular, a system capable of measuring temperature dependent properties of thin lamina and laminates, like those used in PWB manufacture. The thesis has detailed the methods by which the following objectives were realized:

- Development of methods for measuring temperature dependent properties of thin lamina and laminates
- Automation temperature dependent property testing process
- Comparison of sample PWB warpage predictions using: 1) measured temperature dependent property data, and 2) maximum and minimum values of published property data, illustrating the importance of temperature dependent property testing

A crucial aspect of the research was the automation of the temperature dependent property testing process. This section focuses on aspects of the project which can be improved in respect to system automation. Figure 6.1 shows a schematic of the functions required to perform the project objectives. The three subsystems indicate the main

functions of the project, while PWB lay-up design and design decisions are external functions. The schematic illustrates the ability of the system to act as a design tool in the early stages of PWB manufacture. The system functions which are encased in ellipses represent those which have the greatest potential for improvement, either through increased automation or accuracy.

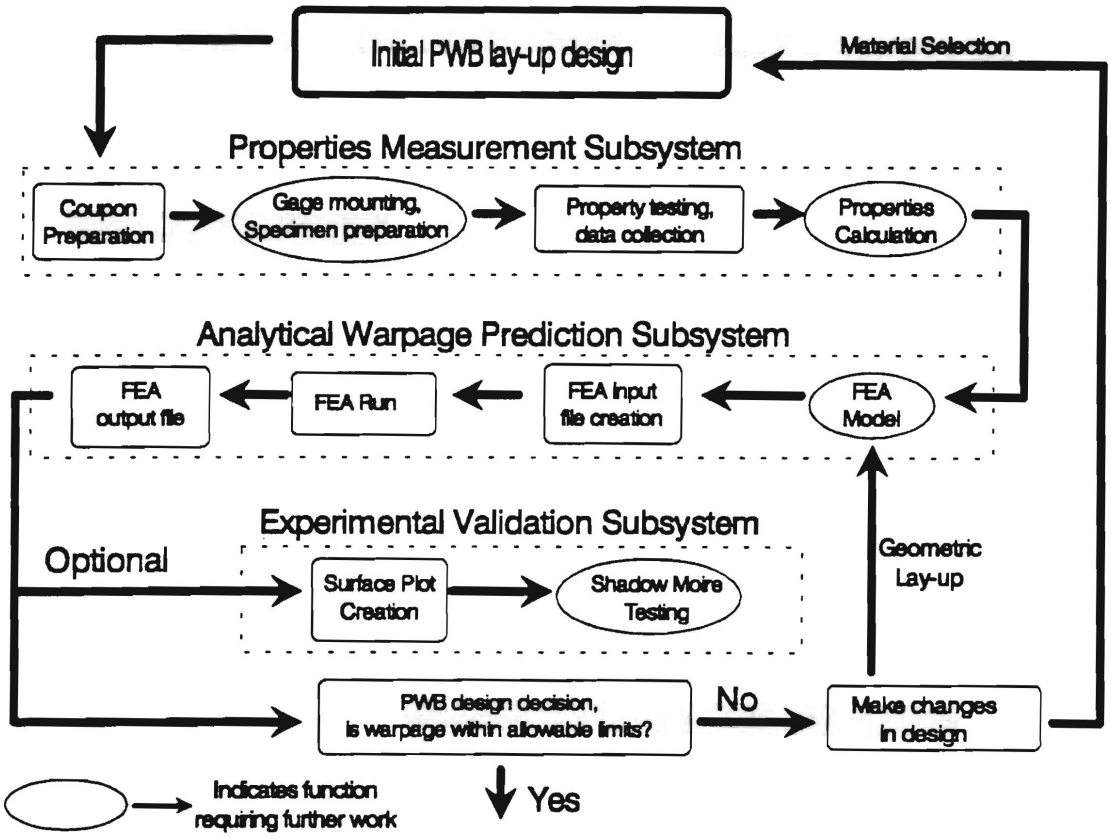

Figure 6.1 Schematic of system functions, with processes requiring further work indicated.

The process of gage mounting was not only time consuming, but was also a source of errors due to gage misalignment, poor bonding, temperature effects, and reinforcement

effects. This function could be greatly improved by the incorporation non-contact techniques.

Properties calculation also proved to be both time consuming and tedious. The use of software to automatically process the data and calculate the required properties would greatly increase overall system performance, as well as reduce the chances for human error. Future enhancements might also include the merger of the data calculation software with the Ansys input file creation program discussed in chapter 5.

Perhaps the most room for improvement lies in the method by which the finite element model of the PWB was determined. Each time a new PWB design enters the system, the model must be updated based upon board configuration. However, the modeling process would require a great amount of refinement based upon comparison with experimental results. Thus, the automation of other system functions should be made a priority, to allow for later development of the FEA model through an iterative process.

The Shadow Moiré system, during this research, was being modified to incorporate closed loop control of pre-test specimen orientation, a long and tedious process. Once the modifications are complete, the time required for experimental warpage measurement will be greatly reduced.

The current project has illustrated the importance of temperature dependent properties testing of PWB core materials to the prediction of warpage due to thermal stresses resulting from the wave soldering process. In addition, the framework for a design tool which can be used in the early stages of the PWB design process has been presented, along with possibilities for future enhancements. The steps taken to automate the temperature dependent property testing system has greatly reduced both the cost and time previously required for material property characterization. These results are just part

of the efforts of the current project which tries to keep pace with the changes taking place in the PWA/PWB manufacturing industry.

Suggestions for Future Research

The predicted warpage values of chapter 5 were based upon the assumption that the temperature varied linearly through the thickness of the board. Better modeling should be achieved by determining the actual temperature profile through the thickness of the board. A possible solution may be the development of an analytical tool for determining the temperature profile based upon lay-up data and temperature profiles for the manufacturing process. The method should be consistent with the overall project goal of system automation.

The sample board used for the current research represented a simplified version of actual PWBs (see chapter 5 for sample PWB configuration), which greatly simplified the modeling process. However, actual PWBs are much more complex, with intricate trace patterns as well as plated-thru and via holes, not to mention components. The modeling process perhaps poses the greatest problem to system implementation, and provides the widest area of future research.

APPENDIX A

STRAIN GAGE USED FOR TESTING THERMO-MECHANICAL PROPERTIES

After intensive collaboration with engineers from Measurements Group, Inc., the EA-13-250AE-350 open faced foil strain gage was chosen. Specifications are given in the figure and table below.

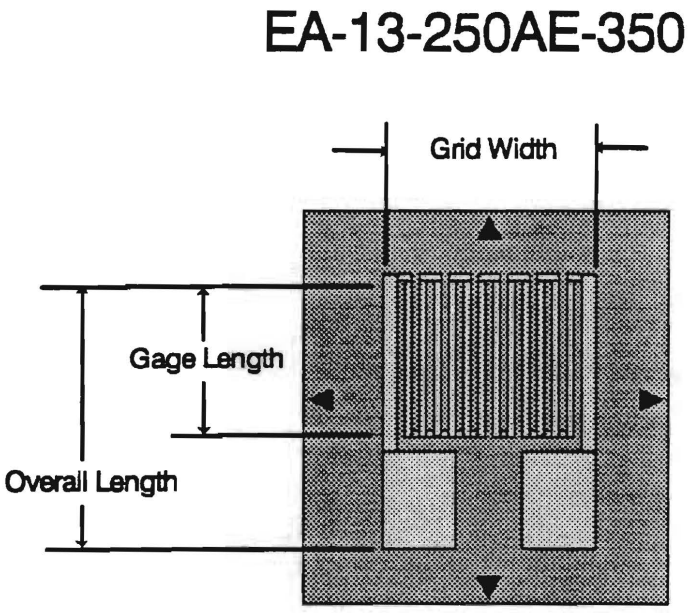

Figure A.1 Foil strain gage used for testing

• Gage Length	Overall Length	Grid Width	Overall Width
0.230 in	0.375 in	0.022 in	0.030 in
5.84 mm	9.53 mm	0.56 mm	0.76 mm
Matrix Size 0.50L x 0.36W in		12.7L x 3.0W mm	

Table A.1 Gage dimensional specifications

APPENDIX B

FINITE ELEMENT MODEL USING TEMPERATURE DEPENDENT PROPERTIES

The following is a listing of the Ansys input file for the model using measured temperature dependent property values. The maximum temperature is 175°C (Note: all values in °F), with the temperature gradient across the thickness of the board assumed linear.

```
/PREP7
/PNUM,KPOI,1
/PNUM,AREA,1
/PNUM,LINE,1
/PNUM,NODE,1
/PNUM,ELEM,1
KAN,0
ITER,-5
ET,1,99
R,1,19,0,1,19,0
RMORE,0,0,0,0,0,0
RMORE,1,0.000000,0.000300,2,90.00000,0.0026300
RMORE,2,90.000000,0.0026300,2,90.00000,0.0026300
RMORE,2,90.000000,0.0026300,3,90.000000,0.001200
RMORE,2,0.000000,0.0026300,2,0.000000,0.0026300
RMORE,2,0.000000,0.0026300,2,0.000000,0.0026300
RMORE,2,0.000000,0.0026300,3,0.000000,0.001200
RMORE,2,90.000000,0.0026300,2,90.000000,0.0026300
RMORE,2,90.000000,0.0026300,2,90.000000,0.0026300
RMORE,2,90.000000,0.0026300,2,90.000000,0.0026300
RMORE,1,90.000000,0.000300,
```

```
***TEMPERATURE TABLE
MPTEMP,1,75,88,97,109,122,135
MPTEMP,7,147,159,171,183,195,207
MPTEMP,13,219,231,243,255,267,279
MPTEMP,19,291,303,315,327,339,345

***MATERIAL 1(OUTER COPPER TRACES)
EX,1,16743000.000000,23500.000000,-184.300003,0.200000,
EY,1,1674000.000000,2350.290039,-18.430000,0.020000,
ALPX,1,0.000010,
ALPY,1,0.000010,
NUXY,1,0.1,
GXY,1,7310139.000000,-7776.919922,0.000000,0.000000,
***MATERIAL 2(PREPREG)
EX,2,2036100.000000,-812.000000,0.340000,0.000000,
EY,2,1418457.000000,1737.699951,-7.500000,0.000000,
ALPX,2,0.000010,
ALPY,2,0.000012,
NUXY,2,0.363948,-0.002315845,0.00000395,0.000000009019,
GXY,2,348259.500000,1628.500000,-11.905000,0.015930,
***MATERIAL 3(COPPER/PREPRPEG HYDBRID)
EX,3,8298071.000000,-7517.149902,0.000000,0.000000,
EY,3,1755473.250000,-157.977097,-0.308530,0.000000,
ALPX,3,0.000011,
ALPY,3,0.000012,
NUXY,3,0.294420,0.000230,0.000000,0.000000,
GXY,3,523088.281250,-25.469999,-0.125660,0.000000,
***BEGIN NODE GENERATION, PERFORMED IN SUCH A WAY AS TO
***ALLOW USE OF OUTPUT IN MATHEMATICA 3-D SURFACE PLOT ROUTINE
N,1,0,0,0
N,2,0.125000,0,0
NGEN,16,2,1,2,,0.250000
NGEN,2,1,32,32,,0.125000
NGEN,17,50,1,33,,,0.250000,,
N,34,0,0.125000,0
NGEN,17,1,34,34,,0.250000,,,
NGEN,16,50,34,50,,,,0.250000,,
E,1,3,53,51,2,35,52,34
E,3,5,55,53,4,36,54,35
E,5,7,57,55,6,37,56,36
E,7,9,59,57,8,38,58,37
E,9,11,61,59,10,39,60,38
E,11,13,63,61,12,40,62,39
```

E,13,15,65,63,14,41,64,40
E,15,17,67,65,16,42,66,41
E,17,19,69,67,18,43,68,42
E,19,21,71,69,20,44,70,43
E,21,23,73,71,22,45,72,44
E,23,25,75,73,24,46,74,45
E,25,27,77,75,26,47,76,46
E,27,29,79,77,28,48,78,47
E,29,31,81,79,30,49,80,48
E,31,33,83,81,32,50,82,49
E,51,53,103,101,52,85,102,84
E,53,55,105,103,54,86,104,85
E,55,57,107,105,56,87,106,86
E,57,59,109,107,58,88,108,87
E,59,61,111,109,60,89,110,88
E,61,63,113,111,62,90,112,89
E,63,65,115,113,64,91,114,90
E,65,67,117,115,66,92,116,91
E,67,69,119,117,68,93,118,92
E,69,71,121,119,70,94,120,93
E,71,73,123,121,72,95,122,94
E,73,75,125,123,74,96,124,95
E,75,77,127,125,76,97,126,96
E,77,79,129,127,78,98,128,97
E,79,81,131,129,80,99,130,98
E,81,83,133,131,82,100,132,99
E,101,103,153,151,102,135,152,134
E,103,105,155,153,104,136,154,135
E,105,107,157,155,106,137,156,136
E,107,109,159,157,108,138,158,137
E,109,111,161,159,110,139,160,138
E,111,113,163,161,112,140,162,139
E,113,115,165,163,114,141,164,140
E,115,117,167,165,116,142,166,141
E,117,119,169,167,118,143,168,142
E,119,121,171,169,120,144,170,143
E,121,123,173,171,122,145,172,144
E,123,125,175,173,124,146,174,145
E,125,127,177,175,126,147,176,146
E,127,129,179,177,128,148,178,147
E,129,131,181,179,130,149,180,148
E,131,133,183,181,132,150,182,149
E,151,153,203,201,152,185,202,184

E,153,155,205,203,154,186,204,185
E,155,157,207,205,156,187,206,186
E,157,159,209,207,158,188,208,187
E,159,161,211,209,160,189,210,188
E,161,163,213,211,162,190,212,189
E,163,165,215,213,164,191,214,190
E,165,167,217,215,166,192,216,191
E,167,169,219,217,168,193,218,192
E,169,171,221,219,170,194,220,193
E,171,173,223,221,172,195,222,194
E,173,175,225,223,174,196,224,195
E,175,177,227,225,176,197,226,196
E,177,179,229,227,178,198,228,197
E,179,181,231,229,180,199,230,198
E,181,183,233,231,182,200,232,199
E,201,203,253,251,202,235,252,234
E,203,205,255,253,204,236,254,235
E,205,207,257,255,206,237,256,236
E,207,209,259,257,208,238,258,237
E,209,211,261,259,210,239,260,238
E,211,213,263,261,212,240,262,239
E,213,215,265,263,214,241,264,240
E,215,217,267,265,216,242,266,241
E,217,219,269,267,218,243,268,242
E,219,221,271,269,220,244,270,243
E,221,223,273,271,222,245,272,244
E,223,225,275,273,224,246,274,245
E,225,227,277,275,226,247,276,246
E,227,229,279,277,228,248,278,247
E,229,231,281,279,230,249,280,248
E,231,233,283,281,232,250,282,249
E,251,253,303,301,252,285,302,284
E,253,255,305,303,254,286,304,285
E,255,257,307,305,256,287,306,286
E,257,259,309,307,258,288,308,287
E,259,261,311,309,260,289,310,288
E,261,263,313,311,262,290,312,289
E,263,265,315,313,264,291,314,290
E,265,267,317,315,266,292,316,291
E,267,269,319,317,268,293,318,292
E,269,271,321,319,270,294,320,293
E,271,273,323,321,272,295,322,294
E,273,275,325,323,274,296,324,295

E,275,277,327,325,276,297,326,296
E,277,279,329,327,278,298,328,297
E,279,281,331,329,280,299,330,298
E,281,283,333,331,282,300,332,299
E,301,303,353,351,302,335,352,334
E,303,305,355,353,304,336,354,335
E,305,307,357,355,306,337,356,336
E,307,309,359,357,308,338,358,337
E,309,311,361,359,310,339,360,338
E,311,313,363,361,312,340,362,339
E,313,315,365,363,314,341,364,340
E,315,317,367,365,316,342,366,341
E,317,319,369,367,318,343,368,342
E,319,321,371,369,320,344,370,343
E,321,323,373,371,322,345,372,344
E,323,325,375,373,324,346,374,345
E,325,327,377,375,326,347,376,346
E,327,329,379,377,328,348,378,347
E,329,331,381,379,330,349,380,348
E,331,333,383,381,332,350,382,349
E,351,353,403,401,352,385,402,384
E,353,355,405,403,354,386,404,385
E,355,357,407,405,356,387,406,386
E,357,359,409,407,358,388,408,387
E,359,361,411,409,360,389,410,388
E,361,363,413,411,362,390,412,389
E,363,365,415,413,364,391,414,390
E,365,367,417,415,366,392,416,391
E,367,369,419,417,368,393,418,392
E,369,371,421,419,370,394,420,393
E,371,373,423,421,372,395,422,394
E,373,375,425,423,374,396,424,395
E,375,377,427,425,376,397,426,396
E,377,379,429,427,378,398,428,397
E,379,381,431,429,380,399,430,398
E,381,383,433,431,382,400,432,399
E,401,403,453,451,402,435,452,434
E,403,405,455,453,404,436,454,435
E,405,407,457,455,406,437,456,436
E,407,409,459,457,408,438,458,437
E,409,411,461,459,410,439,460,438
E,411,413,463,461,412,440,462,439
E,413,415,465,463,414,441,464,440

E,415,417,467,465,416,442,466,441
E,417,419,469,467,418,443,468,442
E,419,421,471,469,420,444,470,443
E,421,423,473,471,422,445,472,444
E,423,425,475,473,424,446,474,445
E,425,427,477,475,426,447,476,446
E,427,429,479,477,428,448,478,447
E,429,431,481,479,430,449,480,448
E,431,433,483,481,432,450,482,449
E,451,453,503,501,452,485,502,484
E,453,455,505,503,454,486,504,485
E,455,457,507,505,456,487,506,486
E,457,459,509,507,458,488,508,487
E,459,461,511,509,460,489,510,488
E,461,463,513,511,462,490,512,489
E,463,465,515,513,464,491,514,490
E,465,467,517,515,466,492,516,491
E,467,469,519,517,468,493,518,492
E,469,471,521,519,470,494,520,493
E,471,473,523,521,472,495,522,494
E,473,475,525,523,474,496,524,495
E,475,477,527,525,476,497,526,496
E,477,479,529,527,478,498,528,497
E,479,481,531,529,480,499,530,498
E,481,483,533,531,482,500,532,499
E,501,503,553,551,502,535,552,534
E,503,505,555,553,504,536,554,535
E,505,507,557,555,506,537,556,536
E,507,509,559,557,508,538,558,537
E,509,511,561,559,510,539,560,538
E,511,513,563,561,512,540,562,539
E,513,515,565,563,514,541,564,540
E,515,517,567,565,516,542,566,541
E,517,519,569,567,518,543,568,542
E,519,521,571,569,520,544,570,543
E,521,523,573,571,522,545,572,544
E,523,525,575,573,524,546,574,545
E,525,527,577,575,526,547,576,546
E,527,529,579,577,528,548,578,547
E,529,531,581,579,530,549,580,548
E,531,533,583,581,532,550,582,549
E,551,553,603,601,552,585,602,584
E,553,555,605,603,554,586,604,585

E,555,557,607,605,556,587,606,586
E,557,559,609,607,558,588,608,587
E,559,561,611,609,560,589,610,588
E,561,563,613,611,562,590,612,589
E,563,565,615,613,564,591,614,590
E,565,567,617,615,566,592,616,591
E,567,569,619,617,568,593,618,592
E,569,571,621,619,570,594,620,593
E,571,573,623,621,572,595,622,594
E,573,575,625,623,574,596,624,595
E,575,577,627,625,576,597,626,596
E,577,579,629,627,578,598,628,597
E,579,581,631,629,580,599,630,598
E,581,583,633,631,582,600,632,599
E,601,603,653,651,602,635,652,634
E,603,605,655,653,604,636,654,635
E,605,607,657,655,606,637,656,636
E,607,609,659,657,608,638,658,637
E,609,611,661,659,610,639,660,638
E,611,613,663,661,612,640,662,639
E,613,615,665,663,614,641,664,640
E,615,617,667,665,616,642,666,641
E,617,619,669,667,618,643,668,642
E,619,621,671,669,620,644,670,643
E,621,623,673,671,622,645,672,644
E,623,625,675,673,624,646,674,645
E,625,627,677,675,626,647,676,646
E,627,629,679,677,628,648,678,647
E,629,631,681,679,630,649,680,648
E,631,633,683,681,632,650,682,649
E,651,653,703,701,652,685,702,684
E,653,655,705,703,654,686,704,685
E,655,657,707,705,656,687,706,686
E,657,659,709,707,658,688,708,687
E,659,661,711,709,660,689,710,688
E,661,663,713,711,662,690,712,689
E,663,665,715,713,664,691,714,690
E,665,667,717,715,666,692,716,691
E,667,669,719,717,668,693,718,692
E,669,671,721,719,670,694,720,693
E,671,673,723,721,672,695,722,694
E,673,675,725,723,674,696,724,695
E,675,677,727,725,676,697,726,696

```
E,677,679,729,727,678,698,728,697
E,679,681,731,729,680,699,730,698
E,681,683,733,731,682,700,732,699
E,701,703,753,751,702,735,752,734
E,703,705,755,753,704,736,754,735
E,705,707,757,755,706,737,756,736
E,707,709,759,757,708,738,758,737
E,709,711,761,759,710,739,760,738
E,711,713,763,761,712,740,762,739
E,713,715,765,763,714,741,764,740
E,715,717,767,765,716,742,766,741
E,717,719,769,767,718,743,768,742
E,719,721,771,769,720,744,770,743
E,721,723,773,771,722,745,772,744
E,723,725,775,773,724,746,774,745
E,725,727,777,775,726,747,776,746
E,727,729,779,777,728,748,778,747
E,729,731,781,779,730,749,780,748
E,731,733,783,781,732,750,782,749
E,751,753,803,801,752,785,802,784
E,753,755,805,803,754,786,804,785
E,755,757,807,805,756,787,806,786
E,757,759,809,807,758,788,808,787
E,759,761,811,809,760,789,810,788
E,761,763,813,811,762,790,812,789
E,763,765,815,813,764,791,814,790
E,765,767,817,815,766,792,816,791
E,767,769,819,817,768,793,818,792
E,769,771,821,819,770,794,820,793
E,771,773,823,821,772,795,822,794
E,773,775,825,823,774,796,824,795
E,775,777,827,825,776,797,826,796
E,777,779,829,827,778,798,828,797
E,779,781,831,829,780,799,830,798
E,781,783,833,831,782,800,832,799

SYMBC,0,1,0.0
SYMBC,0,2,0.0
D,1,UZ,0
WSORT,X
TREF,75
KTEMP,-1
TESIZE,19
```

TE,ALL,86,87.8,91.4,93.2,95,98.6
TEMORE,100.4,102.2,105.8,107.6,109.4,111.2
TEMORE,114.8,116.6,118.4,122,123.8,125.6
TEMORE,129.2
LWRITE
TE,ALL,134.6,138.2,141.8,147.2,150.8,154.4
TEMORE,158,161.6,167,170.6,174.2,177.8
TEMORE,183.2,186.8,190.4,194,197.6,203
TEMORE,206.6
LWRITE
TE,ALL,170.6,174.2,179.6,183.2,186.8,192.2
TEMORE,195.8,199.4,204.8,208.4,212,215.6
TEMORE,221,224.6,228.2,233.6,237.2,240.8
TEMORE,246.2
LWRITE
TE,ALL,219.2,224.6,228.2,233.6,239,242.6
TEMORE,248,251.6,257,262.4,266,271.4
TEMORE,276.8,280.4,285.8,289.4,294.8,300.2
TEMORE,305.6
LWRITE
TE,ALL,264.2,269.6,273.2,278.6,284,287.6
TEMORE,293,298.4,302,307.4,312.8,318.2
TEMORE,321.8,327.2,332.6,336.2,341.6,347
TEMORE,352.4
LWRITE

FINITE ELEMENT MODEL USING MAXIMUM CONSTANT PROPERTIES

The following is a listing of the Ansys input file for the model using maximum constant property values. The maximum temperature is 175°C (Note: all values in °F), with the assumption that the temperature gradient across the thickness of the board is linear. Note, the element generation portion of the file is not shown; however, it is the same as that for the measured temperature dependent properties case immediately preceding this section.

```
/PREP7
/PNUM,KPOI,1
/PNUM,AREA,1
/PNUM,LINE,1
/PNUM,NODE,1
/PNUM,ELEM,1
KAN,0
ITER,-5
ET,1,99
R,1,19,0,1,19,0
RMORE,0,0,0,0,0,0
RMORE,1,0.000000,0.000300,2,90.00000,0.0026300
RMORE,2,90.000000,0.0026300,2,90.00000,0.0026300
RMORE,2,90.000000,0.0026300,3,90.000000,0.001200
RMORE,2,0.000000,0.0026300,2,0.000000,0.0026300
RMORE,2,0.000000,0.0026300,2,0.000000,0.0026300
RMORE,2,0.000000,0.0026300,3,0.000000,0.001200
RMORE,2,90.000000,0.0026300,2,90.000000,0.0026300
RMORE,2,90.000000,0.0026300,2,90.000000,0.0026300
RMORE,2,90.000000,0.0026300,2,90.000000,0.0026300
RMORE,1,90.000000,0.000300,

***MATERIAL 1(OUTER COPPER TRACES)
EX,1,17300000
```

```
EY,1,1730000
ALPX,1,0.0000111
ALPY,1,0.0000111
NUXY,1,0.1
GXY,1,5.6E6
***MATERIAL 2(PREPREG)
EX,2,3700000
EY,2,3700000
ALPX,2,0.0000156
ALPY,2,0.0000156
NUXY,2,0.4
GXY,2,1000000
***MATERIAL 3(COPPER/PREPRPEG HYDBRID)
EX,3,8900000
EY,3,1780000
ALPX,3,0.00001112
ALPY,3,0.0000124
NUXY,3,0.3165
GXY,3,521000
***BEGIN NODE GENERATION, PERFORMED IN SUCH A WAY AS TO
***ALLOW USE OF OUTPUT IN MATHEMATICA 3-D SURFACE PLOT ROUTINE
N,1,0,0,0
N,2,0.125000,0,0
NGEN,16,2,1,2,,0.250000
NGEN,2,1,32,32,,0.125000
NGEN,17,50,1,33,,,0.250000,,
N,34,0,0.125000,0
NGEN,17,1,34,34,,0.250000,,,
NGEN,16,50,34,50,,,0.250000,,

*** NOTE: THE ELEMENT GENERATION SECTION IS NOT SHOWN;
***HOWEVER, IT IS THE SAME AS THAT SHOWN IN APPENDIX C

SYMBC,0,1,0.0
SYMBC,0,2,0.0
D,1,UZ,0
WSORT,X
TREF,75
KTEMP,-1
TESIZE,19
TE,ALL,86,87.8,91.4,93.2,95,98.6
TEMORE,100.4,102.2,105.8,107.6,109.4,111.2
TEMORE,114.8,116.6,118.4,122,123.8,125.6
```

TEMORE,129.2
LWRITE
TE,ALL,134.6,138.2,141.8,147.2,150.8,154.4
TEMORE,158,161.6,167,170.6,174.2,177.8
TEMORE,183.2,186.8,190.4,194,197.6,203
TEMORE,206.6
LWRITE
TE,ALL,170.6,174.2,179.6,183.2,186.8,192.2
TEMORE,195.8,199.4,204.8,208.4,212,215.6
TEMORE,221,224.6,228.2,233.6,237.2,240.8
TEMORE,246.2
LWRITE
TE,ALL,219.2,224.6,228.2,233.6,239,242.6
TEMORE,248,251.6,257,262.4,266,271.4
TEMORE,276.8,280.4,285.8,289.4,294.8,300.2
TEMORE,305.6
LWRITE
TE,ALL,264.2,269.6,273.2,278.6,284,287.6
TEMORE,293,298.4,302,307.4,312.8,318.2
TEMORE,321.8,327.2,332.6,336.2,341.6,347
TEMORE,352.4
LWRITE

FINITE ELEMENT MODEL USING MINIMUM CONSTANT PROPERTIES

The following is a listing of the Ansys input file for the model using minimum constant property values. The maximum temperature is 175°C (Note: all values for °F), with the temperature gradient across the thickness of the board assumed linear.

```
/PREP7
/PNUM,KPOI,1
/PNUM,AREA,1
/PNUM,LINE,1
/PNUM,NODE,1
/PNUM,ELEM,1
KAN,0
ITER,-5
ET,1,99
R,1,19,0,1,19,0
RMORE,0,0,0,0,0,0
RMORE,1,0.000000,0.000300,2,90.00000,0.0026300
RMORE,2,90.000000,0.0026300,2,90.00000,0.0026300
RMORE,2,90.000000,0.0026300,3,90.000000,0.001200
RMORE,2,0.000000,0.0026300,2,0.000000,0.0026300
RMORE,2,0.000000,0.0026300,2,0.000000,0.0026300
RMORE,2,0.000000,0.0026300,3,0.000000,0.001200
RMORE,2,90.000000,0.0026300,2,90.000000,0.0026300
RMORE,2,90.000000,0.0026300,2,90.000000,0.0026300
RMORE,2,90.000000,0.0026300,2,90.000000,0.0026300
RMORE,1,90.000000,0.000300,

***MATERIAL 1(OUTER COPPER TRACES)
EX,1,12000000
EY,1,1200000
ALPX,1,0.00000833
ALPY,1,0.00000833
NUXY,1,0.1
GXY,1,5.6E6
***MATERIAL 2(PREPREG)
EX,2,1600000
```

```
EY,2,1600000
ALPX,2,0.00000611
ALPY,2,0.00000611
NUXY,2,0.02
GXY,2,300000
***MATERIAL 3(COPPER/PREPRPEG HYDBRID)
EX,3,6250000
EY,3,1690000
ALPX,3,0.000008469
ALPY,3,0.0000113
NUXY,3,0.2915
GXY,3,521000
***BEGIN NODE GENERATION, PERFORMED IN SUCH A WAY AS TO
***ALLOW USE OF OUTPUT IN MATHEMATICA 3-D SURFACE PLOT ROUTINE
N,1,0,0,0
N,2,0.125000,0,0
NGEN,16,2,1,2,,0.250000
NGEN,2,1,32,32,,0.125000
NGEN,17,50,1,33,,,0.250000,,
N,34,0,0.125000,0
NGEN,17,1,34,34,,0.250000,,,
NGEN,16,50,34,50,,,0.250000,,

*** NOTE: THE ELEMENT GENERATION SECTION IS NOT SHOWN;
***HOWEVER, IT IS THE SAME AS THAT SHOWN IN APPENDIX C

SYMBC,0,1,0.0
SYMBC,0,2,0.0
D,1,UZ,0
WSORT,X
TREF,75
KTEMP,-1
TESIZE,19
TE,ALL,86,87.8,91.4,93.2,95,98.6
TEMORE,100.4,102.2,105.8,107.6,109.4,111.2
TEMORE,114.8,116.6,118.4,122,123.8,125.6
TEMORE,129.2
LWRITE
TE,ALL,134.6,138.2,141.8,147.2,150.8,154.4
TEMORE,158,161.6,167,170.6,174.2,177.8
TEMORE,183.2,186.8,190.4,194,197.6,203
TEMORE,206.6
LWRITE
```

TE,ALL,170.6,174.2,179.6,183.2,186.8,192.2
TEMORE,195.8,199.4,204.8,208.4,212,215.6
TEMORE,221,224.6,228.2,233.6,237.2,240.8
TEMORE,246.2
LWRITE
TE,ALL,219.2,224.6,228.2,233.6,239,242.6
TEMORE,248,251.6,257,262.4,266,271.4
TEMORE,276.8,280.4,285.8,289.4,294.8,300.2
TEMORE,305.6
LWRITE
TE,ALL,264.2,269.6,273.2,278.6,284,287.6
TEMORE,293,298.4,302,307.4,312.8,318.2
TEMORE,321.8,327.2,332.6,336.2,341.6,347
TEMORE,352.4
LWRITE

APPENDIX C

MATHEMATICA ROUTINE FOR CREATING 3-D PLOT OF WARPED BOARD SURFACE

The following is the mathematica file used to create the 3-D plot of the warped board at different temperature levels.

```
***This group contains the commands used in processing the input file
***to create the three dimensional rendering of the warped printed
***wiring board.

***First clear all variables to be used
Clear[temp];
Clear[surfuprt];
Clear[surfuphalf];
Clear[surftot];

***Store surface in temporary matrix.
temp=%;

***First read in displacement matrix from external text file created in
***Excel Spreadsheet. Note: example filename is shown here.
ReadList["c:\\surf275.txt",Number,RecordLists->True];

***Determine the number of rows(m) and columns(n) in the upper right
***quadrant's surface matrix. The dimensions of the entire board surface
***matrix are given by mtot and ntot.
n=(Length[temp[[1]]]-1)/2+1;
m=n;
***(* -1 is needed to keep from dupliating element*)
mtot=2*m-1;
ntot=2*n-1;
```

```
***This part will Create a matrix to store the upper right quad. of
***the board based upon the temporary matrix.
surfuprt=Table[0,{m},{n}];

***Now remove interor points and create upper right quad. surface
***matrix.
Do[ Do[surfuprt[[i,j]]=temp[[i,2*j-1]],{j,n}] ,{i,m}];
Clear[temp];

***This part will Create a matrix to store the upper half of
***the board based upon the upper right quadrant from the analysis.
surfuphalf=Table[0,{m},{ntot}];

***Now add upper left quadrant of board surface to upper half surface
***matrix.
Do[ Do[surfuphalf[[i,j]]=surfuprt[[i,n-j+1]],{j,n}] ,{i,m}];

***Now add upper right quadrant of board surface to upper half surface
***matrix.  Note that start from second element in original quadrant,
***to keep from repeating the element.
Do[ Do[surfuphalf[[i,j+n-1]]=surfuprt[[i,j]],{j,2,n}] ,{i,m}];

***This part will Create a matrix to store the entire board based upon
***the upper right half created earlier.
surftot=Table[0,{mtot},{ntot}];
surftot[[1]];

***Now clear surfuprt memory.
Clear[surfuprt];

***Now mirror the upper half of the board to the lower half and store in
***new matrix which holds the entire board surface.
Do[ Do[surftot[[i,j]]=surfuphalf[[m-i+1,j]],{j,ntot}] ,{i,m-1}];

***Now add upper half of board surface to total surface matrix.  Note
***that start from second element in original quadrant, to keep from
***repeating the element.
Do[ Do[surftot[[i+m-1,j]]=surfuphalf[[i,j]],{j,ntot}] ,{i,m}];
Clear[surfuphalf];

***Now ready to Plot the surface. Make sure to
***clear the surftot matrix before trying to
***manipulate the created plot!!
```

```
ListPlot3D[surftot];
Clear[surftot];
```

APPENDIX D

ANSYS INPUT FILE CREATION PROGRAM

The following program is used to create the input file necessary for the preprocessor module of the Ansys 4.4a finite element analysis software package. The first section contains the main program module, with the second section containing the utility functions module.

```
#include <conio.h>
#include <stdio.h>
#include <stdlib.h>
#include <ctype.h>
#include <string.h>
#include <alloc.h>
#include <process.h>
#include <graphics.h>
#include "utility.h"

#define TRUE 1
#define FALSE 0

// Functions local to this module
void exit_protocol(void);       // Executed upon abnormal termination
void info(void);                // Gives preliminary info. about program
void input_initial(void);       // Gets # of layers and materials
void query_graphics(void);       // Ask if graphics available
void layer_def(void);           // Defines layer properties
void matl_def(void);            // Defines material properties
void layer_matl_assign(void);   // Assigns material type to each layer
int disp_layer();               // Displays layer attributes
int disp_matl();                // Displays material attributes
void real_const_write(void);    // Write real constants to file
void matl_prop_write(void);     // Write property data to file
void mesh_create(void);
```

```
// Global variables
int layer_num;                  // Total number of layers
int curr_layer;                 // Curret layer for input
int matl_num;                   // Total number of materials used in board
int curr_matl;                  // Curret materialfor input
int graphics_on;                // Graphics device Parameter
int left,top,right,bottom;      // Used for windowing scheme
FILE *input_file;               //  Stream pointer to text file used for input to ANSYS
int num_bdry_elem;                      // Number of elements along boundary
int elem_num;
/* this variable is set up temporarily due to floating pt. warning*/
float dummy;

//Structure for  properties for each material
typedef struct {
  char name[20];
  int matlnum;          // Material #
  float ex[4];                  // Moduli
  float ey[4];
  float vxy[4];           // Poissons Ratio
  float gxy[4];
  float alpha_x;
  float alpha_y;
} MATERIAL;

//Structure for properties for each layer
typedef struct {
  int laynum;                   // Layer number
  int layer_matl;               // Layer material
  float thick;                  // Layer thickness
  float angle;                  //  Angle between Material and Element axes
  int repeats;                  // # of times current layer repeats
}LAYER;


/* Pointer to LAYER and MATERIAL types, will be used when memory is dynamically
allocated based upon layer number input by user*/
LAYER *layer_ptr;
MATERIAL *matl_ptr;
```

```
/*********************************************************************/
/* MAIN FUNCTION OF PROGRAM*/
void main()
{
  // Define function call at abnormal prog. termination
  atexit(exit_protocol);
  // Initiate graphics ability if files available
  query_graphics();
  if (graphics_on) {
    graph_init();
  }
  else {
    printf("This program will automatically create an input\n");
    printf("file for the ANSYS finite element package\n\n");
    printf("Press any key to continue:");
    getch();
  }
  // Matl property input functions
  input_initial();        //Get number layers, number materials
  matl_def();             //Get material properties
  layer_def();            //Get Material data for each layer
  if(graphics_on) layer_plot();
  /// ANSYS input file writing functions
  open_file();            // Open input file to ANSYS (input.dat)
  real_const_write();  // Write real constants to file
  matl_prop_write();  // Write material properties to file
  mesh_create();
  bdry_conditions();
  getch();
  free(layer_ptr);
  free(matl_ptr);
  closegraph();
  fclose(input_file);
  return;
}
/*********************************************************************/
```

```
/*********************************************************************/
```

```
//THESE FUNTIONS HANDLE INPUT OF PROPERTY INFO. BY USER

/* This function allows input of the number of layers then automatically
creates a dynamically allocated array of structures to store layer
information*/
void input_initial(void)
{
   int pass=FALSE;
   do {
        do {
          do {
            clrscr();
            printf("How many total layers in board (2-100)?\n");
            scanf("%i",&layer_num);
            } while( (layer_num<2)||(layer_num>100));
          printf("\nTotal # of layers = %i\n",layer_num);
          do {
            printf("Is this correct,Yes=1 or No=0?  ");
            scanf("%d",&pass);
          }  while((pass!=TRUE)&&(pass!=FALSE));
        } while(pass==FALSE);
        //Dynamically allocate memory if available
        if(NULL == (layer_ptr=(LAYER *)calloc(layer_num,sizeof(LAYER)))) {
          clrscr();
          printf("WARNING!! MEMORY NOT AVAILABLE, ABORTING\n\n");
          printf("Press any key to exit");
          getch();
          exit(0);
        }
        else {
          printf("successful\n");
        }

   } while(pass==FALSE);
   clrscr();
   do {
        do {
          clrscr();
          do {
            printf("How many different materials in board (>0) ?\n");
            scanf("%i",&matl_num);
            if(matl_num>layer_num) {
                 clrscr();
```

```
                printf("WARNING!! NUMBER OF MATERIALS EXCEEDS\n");
                printf("THE NUMBER OF LAYERS IN THE BOARD.\n");
                printf("Press any key to continue\n");
                getch();
                clrscr();
              }
            } while( (matl_num>layer_num)||(matl_num<1));
            printf("Total # of materials = %i\n",matl_num);
            do {
              printf("Is this correct,Yes=1 or No=0?  ");
              scanf("%d",&pass);
            }  while((pass!=TRUE)&&(pass!=FALSE));
          } while(pass==FALSE);
          //Dynamically allocate memory if available
          if(NULL == (matl_ptr=(MATERIAL *)calloc(matl_num,sizeof(MATERIAL)))) {
            clrscr();
            printf("WARNING!! MEMORY NOT AVAILABLE, ABORTING\n\n");
            printf("Press any key to exit");
            getch();
            exit(1);
          }
          else {
            printf("successful\n");
          }
    } while(pass==FALSE);
    return;
}



/* This function allows input of board materials and the temperature
dependent properties determined from automated properties testing
station*/
void matl_def(void) {
    int coeff,pass;
    int done=FALSE;
    for (curr_matl=1; curr_matl<=matl_num;curr_matl++) {
          do {
            clrscr();
            // Material number is set automatically
            (matl_ptr+curr_matl-1)->matlnum=curr_matl;
            // get name
```

```
printf("Input the name for material %d\n",curr_matl);
printf("(Up to 15 characters, no spaces allowed)\n");
printf("or e(X)it:\n");
scanf("%s",&(matl_ptr+curr_matl-1)->name);
// Exit if desired by user
if( toupper( (matl_ptr+curr_matl-1)->name[0] )=='X')  {
  exit(0);
}
//get modulus ex in four coefficient form
printf("\nInput the modulus (Ex) of material %d:\n",curr_matl);
for(coeff=0;coeff<=3;coeff++) {
 printf("Coefficient %d= ",coeff);
 scanf("%f",&dummy);
 ((matl_ptr+curr_matl-1)->ex[coeff])=dummy;
}
// modulus ey
clrscr();
printf("input the modulus (Ey) of material %d:\n",curr_matl);
for(coeff=0;coeff<=3;coeff++) {
  printf("Coefficient %d= ",coeff);
  scanf("%f",&dummy);
  ((matl_ptr+curr_matl-1)->ey[coeff])=dummy;
}
// poisson's ratio
clrscr();
printf("input Poissons ratio of material %d:\n",curr_matl);
for(coeff=0;coeff<=3;coeff++) {
  printf("Coefficient %d= ",coeff);
  scanf("%f",&dummy);
  ((matl_ptr+curr_matl-1)->vxy[coeff])=dummy;
}
// shear modulus
clrscr();
printf("Input shear modulus (G) of material %d:\n",curr_matl);
for(coeff=0;coeff<=3;coeff++) {
  printf("Coefficient %d= ",coeff);
  scanf("%f",&dummy);
  ((matl_ptr+curr_matl-1)->gxy[coeff])=dummy;
}
// CTE in the x direction
clrscr();
printf("Input CTE in x-dir. of material %d:\n",curr_matl);
scanf("%f",&dummy);
```

```
            ((matl_ptr+curr_matl-1)->alpha_x)=dummy;

            // CTE in the y-direction
            clrscr();
            printf("Input CTE in y-dir. of material %d:\n",curr_matl);
            scanf("%f",&dummy);
            ((matl_ptr+curr_matl-1)->alpha_y)=dummy;

            // display current attributes and verify
            done=disp_matl();
          } while(done==FALSE);
    }
    return;
}


/* This function is called to initialize the properties for
each layer of the board*/
void layer_def(void) {
    int coeff,pass;
    int done=FALSE;
    int count;
    for (curr_layer=1; curr_layer<=layer_num;curr_layer++) {
          do {
            clrscr();
            // Layer number is set automatically
            (layer_ptr+curr_layer-1)->laynum=curr_layer;


            // get layer material
            layer_matl_assign();

            // get thickness
            do {
              clrscr();
              printf("Input the thickness of layer %d:\n",curr_layer);
              scanf("%f",&dummy);
              if(dummy<0) {
                    printf("\nTHICKNESS MUST BE POSITIVE!");
                    printf("\nPress any key to continue");
                    getch();
              }
```

```
        } while(dummy<0);

        ((layer_ptr+curr_layer-1)->thick)=dummy;

        // get angle
        do {
          clrscr();
          printf("Input the angle of material axis layer %d:\n",curr_layer);
          printf("(0-90)");
          scanf("%f",&dummy);
          if((dummy<0)||(dummy>90)) {
               printf("\nANGLE MUST BE POSITIVE!\n");
               printf("Press any key to continue.");
               getch();
          }
        } while((dummy<0)||(dummy>90));
        ((layer_ptr+curr_layer-1)->angle)=dummy;

        // does the layer repeat

        do {
          printf("\n\nHow many times does the layer repeat?\n");
          printf("Do not include current layer, (0 for none): ",curr_layer);
          scanf("%d",&(layer_ptr+curr_layer-1)->repeats);
          if((((layer_ptr+curr_layer-1)->repeats) + curr_layer)>layer_num) {
               clrscr();
               printf("\n\nWARNING!! LAYER REPETITIONS EXTEND BEYOND
\n");
               printf("THE TOTAL NUMBER OF %d LAYERS INITIALLY
\n",layer_num);
               printf("SPECIFIED, PLEASE REENTER THE NUMBER OF \n");
               printf("REPETITIONS.\n");
               clrscr();
               pass=FALSE;
          }
          else if ((layer_ptr+curr_layer-1)->repeats<0) {
               clrscr();
               printf("\n\nREPETITIONS CANNOT BE  NEGATIVE\n");
               pass=FALSE;
          }
          else {
               pass=TRUE;
          }
```

```
            } while(pass==FALSE);

            // copy layer the number off repeated times
            for (count=curr_layer;count<=curr_layer+((layer_ptr+curr_layer-1)-
>repeats);count++) {
              *(layer_ptr+count)=*(layer_ptr+count-1);
            }
            // display current attributes and verify

            done=disp_layer();

            // check and see if current layer repeats
          } while( done==FALSE);
    }
    return;
}
```

```
/* This function allows the user to determine what material the current
board layer is made of.*/
void layer_matl_assign(void) {
        int count;
        int temp;
        do {
          clrscr();
          printf("Input the material NUMBER for layer %d\n\n",curr_layer);
          for(count=0;count<matl_num;count++)  {
            printf("(%d)  %s\n",count+1,(matl_ptr+count)->name);
          }
          printf("\nor  <-1> to exit:\n");
          scanf("%d",&temp);
          if ((temp<-1)||(temp>matl_num)) {
            printf("MATERIAL NUMBER NOT WITHIN RANGE\n");
            printf("Press any key to continue.");
            getch();
          }
        } while((temp<-1)||(temp>matl_num));
        (layer_ptr+curr_layer-1)->layer_matl=temp;
        // Exit if desired by user
        if(temp==(-1))  {
```

```
            exit(0);
          }
          return;
}



/* This funtion displays current layer material properties as well
as creating repeated layers of current layer input*/
int disp_layer() {
          int correct;
          clrscr();
          if (((layer_ptr+curr_layer-1)->repeats)==0) {
          printf("INFORMATION FOR LAYER %i\n\n", (layer_ptr+curr_layer-1)-
>laynum);
          }
          else {
            printf("INFORMATION FOR LAYERS %i ", (layer_ptr+curr_layer-1)-
>laynum);
            printf("THRU %i\n\n",(layer_ptr+curr_layer-1)->laynum+(layer_ptr+curr_layer-
1)->repeats);
          }
          printf("Material name          %s\n",(matl_ptr+((layer_ptr+curr_layer-1)-
>layer_matl)-1)->name);
          printf("Layer thickness (in)     %f\n",(layer_ptr+curr_layer-1)->thick);
          printf("Material angle (degrees)  %f\n",(layer_ptr+curr_layer-1)->angle);
          printf("Layer repeats          %d\n",(layer_ptr+curr_layer-1)->repeats);
          printf("\nIS THIS INFORMATION CORRECT? YES=1 NO=0 : ");
          scanf("%d",&correct);
          if(correct==TRUE) curr_layer=curr_layer+(layer_ptr+curr_layer-1)->repeats;
          return(correct);
}



/* This funtion displays current layer material properties, and asks
for verification*/
int disp_matl() {
          int correct,count;
          clrscr();
```

```
        printf("INFORMATION FOR MATERIAL %i\n\n", (matl_ptr+curr_matl-1)-
>matlnum);
        printf("Material name          %s\n",(matl_ptr+curr_matl-1)->name);
        printf("Modulus (Ex)           %f\n",(matl_ptr+curr_matl-1)->ex[0]);
        for (count=1;count<=3;count++) {
          printf("                     %f\n",(matl_ptr+curr_matl-1)->ex[count]);
        }
        printf("\nModulus (Ey)           %f\n",(matl_ptr+curr_matl-1)->ey[0]);
        for (count=1;count<=3;count++) {
          printf("                     %f\n",(matl_ptr+curr_matl-1)->ey[count]);
        }
        printf("\nPoisson's ratio (vxy)    %f\n",(matl_ptr+curr_matl-1)->vxy[0]);
        for (count=1;count<=3;count++) {
          printf("                     %f\n",(matl_ptr+curr_matl-1)->vxy[count]);
        }
        printf("\nCTE in X               %f\n",(matl_ptr+curr_matl-1)->alpha_x);
        printf("\nCTE in Y               %f\n",(matl_ptr+curr_matl-1)->alpha_y);
        printf("\nIS THIS INFORMATION CORRECT? YES=1 NO=0 : ");
        scanf("%d",&correct);
        return(correct);
}
/*************************************************************************/


/* Exit function, called in event of abnormal program termination*/
void exit_protocol(void) {
        free(layer_ptr);
        free(matl_ptr);
        closegraph();
        fclose(input_file);
        return;
}


/* Write real constants to ANSYS input file*/
void real_const_write() {
  int count;
  // Go to beginning of file
  fputs("/PREP7\n",input_file);
  fputs("/PNUM,KPOI,1\n",input_file);
  fputs("/PNUM,AREA,1\n",input_file);
```

```
  fputs("/PNUM,LINE,1\n",input_file);
  fputs("/PNUM,NODE,1\n",input_file);
  fputs("/PNUM,ELEM,1\n",input_file);
  fputs("KAN,0\n",input_file);
  fputs("ET,1,99\n",input_file);
  // Beginning of Real constant input
  fprintf(input_file,"R,1,%d,0,1,%d,0\n",layer_num,layer_num);
  fprintf(input_file,"RMORE,0,0,0,0,0,0");
  for (count=1;count<=layer_num/2;count++) {
    fprintf(input_file,"\nRMORE,%d,",(layer_ptr+(2*count-2))->layer_matl);
    fprintf(input_file,"%f,",(layer_ptr+(2*count-2))->angle);
    fprintf(input_file,"%f,",(layer_ptr+(2*count-2))->thick);
    fprintf(input_file,"%d,",(layer_ptr+2*count-1)->layer_matl);
    fprintf(input_file,"%f,",(layer_ptr+2*count-1)->angle);
    fprintf(input_file,"%f\n",(layer_ptr+2*count-1)->thick);
   }
   // If odd number of layers, be sure to include last layer
   if ( ((layer_num/2)*2)!=(layer_num)) {
     fprintf(input_file,"RMORE,%d,",(layer_ptr+(2*count-2))->layer_matl);
     fprintf(input_file,"%f,",(layer_ptr+(2*count-2))->angle);
     fprintf(input_file,"%f,",(layer_ptr+(2*count-2))->thick);
   }
  return;
}



/* Write real constants to ANSYS input file*/
void matl_prop_write() {
  int count;
  int temp;
  // Beginning of Property data input
  for (count=1;count<=matl_num;count++) {
    fprintf(input_file,"\nEX,%d,",(matl_ptr+(count-1))->matlnum);
    for (temp=0;temp<=3;temp++) {
        fprintf(input_file,"%f,",(matl_ptr+(count-1))->ex[temp]);
    }
    fprintf(input_file,"\nEY,%d,",(matl_ptr+(count-1))->matlnum);
    for (temp=0;temp<=3;temp++) {
        fprintf(input_file,"%f,",(matl_ptr+(count-1))->ey[temp]);
    }
    //fprintf(input_file,"\nEZ,%d,",(matl_ptr+(count-1))->matlnum);
```

```
    //for (temp=0;temp<=3;temp++) {
    //    fprintf(input_file,"%f,",(matl_ptr+(count-1))->ey[temp]);
    //}
    fprintf(input_file,"\nALPX,%d,",(matl_ptr+(count-1))->matlnum);
    fprintf(input_file,"%f,",(matl_ptr+(count-1))->alpha_x);
    fprintf(input_file,"\nALPY,%d,",(matl_ptr+(count-1))->matlnum);
    fprintf(input_file,"%f,",(matl_ptr+(count-1))->alpha_y);

    fprintf(input_file,"\nNUXY,%d,",(matl_ptr+(count-1))->matlnum);
    for (temp=0;temp<=3;temp++) {
        fprintf(input_file,"%f,",(matl_ptr+(count-1))->vxy[temp]);
    }
    fprintf(input_file,"\nGXY,%d,",(matl_ptr+(count-1))->matlnum);
    for (temp=0;temp<=3;temp++) {
        fprintf(input_file,"%f,",(matl_ptr+(count-1))->gxy[temp]);
    }
  }
  return;
}
```

SECOND MODULE OF ANSYS INPUT FILE CREATION PROGRAM

This is the second module of the Ansys input file creation program. The following module contains utility routines used in the program.

```
#include <conio.h>
#include <stdio.h>
#include <ctype.h>
#include <string.h>
#include <stdlib.h>
#include <graphics.h>
#include <dos.h>



// External Global declarations
extern int matl_num;            // Total number of materials in board, from "main.cpp"
extern int layer_num;  // Total number of layers in board, from "main.cpp"
extern int _wscroll;
extern int left,top,right,bottom;
extern int graphics_on;
//extern *layer_ptr;
//extern *material_ptr;
extern FILE *input_file;
extern int num_bdry_elem;           // Number of elements along boundary
extern int elem_num;                // Total number of elements


// Functions local to this module, declarations in "utility.h"
void open_file(void);
void graph_init(void);
void viewport_center(void);
void layer_plot(void);
void real_const_write(void);  // Write real constants to file
void mesh_create(void);
void info(void);
void text_box(void);
```

```
int left1=400,top1=0,right1=630,bottom1=350;
int left2=403,top2=20,right2=625,bottom2=347;

//*************************************************************************
/* File utility functions


/* this function will open a stream to a file chosen by the user*/
void open_file()
{
   char file_name[]="c:\\conf1a.dat";
   int temp;
   int done=0;

   do {
      if( (toupper(file_name[0])=='A')&&(file_name[1]==NULL)) //end if A entered
      {
        printf("Operation aborted");
        exit(1);
        return;
      }
      // Old file overwritten
      if((input_file=fopen(file_name,"w+t"))==NULL)
      {
        printf("Could not open file!!");
        printf("Enter to continue, or <a> for abort? ");
        if(toupper(getche())=='A')
        {
          printf("\nOperation aborted, Press any key to continue ");
          getch();
          fclose(input_file);
          exit(1);
          return;
        }
      }
      else
      {
        printf("file opened successfully.\n");
        printf("Press any key to continue.\n");
        getch();
        done=1;
        /* print file to the screen  */
```

```
            /*while(!feof(f_in)) {
              putchar(fgetc(f_in));
             }
            fclose(f_in);*/
          }

    } while(done==0);
    return;
}
```

```
//*************************************************************************
**//
/* Graphics interface functions */

void graph_init(void)  {
        _wscroll=0;
        int graphdrv=DETECT;
        int graphmode;
        int errorcode;

        int choice;
        //Initialize graphics drivers
        do {
          clrscr();
          printf("BGI files in current dir. <1> or default <0>");
          scanf("%d",&choice);
        } while ((choice!=0)&&(choice!=1));
        if (choice==1) {
          initgraph(&graphdrv,&graphmode,"");
        }
        else {
          initgraph(&graphdrv,&graphmode,"c:\\borlandc\\bgi");
        }
        /* read result of initialization */
        errorcode = graphresult();
        if (errorcode != grOk)  /* an error occurred */
        {
          printf("Graphics error: %s\n", grapherrormsg(errorcode));
          printf("Press any key to halt:");
```

```
        getch();
        exit(1); /* terminate with an error code */
      }
      // Give information about program
      info();
      // Create box around text entry
      //text_box();
      //set text window
      window(1,1,48,24);
      textcolor(BLACK);
      textbackground(WHITE);
      //set the viewport
      setviewport(left1,top1,right1,bottom1,1);
      setlinestyle(SOLID_LINE,0,3);
      setcolor(EGA_WHITE);

      rectangle(0,0,230,350);
      setcolor(EGA_CYAN);
      rectangle(3,3,227,347);


      //rectangle(1,25,225,350);
      //viewort is 270x290
      moveto(80,1);
      setcolor(EGA_LIGHTMAGENTA);
      outtext("VIEWPORT");
      setcolor(EGA_WHITE);
      /*create another viewport that is clearable by
      each function that calls it without removing viewport
      border and heading*/
      setviewport(left2,top2,right2,bottom2,1);
      /* Now calculate left and right offset for drawing objects in
      the actual viewport, labeled by #####2.*/
      //left=left2-left1;
      //top=top2-top1;
      //bottom=bottom1
      return;
}

void info(void) {
  setviewport(100,50,600,400,1);
  setlinestyle(SOLID_LINE,0,3);
  setcolor(EGA_MAGENTA);
```

```
  rectangle(0,0,500,350);
  setlinestyle(SOLID_LINE,0,3);
  setcolor(EGA_CYAN);
  rectangle(3,3,497,347);
  setcolor(EGA_WHITE);
  settextstyle(1, HORIZ_DIR, 4);
  outtextxy(20,70,"ANSYS INPUT FILE CREATION");
  outtextxy(160,110,"PROGRAM");
  settextstyle(1, HORIZ_DIR, 3);
  outtextxy(80,220,"by Jeff Garratt,MS. Student");
  outtextxy(155,250,"Georgia Tech");
  outtextxy(200,280,"1993");
  getch();
  settextstyle(1, HORIZ_DIR, 1);
  cleardevice();
  return;
}


void text_box(void) {
  setviewport(0,0,388,470,1);
  setlinestyle(SOLID_LINE,0,3);
  setcolor(EGA_MAGENTA);
  rectangle(0,0,388,470);
  setlinestyle(SOLID_LINE,0,3);
  setcolor(EGA_CYAN);
  rectangle(3,3,385,467);
  setcolor(EGA_WHITE);
  return;
}



/* this function is just giving preliminary information about program*/
void query_graphics(void)
{
        clrscr();
        do {
          clrscr();
```

```
            printf("ARE C++ BGI GRAPHICS FILES AVAILABLE ? YES<1> OR
NO<0>: ");
            scanf("%d",&graphics_on);
          } while((graphics_on!=0)&&(graphics_on!=1));

          clrscr();
          return;
}


/* this function automatically plots board layers in drawing
viewport(i.e. viewport 2)*/
void layer_plot(void) {
  // Center of graphics viewport based upon number of layers
  int height;             // Height of drawing viewport(i.e. viewport 2)
  int layer_thickness;  // Thickness of each layer for graphics purposes only
  int layer;
  int step;
  int vert_spacing=15;// Spacing of layers from border
  int dp;

  dp=350/layer_num+layer_num;
  //int horiz_spacing=10;
  height=bottom2-top2;
  layer_thickness= (height/2-vert_spacing)/(layer_num);
  setlinestyle(SOLID_LINE,0,1);
  setcolor(EGA_LIGHTGREEN);
  for (layer=1;layer<=layer_num;layer++) {
    bar3d(25,height-vert_spacing-2*(layer-1)*layer_thickness,150,height-vert_spacing-
(2*(layer-1)*layer_thickness-layer_thickness),dp,1);
    delay(150);
  }
  setcolor(EGA_WHITE);
  return;
}



/*****************************************************************************
***/
/* THESE FUNCTIONS ARE USED FOR WRITING DATA TO INPUT FILE FOR
ANSYS FEA PACKAGE*/
```

```
void mesh_create(void) {
  int count,row_count;                    // Counters
  int node_num;              // Counter for node generation loop
  float node_distance;       // Distance between nodes
  float quad_length;         // Length of one edge of square quadrant of board
  float elem_length;         // Length of element
  int tot_num_nodes;         // Total number of nodes
  int i,j,k,l,m,n,o,p;       // Node locations on element

  //float x_postion=0,y_position=0;

  //Get length of one quadrant of board
  do {
    clrscr();
    printf("Enter length of edge of board quadrant\n");
    printf("(.1 to 15 inches)\n");
    scanf("%f",&quad_length);
  } while ((quad_length<.1)||(quad_length>15));
  // Get number of elements along one side of board
  do {
    clrscr();
    printf("How man elements along the edge?\n ");
    printf("(4 to 100 elements)\n");
    scanf("%d",&num_bdry_elem);
  } while ((num_bdry_elem<4)||(num_bdry_elem>100));
  // Assuming square quadrant
  elem_num=(num_bdry_elem)*(num_bdry_elem);
  elem_length=(quad_length/num_bdry_elem);

  // Create x-boundary nodes
  fprintf(input_file,"\nN,1,0,0,0\n");
  fprintf(input_file,"N,2,%f,0,0\n",elem_length/2);
  fprintf(input_file,"NGEN,%d,2,1,2,,%f\n",num_bdry_elem,elem_length);

fprintf(input_file,"NGEN,2,1,%d,%d,,%f\n",num_bdry_elem*2,num_bdry_elem*2,elem_l
ength/2);
  // Now copy this row up to match with all element upper boundaries
  fprintf(input_file,"NGEN,%d,",num_bdry_elem+1);
  fprintf(input_file,"%d,",num_bdry_elem*2+num_bdry_elem+2);
  fprintf(input_file,"1,%d,,,%f,,\n",num_bdry_elem*2+1,elem_length);
```

```
  //Now create midside nodes
  fprintf(input_file,"N,%d,0,%f,0\n",num_bdry_elem*2+2,elem_length/2);
  fprintf(input_file,"NGEN,%d,1,%d,",num_bdry_elem+1,num_bdry_elem*2+2);
  fprintf(input_file,"%d,,%f,,,\n",num_bdry_elem*2+2,elem_length);
  //Now copy this row up

fprintf(input_file,"NGEN,%d,%d,%d,",num_bdry_elem,num_bdry_elem*2+2+num_bdry_
elem,num_bdry_elem*2+2);
  fprintf(input_file,"%d,,,%f,,\n",num_bdry_elem*2+2+num_bdry_elem,elem_length);


  // Now begin loop to create elements
  for (row_count=1;row_count<=num_bdry_elem;row_count++) {
    for (count=1;count<=num_bdry_elem*2-1;count=count+2) {
        i=count+(row_count-1)*((num_bdry_elem*2+1) +(num_bdry_elem+1));
        j=i+2;
        k=j+num_bdry_elem*2+1+num_bdry_elem+1;
        l=k-2;
        m=i+1;
        n=count/2+2+(row_count-1)*(num_bdry_elem+1)
+row_count*(num_bdry_elem*2+1);
        o=k-1;
        p=n-1;
        fprintf(input_file,"E,%d,%d,%d,%d,%d,%d,%d,%d\n",i,j,k,l,m,n,o,p);
    }
  }

  return;
}



void bdry_conditions(void) {
  fprintf(input_file,"\nSYMBC,0,1,0.0");
  fprintf(input_file,"\nSYMBC,0,2,0.0");
  fprintf(input_file,"\nWSORT,X");
  fprintf(input_file,"\nTREF,75");
  fprintf(input_file,"\nTUNIF,275");
  fprintf(input_file,"\nKTEMP,0");
  //fprintf(input_file,"\nAFWRIT");
  //fprintf(input_file,"\nFINISH");
  // fprintf(input_file,"\n/POST1");
```

```
  //fprintf(input_file,"\nSET,1");
  //fprintf(input_file,"\nPRDISP");


  return;

}
```

APPENDIX E

MANUFACTURER INFORMATION FOR PREPREG AND BOARD LAY-UP

WARPAGE STUDY GLASS CLOTH FIBER COUNTS, etc.

1080 Style cloth

1.45 oz / square yard

.0025 inch thick pressed out

60 x 47 ends / inch

.00023 inch diameter filaments

45,000 Yds / lb

Unplied

Data provided from Joel Roth Laminations Engineering IBM Endicott.

2) VARIABLE CLOTH BOARDS:

NOTE: traces alternate between north-south and east-west
glass cloth alternate warp between north-south and east-west

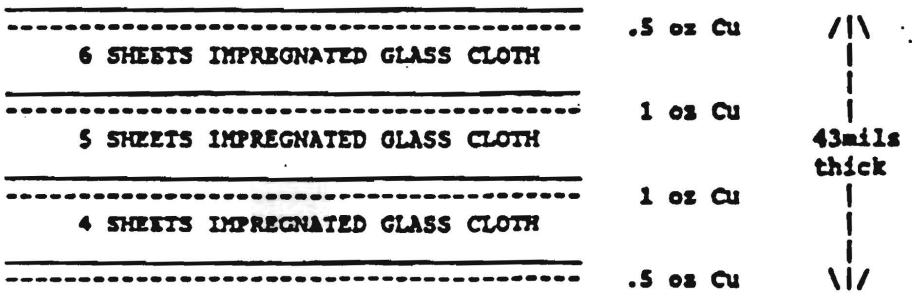

BIBLIOGRAPHY

[1] Bhagwan, D. and Broutman, L, *Analysis and Performance of Fiber Composites*, John Wiley & Sons, Inc., New York, 1990.

[2] Dally, J. and Riley, W., *Experimental Stress Analysis, 3rd ed.*, McGraw-Hill, Inc., New York, 1991.

[3] Daniel, I., Pipes, R., and Whitney, J., *Experimental Mechanics of Fiber Reinforced Composite Materials*, Society for experimental Stress Analysis, Prentice-Hall,Inc., Englewood Cliffs, New Jersey, 1982.

[4] Datoo, M., *Mechanics of Fibrous Composites*, Elsevier Applied Science, London and New York, 1991.

[5] "Errors Due to Transverse Sensitivity in Strain Gages", *M-M Tech Note TN-509: Transverse Sensitivity Errors*, Measurements Group, Inc., Raleigh, NC., 1982.

[6] Fulton, R.E., et al., *An Integrated Approach to Printed Wiring Board Design: Thermal Mechanical Behavior and Engineering Information Integration, Final Report: June 1991-September 1992*, Manufacturing Research Center, Georgia Tech, Atlanta, GA.

[7] Handbook of Ceramics and Composites, ed. Nicholas P. Cheremisinoff, New York, 1990.

[8] Haque, A. ,et al., "Moisture and Temperature induced degradation in tensile properties of Kevlar-graphite/epoxy hybrid Composites", *Journal of Reinforced Plastics and Composites*, v 10 n 2, p 132-145, March 1991.

[9] Hedden, R. P., *Cost Engineering in Printed Circuit Board Manufacturing*, Marcel Dekker, Inc., 1987.

[10] Herakovich, C. and Pindera,M., "Shear Characterization of Unidirectional Composites with the Off-Axis Tension Test", *Experimental Mechanics,* vol. 26(1), p.103, 1986.

[11] Hines, William W., and Montgomery, Douglas C., *Probability and Statistics in Engineering and Management Science 3rd. ed*, John Wiley & Sons, New York, 1990, pp. 11-14,230-231.

[12] Houston, T., *A Letter from IBM to Dr. Charles Ume of Georgia Tech*, April 1993.

[13] Lynch, L. and Nesbitt, R., "Rigid Printed Wiring Board Fabrication Techniques", *Electronic Materials Handbook, Volume 1: Packaging*, ASM International, Ohio, p. 538, 1990.

[14] Martin, T., "Finite Element Analysis of Printed Wiring Board Deformations During Thermal Cycles involved in the Solder Masking Process", *Masters Thesis*, Georgia Institute of Technology, May 1992.

[15] "Measurement of Thermal Expansion Coefficient Using Strain Gages", *M-M Tech Note TN-513-1: Thermal Expansion Measurement*, Measurements Group, Inc., Raleigh, NC., 1986.

[16] "M-Line Strain Gage Accessories", *Catalog A-110-6*, Measurements Group, Inc., Raleigh, NC., 1992.

[17] "Optimizing Strain Gage Excitation Levels", *M-M Tech Note TN-502: Strain Gage Excitation Levels*, Measurements Group, Inc., Raleigh, NC., 1979.

[18] Prasad, R.P., *Surface Mount Technology, Principles and Practice*, Van Nostrand Reinhold, New York, 1989.

[19] Shigley, J. and Mischke, C., *Mechanical Engineering Design 5th ed.*, McGraw-Hill Book Company, 1989.

[20] "Standard Test Method for Tensile Properties of Fiber-Resin Composites", Designation: D 3039-76, *Book of ASTM Standards*, ASTM, 1989.

[21] "Strain Gage Selection, Criteria, Procedures, Recommendations", *M-M Tech Note TN-505-2: Strain Gage Selection,* Measurements Group, Inc., Raleigh, NC., 1989.

[22] "Strain Gage Thermal Output and Gage Factor Variation with Temperature", *M-M Tech Note TN-504-1: Strain Gage Temperature Effects*, Measurements Group, Inc., Raleigh, NC., 1992.

[23] Swanson Analysis Systems, Inc., *Ansys User Manual, Vol. 1 &2, Version 4.4A*, Houston, PA., 1990.

[24] "Testware-SX Application Manual", *Testar Materials Testing Workstation*, MTS Systems Corporation, 1991.

[25] Upthegrove, Clair, "Elevated temperature properties of coppers and copper-base alloys. Data compiled and issued under the auspices of the Data and Publications Panel of the ASTM-ASME Joint Committee on Effect of Temperature on the Properties of Metals", *American Society for Testing and Materials. Special Technical Publication*, American Society for Testing Materials, Philadelphia, PA., 1956.

[26] Yeh, C.P., et al., "Experimental and Analytical Investigation of Thermally Induced Warpage for PWBs", *Proceedings of IEEE 41st Electronic Component Technology Conference (ECTC)*, Atlanta, GA., May 1991.

[27] Zhou, W., *Project work for Dr. R. Fulton*, Georgia Institute of Technology, Summer Quarter, 1993.